

ผลของการเติมผลึกเหลวโมเลกุลต่ำต่อโครงสร้างผลึกของซินติโอแทกติกพอลิสไตรีน



นาย อาษาไนย บัวศรี

สถาบันวิทยบริการ  
จุฬาลงกรณ์มหาวิทยาลัย

วิทยานิพนธ์นี้เป็นส่วนหนึ่งของการศึกษาตามหลักสูตรปริญญาวิศวกรรมศาสตรมหาบัณฑิต

สาขาวิศวกรรมเคมี ภาควิชาวิศวกรรมเคมี

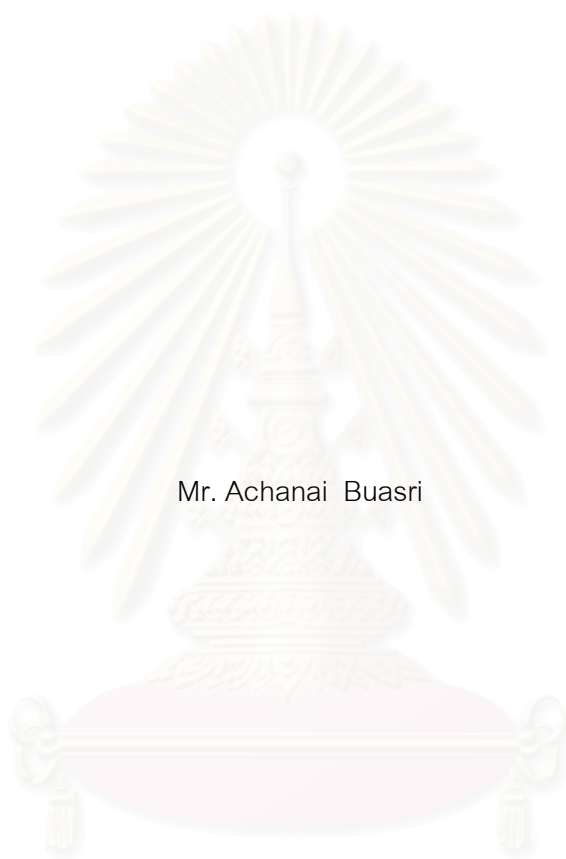
คณะวิศวกรรมศาสตร์ จุฬาลงกรณ์มหาวิทยาลัย

ปีการศึกษา 2546

ISBN 974-17-4858-2

ลิขสิทธิ์ของจุฬาลงกรณ์มหาวิทยาลัย

EFFECTS OF LOW MOLAR MASS LIQUID CRYSTAL ADDITION ON  
CRYSTAL STRUCTURE OF SYNDIOTACTIC POLYSTYRENE



Mr. Achanai Buasri

สถาบันวิทยบริการ

A Thesis Submitted in Partial Fulfillment of the Requirements  
for the Degree of Master of Engineering in Chemical Engineering

Department of Chemical Engineering

Faculty of Engineering

Chulalongkorn University

Academic Year 2003

ISBN 974-17-4858-2

Thesis Title                    EFFECTS OF LOW MOLAR MASS LIQUID CRYSTAL ADDITION  
ON CRYSTAL STRUCTURE OF SYNDIOTACTIC POLYSTYRENE  
By                                    Mr. Achanai Buasri  
Field of Study                    Chemical Engineering  
Thesis Advisor                    Assistant Professor ML. Supakanok Thongyai, Ph.D.

---

Accepted by the Faculty of Engineering, Chulalongkorn University in  
Partial Fulfillment of the Requirements for the Master's Degree.

..... Dean of Faculty of Engineering  
(Professor Direk Lavansiri, Ph.D.)

Thesis Committee

..... Chairman  
(Associate Professor Suttichai Assabumrungrat, Ph.D.)

..... Thesis Advisor  
(Assistant Professor ML. Supakanok Thongyai, Ph.D.)

..... Member  
(Assistant Professor Seerong Prichanont, Ph.D.)

..... Member  
(Bunjerd Jongsomjit, Ph.D.)

อาชาไนย บัณฑิต: ผลของการเติมผลึกเหลวมวลโมเลกุลต่ำต่อโครงสร้างผลึกของซินดีโอแทกติกพอลิสไตรีน (Effects of Low Molar Mass Liquid Crystal Addition on Crystal Structure of Syndiotactic Polystyrene) อาจารย์ที่ปรึกษา: ผศ. ดร. มล. ศุภกนก ทองใหญ่, 110 หน้า, ISBN 974-17-4858-2.

การเกิดพอลิเมอร์แบบของเหลวผสมของสไตรีนด้วยระบบตัวเร่งปฏิกิริยาเพนทาเมทิลไซโคลเพนทาไดอีนิลไทเทเนียมไตรคลอไรด์ร่วมกับตัวเร่งปฏิกิริยาร่วมซึ่งเป็นสารประกอบของโบรอนและไตรไอโซบิวทิลอะลูมิเนียม ถูกค้นคว้าเพื่อศึกษาผลของเวลาในการเกิดปฏิกิริยาพอลิเมอร์เซชันที่มีต่อคุณสมบัติของซินดีโอแทกติกพอลิสไตรีน จากผลการทดลองพบว่าเปอร์เซ็นต์ซินดีโอแทกติกของพอลิสไตรีนที่ได้จะแตกต่างกันเล็กน้อย ดังนั้นเปอร์เซ็นต์ซินดีโอแทกติกของพอลิเมอร์จะไม่สัมพันธ์กับเวลาในการเกิดปฏิกิริยา นอกจากนี้ยังศึกษาผลของการเติมสารเติมแต่งที่มีต่อระดับความเป็นผลึกของพอลิเมอร์ พอลิเมอร์ผสมถูกเตรียมขึ้นโดยวิธีการกวนผสมแบบหลอมเหลวด้วยความร้อนที่อัตราส่วน 1.0 เปอร์เซ็นต์โดยน้ำหนักของไซโคลเฮกซิลไบฟีนิลไซโคลเฮกเซนซึ่งเป็นผลึกเหลวมวลโมเลกุลต่ำหรือกลีเซอรอลมอนอสเตียเรตซึ่งเป็นสารหล่อลื่นทางการค้า พอลิเมอร์ที่ได้จะถูกนำไปทดสอบหาอุณหภูมิกลาสทรานซิชัน อุณหภูมิก่อผลึก อุณหภูมิหลอมเหลว ระดับความเป็นผลึก ลักษณะทางกายภาพและการกระเจิงแสงเปรียบเทียบกับพอลิเมอร์บริสุทธิ์ พบว่าสารผลึกเหลวและสารหล่อลื่นจะทำให้โมเลกุลของสารผสมเคลื่อนที่ได้มากขึ้น ดังนั้นการเติมสารเติมแต่งส่งผลให้ระดับความเป็นผลึกและการกระเจิงแสงเพิ่มขึ้น แต่จะไปลดอุณหภูมิก่อผลึกและอุณหภูมิหลอมเหลวของพอลิเมอร์ผสม

ภาควิชา.....วิศวกรรมเคมี  
สาขาวิชา.....วิศวกรรมเคมี  
ปีการศึกษา.....2546.....

ลายมือชื่อนิสิต.....  
ลายมือชื่ออาจารย์ที่ปรึกษา.....

# # 4570651621: MAJOR CHEMICAL ENGINEERING

KEY WORD: SYNDIOTACTIC POLYSTYRENE / LOW MOLAR MASS LIQUID CRYSTAL / LUBRICANT / POLYMER BLEND.

ACHANAI BUASRI: EFFECTS OF LOW MOLAR MASS LIQUID CRYSTAL ADDITION ON CRYSTAL STRUCTURE OF SYNDIOTACTIC POLYSTYRENE.

THESIS ADVISOR: ASSISTANT PROFESSOR ML. SUPAKANOK THONGYAI, Ph.D.,  
110 pp. ISBN 974-17-4858-2.

The slurry polymerization of styrene with pentamethylcyclopentadienyltitanium trichloride ( $Cp^*TiCl_3$ ) in combination with boron compound ( $[PhNMe_2H]^+[B(C_6F_5)]$ ) and triisobutylaluminum (TIBA) was investigated to study the effect of polymerization time on property of syndiotactic polystyrene. From the experimental results, it was found that the % syndiotactic index (% S.I.) of polystyrene obtained with various polymerization times had the slight difference in every polymerization time. Also, they did not appear to be related to the polymerization time. Furthermore, study the effect of additive addition on crystallinity of blended polymer. Stirring melt mix was utilized in blending of syndiotactic polystyrene and additive with content at 1.0 percent by weight of cyclohexylbiphenylcyclohexane (CBC-33), which it was low molar mass liquid crystal or glycerol monostearate (GMS), which it was commercial lubricant. The glass transition temperature ( $T_g$ ), crystalline temperature ( $T_c$ ), melting temperature ( $T_m$ ), % Crystallinity, morphology and light scattering of the resulting blends were investigated and compared with the base polymer. The results showed that the major effect of liquid crystal and lubricant were to increase the molecular mobility of the blends. Therefore the additive addition to base polymer by affect the increasing of % crystallinity and light scattering whereas would reducing of  $T_c$  and  $T_m$  in blended polymer.

Department.....Chemical Engineering.....

Student's signature.....

Field of study.....Chemical Engineering.....

Advisor's signature.....

Academic Year.....2003.....

## ACKNOWLEDGEMENTS

I would like to express my deeply gratitude to my advisor, Assistant Professor Dr. ML. Supakanok Thongyai, Ph.D. to his continuous guidance, enormous number of invaluable discussions, helpful suggestions, warm encouragement and patience to correct my writing. I am grateful to Associate Professor Suttichai Assabumrungrat, Ph.D., Assistant Professor Seerong Prichanont, Ph.D. and Bunjerd Jongsomjit, Ph.D. for serving as chairman and thesis committees, respectively, whose comments were constructively and especially helpful.

Since thanks are made to the Scientific and Technological Research Equipment Centre (STREC), Chulalongkorn University for using Scanning Electron Microscope (SEM), Metallurgy and Materials Science Research Institute (MMRI), Chulalongkorn University for using Wide-Angle X-ray Diffraction (WAXD), Polymer Engineering Research Laboratory (PEL), Chulalongkorn University for using Small-Angle Light Scattering (SALS) and Central Instrument Facility (CIF), Mahidol University for using Differential Scanning Calorimetry (DSC)

Sincere thanks to all my friends and all members of the Center of Excellent on Catalysis & Catalytic Reaction Engineering (Petrochemical Engineering Research Laboratory), Department of Chemical Engineering, Chulalongkorn University for their assistance and friendly encouragement.

Finally, I would like to dedicate this thesis to my parents and my families, who generously supported and encouraged me through the year spent on this study.

# CONTENTS

## PAGE

ABSTRACT (IN THAI).....	iv
ABSTRACT (IN ENGLISH).....	v
ACKNOWLEDGEMENTS.....	vi
CONTENTS.....	vii
LIST OF FIGURES.....	x
LIST OF TABLES.....	xiii
CHAPTERS	
I INTRODUCTION.....	1
1.1 The Objective of This Thesis.....	3
1.2 The Scope of This Thesis.....	4
II LITERATURE REVIEWS.....	5
III THEORY.....	13
3.1 Categories of Metallocene Catalyst Systems.....	13
3.1.1 Metallocene.....	13
3.1.2 Aluminoxane.....	15
3.2 Cocatalysts and Modifiers.....	16
3.2.1 Lewis Acids.....	17
3.2.2 Miscellaneous Additives.....	18
3.3 Polystyrene.....	18
3.4 The Polystyrene of the Further.....	20
3.5 Styrene Polymerization.....	21
3.5.1 Radical Polymerization.....	22
3.5.2 Anionic Polymerization.....	24
3.5.3 Cationic Polymerization.....	25
3.5.4 Coordination Polymerization.....	26
3.6 Polymer Morphology.....	26
3.6.1 The Amorphous State.....	26
3.6.2 Glass Transition Temperature.....	27
3.6.3 The Crystalline Polymer.....	27
3.7 Melting Phenomena.....	29
3.8 Thermal Properties.....	29
3.9 Structure of Crystalline Polymers.....	30
3.10 Crystal Structure in Polymers.....	31
3.10.1 Crystallization from Dilute Solution.....	31
3.10.1.1 Polymer Single Crystals.....	31
3.10.1.2 The Folded Chain Model.....	32
3.10.1.3 The Switchboard Model.....	33
3.10.2 Crystallization from the Melt.....	34
3.10.2.1 Spherulitic Morphology.....	34
3.10.2.2 Mechanism of Spherulite Formation.....	35
3.10.2.3 Spherulites in Polymer Blends.....	36
3.10.2.4 Effect of Crystallinity on Glass Transition Temperature.....	36

## CONTENTS (Cont.)

	<b>PAGE</b>
3.11 Introduction to Plastics Additives.....	36
3.12 Functions of Additives.....	36
3.13 Liquid Crystal.....	38
3.13.1 The History of Liquid Crystal.....	38
3.13.2 Introduction to Liquid Crystal.....	38
3.13.3 Main-Chain Polymer Liquid Crystals.....	39
3.13.4 Side Chain Polymer Liquid Crystals.....	41
3.13.5 Type of Liquid Crystal.....	42
3.13.6 Liquid Crystal Phases.....	43
3.13.7 Mesophasic Transition Temperature.....	45
3.13.8 Application of Liquid Crystals.....	45
3.13.9 Structural Considerations of Low Molecular Weight Liquid Crystal Systems.....	46
3.14 Polymer Blends.....	49
3.14.1 Melt Mixing.....	49
3.14.2 Solvent Casing.....	49
3.14.3 Freeze Drying.....	50
3.14.4 Emulsions.....	50
3.14.5 Reactive Blend.....	50
3.15 Light Scattering Theory.....	50
IV EXPERIMENT.....	54
4.1 Chemicals.....	54
4.2 Equipments.....	55
4.2.1 Schlenk Line.....	55
4.2.2 Schlenk Tube.....	55
4.2.3 Glove Box.....	56
4.2.4 Vacuum Pump.....	56
4.2.5 Inert Gas Supply.....	57
4.2.6 Glass Reactor.....	57
4.2.7 Magnetic Stirrer and Hot Plate.....	57
4.2.8 Digital Hot Plate Stirrer.....	57
4.2.9 Cooling System.....	57
4.2.10 Syringe, Needle and Septum.....	58
4.3 Characterization Instruments.....	58
4.3.1 Soxhlet Extractor.....	58
4.3.2 Differential Scanning Calorimetry.....	58
4.3.3 Scanning Electron Microscope.....	58
4.3.4 Small-Angle Light Scattering.....	58
4.3.5 Wide-Angle X-ray Diffraction.....	59
4.4 Polymerization Procedure.....	60
4.4.1 Preparation of Catalyst.....	60
4.4.2 Preparation of Cocatalyst.....	60
4.4.3 Preparation of Styrene Monomer.....	60
4.4.4 Styrene Polymerization.....	60



## CONTENTS (Cont.)

	<b>PAGE</b>
4.5 Blend Polymer between Syndiotactic Polystyrenes and Additives .....	60
4.6 Characterization of All Polystyrene Products .....	61
4.6.1 Catalytic Activity .....	61
4.6.2 Stereospecificity .....	61
4.6.3 Glass Transition, Crystalline and Melting Temperature .....	61
4.6.4 Morphology .....	61
4.6.5 Light Scattering .....	61
4.6.6 Crystalline Structure .....	61
V RESULTS AND DISCUSSION .....	62
5.1 Polymerization of Styrene with Pentamethylcyclopentadienyltitanium Trichloride as Catalyst .....	62
5.1.1 The Effect of Polymerization Time on Catalytic Activity .....	62
5.2 Characterization of All Polystyrene Products and Additives .....	64
5.2.1 Stereospecificity .....	64
5.2.2 Glass Transition, Crystalline and Melting Temperature .....	65
5.2.3 Morphology .....	68
5.2.4 Light Scattering Measurement .....	76
5.2.4.1 Scattered Light Photographs .....	76
5.2.4.2 Digital Intensity Data .....	78
5.2.4.2.1 Smoothing Digital Intensity Data .....	79
5.2.5 Crystalline Structure .....	82
VI CONCLUSIONS AND SUGGESTIONS .....	89
6.1 Conclusions .....	89
6.2 Suggestions .....	90
REFERENCE .....	91
APPENDIX .....	98
VITA .....	110

## LIST OF FIGURES

FIGURE	PAGE
3.1 Plausible structure of methylaluminoxane.....	16
3.2 Structure of polystyrene.....	18
3.3 Free radical polymerization.....	19
3.4 Structure of high-impact polystyrene.....	19
3.5 Phase separate of polybutadiene and polystyrene homopolymer.....	20
3.6 Tacticity of polystyrene.....	21
3.7 Three different configurations of a mono-substituted polyethylene.....	28
3.8 The fringed micelle model.....	30
3.9 Electron micrograph of a single crystal of nylon-6 grown by precipitation from dilute glycerine solution.....	31
3.10 Optical micrograph showing corrugations in single crystal of linear polyethylene grown from a solution in perchloroethylene.....	32
3.11 Electron micrograph showing pleats in a crystal of linear polyethylene grown from a solution in perchloroethylene.....	32
3.12 Schematic view of a polyethylene single crystal exhibiting adjacent reentry.....	33
3.13 Switchboard Model.....	33
3.14 Different types of light scattering patterns are obtained from spherulitic polyethylene using.....	34
3.15 Model of spherulitic structure.....	35
3.16 The structure of MC-PLCs and SC-PLCs.....	39
3.17 The structure of MC-PLC.....	39
3.18 The structure of MC-PLC.....	40
3.19 The random orientation of monomers in the polymer chain.....	40
3.20 The irregularity of polymer substitute in polymer chain.....	41
3.21 120-degree kinks in the polymer chain.....	41
3.22 The structure of SC-PLCs.....	41
3.23 The spacer of methylene units and the mesogen of aromatic rings.....	42
3.24 The tangle conformation and orientation of the mesogens.....	42
3.25 The structure of smectic phase.....	44
3.26 The structure of nematic phase.....	44
3.27 The structure of cholesteric phase.....	44
3.28 The general structure of aromatic system.....	46
3.29 The general structure of alicyclic system.....	47
3.30 The structure of cholesteric system.....	48
3.31 The structure of diskogens system.....	48
3.32 A typical photographic light scattering apparatus.....	51
3.33 Typical light scattering photographs.....	52
3.34 The arrangement of induced dipoles and the expected Vv scattering patterns for spherulites.....	52
3.35 The arrangement of induced dipoles in a tangentially polarizable spherulite which will contribute to Hv scattering.....	53
4.1 Schlenk line.....	55
4.2 Schlenk tube.....	55
4.3 Glove box.....	56
4.4 Vacuum pump.....	56

## LIST OF FIGURES (Cont.)

FIGURE	PAGE
4.5 Inert gas supply system.....	57
4.6 A schematic diagram of static light scattering equipment.....	59
5.1 % Yield of polystyrene produced at different polymerization times.....	63
5.2 Catalytic activity of polystyrene produced at different polymerization times.....	63
5.3 % S.I. of polystyrene products at various polymerization times.....	64
5.4 SEM image of GMS.....	69
5.5 SEM image of CBC-33.....	69
5.6 SEM image of polystyrene 1.0 hr (before extracted).....	70
5.7 SEM image of polystyrene 1.0 hr (after extracted).....	70
5.8 SEM image of polystyrene 1.0 hr blended with GMS.....	71
5.9 SEM image of polystyrene 1.0 hr blend with CBC-33.....	71
5.10 SEM image of polystyrene 1.5 hr (before extracted).....	72
5.11 SEM image of polystyrene 1.5 hr (after extracted).....	72
5.12 SEM image of polystyrene 1.5 hr blend with GMS.....	73
5.13 SEM image of polystyrene 1.5 hr blend with CBC-33.....	73
5.14 SEM image of polystyrene 2.0 hr (before extracted).....	74
5.15 SEM image of polystyrene 2.0 hr (after extracted).....	74
5.16 SEM image of polystyrene 2.0 hr blend with GMS.....	75
5.17 SEM image of polystyrene 2.0 hr blend with CBC-33.....	75
5.18 Scattered light photographs of pure sPS 1.0, 1.5 and 2.0 hr that vary intensity of light.....	77
5.19 Scattered light photographs of additives, pure polymers and their blends.....	78
5.20 Scattered light contour graph of pure sPS 1.0, 1.5 and 2.0 hr.....	78
5.21 Schematic diagram of smoothing procedure.....	79
5.22 Contour graphs of trial and error in smoothing intensity data.....	80
5.23 Smoothed contour graphs of additives, pure polymers and their blends.....	81
5.24 XRD patterns of GMS.....	82
5.25 XRD patterns of CBC-33.....	82
5.26 XRD patterns of polystyrene 1.0 hr.....	83
5.27 XRD patterns of polystyrene 1.0 hr blended with GMS.....	83
5.28 XRD patterns of polystyrene 1.0 hr blend with CBC-33.....	83
5.29 XRD patterns of polystyrene 1.5 hr.....	84
5.30 XRD patterns of polystyrene 1.5 hr blend with GMS.....	84
5.31 XRD patterns of polystyrene 1.5 hr blend with CBC-33.....	84
5.32 XRD patterns of polystyrene 2.0 hr.....	85
5.33 XRD patterns of polystyrene 2.0 hr blend with GMS.....	85
5.34 XRD patterns of polystyrene 2.0 hr blend with CBC-33.....	85
5.35 XRD patterns of all pure polymers and blend polymers.....	86
A.1 DSC curve of GMS.....	99
A.2 DSC curve of CBC-33.....	100
A.3 DSC curve of polystyrene 1.0 hr.....	101
A.4 DSC curve of polystyrene 1.0 hr blended with GMS.....	102
A.5 DSC curve of polystyrene 1.0 hr blended with CBC-33.....	103
A.6 DSC curve of polystyrene 1.5 hr.....	104
A.7 DSC curve of polystyrene 1.5 hr blended with GMS.....	105

**LIST OF FIGURES (Cont.)**

FIGURE	PAGE
A.8 DSC curve of polystyrene 1.5 hr blended with CBC-33.....	106
A.9 DSC curve of polystyrene 2.0 hr.....	107
A.10 DSC curve of polystyrene 2.0 hr blended with GMS.....	108
A.11 DSC curve of polystyrene 2.0 hr blended with CBC-33.....	109



สถาบันวิทยบริการ  
จุฬาลงกรณ์มหาวิทยาลัย

## LIST OF TABLES

TABLE	PAGE
3.1 Metallocene catalyst systems.....	14
3.2 Representative examples of metallocenes.....	15
5.1 % Yield and catalytic activity of polystyrene produced at different polymerization times.....	62
5.2 % Syndiotactic index (% S.I.) of polystyrene products at various polymerization times.....	64
5.3 Glass transition, crystalline and melting temperature of the obtained polymer.....	65
5.4 Melting enthalpy and % crystallinity of the obtained polymer.....	67
5.5 % Crystallinity of the obtained polymer.....	87



สถาบันวิทยบริการ  
จุฬาลงกรณ์มหาวิทยาลัย

# CHAPTER I

## INTRODUCTION

Plastics have an influence on life at nearly every level in society today. Their resistance to corrosion and tremendous technological flexibility has enabled them even to supersede and replace metals in the construction of many household tools and creature comforts [1]. Polyolefins are the most common and at the same time simplest polymer group. For the above reason, the polyolefin process technologies were widely interested and developed in terms of economics, versatility, safety and environmental efficiency. In 1995, 53.6 million metric tons of polyolefins were produced worldwide. This amount makes up 47 % of the entire production of plastics. The production of polyolefins has grown to a huge industry. Especially, polyethylene (PE) is the world's largest volume bulk plastic with annual consumption. Polypropylene (PP) is the third-ranked bulk plastic with annual consumption. These two polyolefins alone account for 35 % of all thermoplastics and elastomers [2].

Classical polymers such as polyethylene, polypropylene and polystyrene (PS) are again of great interest for science and industry. These polymers are not only the most extensively used plastics but also they show an above-average growth rate as materials. This increase is caused largely by new catalysts which are able to tailor the polymer structure and by this, the physical properties [3].

In 1933, polyethylene was discovered by Fawcett and Gibson [4-5]. Karl Ziegler [6-7], Giulio Natta [8-9] and Pual Hogen [10] discovered the revolutionary first-generation Ziegler-Natta transition metal catalyst system in 1953. The second-generation  $MgCl_2$  and/or donor supported Ziegler-Natta transition metal catalyst system, which was at least 100 times more active, led to the development of the low pressure polymerization process for polyolefins and synthetic elastomers [11]. This revolutionary catalyst system resulted in the development of simplified gas-phase low pressure polymerization plant operation without the need for the removal of residual trace catalyst from the polymer. It was estimated that more than 36 billion kilograms of polymers were produced globally with the Ziegler-Natta transition metal catalyst system in 1997 [4].

However, the Ziegler-Natta catalyst has the property to provide polymers with a wide molecular weight distribution (MWD) and composition distributions due to multiple active sites or multi-site catalysts. In contrast, metallocene catalyst that can control composition distribution, molecular weight distribution, incorporation of various comonomers and stereoregularity, was developed for polyolefin production [12]. The metallocene catalysts are generally called single-site catalysts because of the equality of each catalyst site.

Metallocene catalysts have been used to produce polyolefins commercially since 1991. In addition, metallocene can readily polymerize bulky monomer such as styrene and norbornene to make novel polymer with physical properties competitive with high performance engineering plastics such as nylon, polycarbonates and polyesters [2]. However, the polymer yield produced from metallocene catalyst,

although very much higher, was still too low if applied the support systems and catalyst system costs remained too high because of high Al:M (M = Ti, Zr and Hf) ratios for using olefin polymerization.

For the first time the synthesis of syndiotactic polystyrene (sPS) has been succeeded by Ishihara et al. with the usage homogeneous metallocene catalyst of titanium compounds and methylaluminoxane (MAO) [13]. With a melting point of 270 °C, which is the highest of all the homopolymer and a crystalline nature, sPS has excellent heat resistance, chemical resistance, water/steam resistance and insulating properties. Moreover, the crystallization rate of sPS is much faster than isotactic polystyrene (iPS), which allows the practical use sPS in many forming operations, such as injection molding, extrusion and thermoforming. sPS is thought of as a potential engineering polymer and it has aroused wide attention and research interest [14]. Bulk polymerization has been chosen as the main polymerization method in many recent patents for sPS polymerization technology, because its reaction apparatuses are relative small and the posttreatment is relatively simple. In the bulk syndiotactic polymerization of styrene with homogeneous metallocene, the reacting mixture is first in a slurry state and becomes a wet and then dry powder because of the crystallization of the sPS. The polymerization proceeds further in the solid phase and the conversion increases. Thus, a homogeneous high viscous period does not occur as in the radical polymerization of styrene.

Beyond the improvements in activity and the reduction of the high cost of the cocatalyst, these catalysts also offer opportunities to make polymers with properties well beyond the capabilities of any previous-known technology [12]. The study of metallocene catalyst synthesis for olefin polymerization is one of the areas of greatest interest. Development of new catalyst systems is the greatest challenges and lead to a wide range of new polymeric materials.

Many thermoplastics are now accepted as engineering material that probably originated as a classification to distinguish the materials that could substitute metals in many applications. By such a criterion, thermoplastics have a disadvantage compared with metals because their properties change with time and have inferior strengths except in rather special circumstances. However, these disadvantages can be compensated by other advantages such as their low strength to density ratio, their resistance to many of the liquids that corrode metals.

Generally, polystyrene is one of the most important commodity polymers in the industry. Its applications range from high modulus, transparent grade to rubber modified, tough resins and blends with outstanding impact resistance and mechanical properties. Recently, coordination polymerization techniques were introduced for preparation of polystyrene, which has an entirely new range of possibilities and the feasibility to prepare a highly stereoregular, sPS was demonstrated [15]. Also, sPS has been reported to show polymorphism according to crystallization conditions like as isotactic polypropylene (iPP), isotactic poly (butene), isotactic poly (1-butene) and syndiotactic poly (1-butene). However, because sPS has some economic disadvantages such as low strength, higher processing temperature and efficiency of polymerization catalyst, it has been restricted to a few applications. So, many researchers are still interested in blending with secondary polymer materials to reduce the product cost.

The engineering polymers especially syndiotactic polystyrene have a high viscosity and require higher processing temperatures than other thermoplastics to lower down the processing viscosity. However high processing temperature may deteriorate the excellent properties by thermal degradation. There are several processing additives to improve the processing properties at lower processing temperature such as lubricant and plasticizer, but they may cause negative effects to other important properties, especially mechanical properties of the final products.

Polymer blends [16] have been one of the most promising routes to produce new materials. Blending is an efficient means to create new materials having many more varied physical properties than do the individual polymers. There were many ways to mix polymers together such as by heat (melt mixing), solvent (solution casting, freeze-drying) and others. The primary properties, at which improvements are aimed in blending, are mechanical, thermal properties and cost per processability.

Lubricant [17] is a substance that when added in small quantities, provides a considerable decrease in resistance to the movement of chains or segments of a polymer or at least partly amorphous structure. There are two kinds of lubricant that are internal lubricant and external lubricant. In general, if a lubricant appears to be effective in improving flow but does not have much effect on surface tension, it is considered internal lubricant. If it is found on the surface or on adjacent surfaces or if it modifies observables associated with the surface, it is considered external lubricant. If it behaves in one way under one set of conditions and in another way under a different set of circumstances, it is considered both an internal and external lubricant. These are referred to as balanced, combination or multifunctional lubricants.

Plasticizers [166] are most effective in crystalline-type thermoplastic polymers, where they are essential aids in imparting flexibility, melt flow, impact resistance and added strength to the polymer compositions.

In the plastic industry, polymer blends are preferred than the synthesis of new polymers due to its lower production cost and adaptability to fulfill the various and multiple material properties in use.

### **1.1 The Objective of This Thesis**

Study on the effect of two types of additives with syndiotactic polystyrenes, which synthesized by homogeneous half-metallocene catalyst system using various polymerization times that influence on the crystallinity of the polymer blends by differential scanning calorimetry (DSC) and wide-angle X-ray diffraction (WAXD). Furthermore, to produce light scattering behavior database of polymer blends by using the new modification of small-angle light scattering (SALS) technique, the new numerical analysis of 2-dimensions and the computer program.



## 1.2 The Scope of This Thesis

1.2.1 Study and prepare the syndiotactic polystyrenes by using homogeneous half-metallocene catalyst system, which various polymerization times.

1.2.2 Syndiotactic polystyrenes, having the different polymerization times, were blended with glycerol monostearate (GMS), which it was commercial lubricant or cyclohexylbiphenylcyclohexane (CBC-33), which it was low molar mass liquid crystal at concentration about 1.0 % (w/w) by using melt mixing.

1.2.3 Characterize pure syndiotactic polystyrene products, blend polymer products and additives with conventional techniques: Differential Scanning Calorimetry (DSC), Scanning Electron Microscopy (SEM), Small-Angle Light Scattering (SALS) and Wide-Angle X-ray Diffraction (WAXD), also determine the % syndiotacticity of polymer.



สถาบันวิทยบริการ  
จุฬาลงกรณ์มหาวิทยาลัย

## CHAPTER II

### LITERATURE REVIEWS

The first homogeneous metallocene catalysts were discovered in 1957 by Natta [18] and Breslow [19], who used bis (cyclopentadienyl) titanium (IV) compounds together with aluminium alkyls for ethylene polymerization. These catalysts systems, replacing the chloride ligand of the Ziegler-Natta transition metal catalyst system by cyclopentadienyl (Cp) derivative compounds, were mainly used in mechanistic studies [20-21]. Subsequently, Kaminsky and his coworkers found that the addition of water to the trialkyl aluminum in a molar ratio of 1:1 during ethylene polymerization significantly increased the catalytic activity [22-23]. The reaction of trialkyl aluminum with water was shown to produce alkyl aluminoxane. In 1980 Kaminsky and coworkers [22] used oligomeric methylaluminoxane (MAO) with group 4B metallocene compounds to obtain ethylene polymerization catalysts having extremely high activities. For instance  $\text{Cp}_2\text{TiCl}_2/\text{MAO}$  has polyethylene (PE) productivity of  $9.3 \times 10^6$  g PE/(mol Ti.hr.atm) at 20 °C, the productivity is  $9 \times 10^7$  g PE/(mol Zr.hr.atm) at 70 °C with  $\text{Cp}_2\text{ZrCl}_2/\text{MAO}$ . However, these catalysts are non-stereospecific producing only atactic polypropylene (aPP), because of the symmetric feature of their active centers.

N. Ishihara, M. Kuramoto and M. Voi [24] found that a mixture of titanium compounds such as  $\text{TiCl}_4$ ,  $\text{Ti}(\text{OEt})_4$  or  $(\eta\text{-C}_5\text{H}_5)\text{TiCl}_3$  with methylaluminoxane catalyzed the polymerization of styrene, even above room temperature, to the pure syndiotactic polystyrene (sPS), which had a narrow molecular weight distribution ( $\text{MWD} = \text{Mw}/\text{Mn} = 2$ ). Pure syndiotactic polymers were also obtained with ring-substituted styrenes. Monomer reactivity was enhanced by electron-releasing substituents on the aromatic ring.

$(\eta^5\text{-Tetramethylcyclopentadienyl})\text{-}$ ,  $(\eta^5\text{-tetraphenylcyclopentadienyl})\text{-}$ ,  $(\eta^5\text{-}(diphenylphosphino)\text{ tetramethylcyclopentadienyl})\text{-}$  and  $(\eta^5\text{-}(trimethylsilyl)\text{ tetramethylcyclopentadienyl})\text{ titanium triisopropoxide}$  have been synthesized and characterized by A. Kucht and H. Kucht et al. [25]. Their catalytic activities for syndiotactic styrene polymerization have been compared with the reference compound  $(\eta^5\text{-cyclopentadienyl})\text{ titanium triisopropoxide}$ ,  $(\eta^5\text{-tetramethylcyclopentadienyl})\text{ titanium triisopropoxide}$  was the best catalyst precursor, giving rise to catalysts having the highest activity to produce polystyrene with the highest syndiotactic yield and molecular weight (MW).

T. E. Ready, J. C. W. Chein and M. D. Rausch [26] discovered that a variety of 1- and 3-substituted alkylindenes ( $\text{R} = \text{H}, \text{Me}, \text{Et}, \text{tert-butyl}$  and  $\text{Me}_3\text{Si}$ ) as well as 2-methylindene have been prepared in good yields. The substituted indenenes were converted into trimethylsilyl derivatives via reactions of intermediate organolithium complexes with chlorotrimethylsilane. The corresponding titanium complexes,  $(\text{R-Ind})\text{TiCl}_3$ , were synthesized in excellent yield from reactions of the trimethylsilyl derivatives with  $\text{TiCl}_4$ . The titanium complexes were evaluated as styrene polymerization catalysts in toluene solution when activated by methylaluminoxane.

Activities increased in the order: Cp < H<sub>4</sub>Ind < Ind < 1-(Me)Ind < 2-(Me)Ind. A steep drop in activity was observed when R = Et, tert-buthyl and Me<sub>3</sub>Si, corresponding to an increase in the steric bulk of substituent in the catalyst precursor. 1-(Me<sub>3</sub>Si)IndTiCl<sub>3</sub> was found to be ineffective as a styrene polymerization catalyst. Syndiospecificities of the titanium complexes were generally very good (65-98 %).

W. Kaminsky, et al. [27] investigated fluorinated half-sandwich complexes catalysts in syndiospecific styrene polymerization. It was found that fluorinated half-sandwich complexes of titanium, such as cyclopentadienyltitanium trifluoride (CpTiF<sub>3</sub>), showed an increase in activity of up to a factor of 50 compared to chlorinated compounds. In a temperature range of 10-70 °C the methylaluminoxane could be reduced to an Al:Ti ratio of 300. If the cyclopentadienyl ligand in the metallocene is changed to a pentamethylcyclopentadienyl (Cp\*) ligand that is a stronger electron donor and exerts a greater sterically hindrance, the polymerization activity is lowered. But the pentamethylcyclopentadienyltitanium trifluoride (Cp\*TiF<sub>3</sub>) could be produced the polystyrene with highest melting point of 277 °C.

Qing Wu, Zhong Ye and Shangan Lin [28] investigated syndiotactic polymerization of styrene with cyclopentadienyltribenzyloxytitanium/methylaluminoxane catalyst. The reaction conditions e.g., [Ti], [MAO], [Styrene], temperature and the content of retained trimethylaluminum (TMA) in MAO effected on the catalytic activity, syndiotacticity and molecular weight of the polymer. With [MAO] = 0.17 mol/l, the catalyst exhibits higher activities. The catalytic activity increased with increase of [MAO] and reaches a maximum value at [MAO] of 0.5 mol/l. The molecular weight of the polymer decreased and the molecular weight distribution became narrow with increasing the [MAO]. The [MAO] was necessary for activating the titanocene molecules and scavenging of impurities. Additionally, the MAO acted as a chain transfer agent, so that the higher the [MAO] used, the lower is the molecular weight of the polystyrene produced. The catalytic activity was directly proportional to the monomer concentration.

A variety of methoxy-substituted (indenyl) trichlorotitanium complexes, ( $\eta^5$ -(2-methoxyethyl) cyclopentadienyl) trichlorotitanium, ( $\eta^5$ -1-(2-methoxyethyl) indenyl) trichlorotitanium and ( $\eta^5$ -1-(2-methoxyphenyl) indenyl) trichlorotitanium were synthesized by P. Foster, M. O. Raush and J. C. W. Chein [29]. These precursors were used to polymerize styrene, ethylene and propylene. The complexes, when activated with methylaluminoxane, show only low activity for  $\alpha$ -olefin polymerization. Since MAO was a polymeric species, when oxygen-aluminum coordination took place the amount of steric hindrance around the catalytic center is dramatically increased, which could inhibit monomer coordination. Furthermore, the oxygen-aluminum coordination could substantially decrease the ability of MAO to abstract an anionic ligand from titanium to form the cationic organotitanium active species.

Y. Kim, B. H. Koo and Y. Do [30] synthesized five substituted indenyl trichlorotitanium compounds with spectroscopic methods. Their catalytic behavior for the polymerization of styrene was studied in the presence of methylaluminoxane as a cocatalyst. Substituted indenyl ligands include 1,3-dimethyl, 1-methyl, 1-ethyl, 1-isopropyl and 1-(trimethylsilyl) indenyl groups. All five compounds gave extremely pure syndiotactic polystyrene and conversion rates of at least 95 %. The UV-visible

and  $^{47,49}\text{Ti}$  nuclear magnetic resonance (NMR) Spectra provided a consistent measure of the electron densities at the metal centers of five substituted indenyltrichlorotitanium compounds. The catalytic activity was enhanced by less bulky and better electron-releasing substituents of the indenyl ligand.

Cyclopentaphenanthrenetitanium trichloride and its 2-methyl and phenyl derivatives were synthesized by N. Schneider, M. H. Prosenc and H. H. Brintzinger [31]. The crystal structure of 2-methyl-substituted complex was determined by X-ray diffraction (XRD) analysis. In the presence of methylaluminoxane, these complexes give highly active catalysts for the syndiotactic polymerization of styrene. The 2-phenyl-substituted complex exceeded all previously described catalysts in its catalytic activity.

$(\eta^5\text{-trimethylsiloxytetramethylcyclopentadienyl})$  and  $(\eta^5\text{-2-trimethylsiloxyindenyl})$  trichlorotitanium have been synthesized and characterized by G. Tian, S. Xu, Y. Zhang, B. Wang and X. Zhou [32]. Their catalytic behavior for the polymerization of styrene was studied in the presence of methylaluminoxane as a cocatalyst. The cocatalyst MAO, as a Lewis-acid, might coordinate with oxygen atom of siloxy group. The coordination suppressed the resonance effect and enhances the inductive effect of the siloxy group. As a result, the compounds showed only low activity for styrene polymerization.

C. Schwecke and W. Kaminsky [35] synthesized benzyl cyclopentadienyl titaniumtrichloride ( $\text{BzCpTiCl}_3$ ) from benzyl bromide, cyclopentadienyllithium and titanium tetrachloride and used in combination with methylaluminoxane for the syndiospecific polymerization of styrene. Kinetic measurements of the polymerization were carried out at different temperatures. The polymerization with  $\text{BzCpTiCl}_3/\text{MAO}$  differs from the polymerization with cyclopentadienyltitanium trichloride ( $\text{CpTiCl}_3$ ) in its behaviour toward the Al/Ti ratio. In addition, high activities are observed at high Al/Ti ratios. By analyzing the polymerization runs and the physical properties of the polymers with differential scanning calorimetry (DSC),  $^{13}\text{C}$  NMR spectroscopy, wide-angle X-ray diffraction (WAXD) scattering measurements and gel permeation chromatography (GPC), they found that the phenyl ring coordinates to the titanium atom during polymerization. Other known substitutions of the cyclopentadienyl ring in principle influence the polymerization activity. The physical properties of the polymers produced by the catalysts already known are nearly identical.  $\text{BzCpTiCl}_3$  is the first catalyst that leads to polystyrene obviously different from the polystyrene produced by other highly active catalysts.

Y. Kim and Y. Do [36] prepared a new type of the half-metallocene catalysts for the syndiospecific polymerization of styrene by the reaction of various kinds of trialkanolamine with pentamethylcyclopentadienyltitanium trichloride ( $\text{Cp}^*\text{TiCl}_3$ ) in the presence of triethylamine. All seven compounds have a highly thermal stability and they show fairly good activities in the presence of cocatalyst modified methylaluminoxane (MMAO) in styrene polymerization. Especially, highly bulky and electronically deficient system affords syndiospecific polystyrene with very high molecular weight.

(<sup>t</sup>BuC<sub>5</sub>H<sub>4</sub>)TiCl<sub>2</sub>(O-2,6-<sup>i</sup>Pr<sub>2</sub>C<sub>6</sub>H<sub>3</sub>) exhibited relatively high catalytic activity for syndiospecific polymerization of styrene at 25 °C if both [PhMe<sub>2</sub>NH]B(C<sub>6</sub>F<sub>5</sub>)<sub>4</sub> and a mixture of Al<sup>t</sup>Bu<sub>3</sub>/Al(n-C<sub>8</sub>H<sub>17</sub>)<sub>3</sub> were used as the cocatalyst. Effects of both organoaluminum and organoboron compounds were explored and the effect of cocatalyst was different from that observed by K. Nomura and A. Fudo [37] in 1-hexene polymerization catalyzed by Cp\*TiCl<sub>2</sub>(O-2,6-<sup>i</sup>Pr<sub>2</sub>C<sub>6</sub>H<sub>3</sub>). Resulting syndiospecific polystyrene possessed narrow molecular weight distribution under the optimized conditions and M<sub>w</sub> values were unchanged during the time course.

R. Fan, K. Cao, B. Li, H. Fan and Bo-Geng Li [38] synthesized powdery syndiotactic polystyrene in a bulk process with the homogeneous metallocene catalyst system, pentamethylcyclopentadienyltitanium trichloride/methylaluminoxane/triisobutylaluminum (TIBA). The morphology of the nascent polymer particles were investigated and an interesting splaying morphology was observed when the conversion ranged from 0.9-1.7 %. The crystallinities of the as-polymerized polymer samples at different conversions were studied also. The experimental results suggested that manipulating the relative crystallizing rate to exceed the relative polymerizing rate in the initial stage of the polymerization is feasible to prepare the powdery product.

S. K. Noh, S. Kim, Y. Yang, W. S. Lyoo and Dong-Ho Lee [39] prepared as a new kind of dinuclear metallocene four doubly bridged dinuclear metallocene (DBDM) that hold two different bridging units linking two metallocenes and their polymerization properties have been pursued. The selected bridging ligands for DBDM were polymethylene and dialkoxy terminated to bond two cyclopentadienyls and two titanium centers, respectively. The most significant feature from this study is that the second bridging dialkoxy terminated ligands connecting two titanium centers likely exert more pronounced influence than the polymethylene bridges between two Cp groups on the activity of the catalyst as well as the stereochemistry of the generated polymers.

F. M. Rabagliati, M. A. Perez and R. Quijada [40] studied the polymerization of styrene using the combined system diphenylzinc-bis(n-butylcyclopentadienyl) titanium dichloride (Ph<sub>2</sub>Zn-(n-BuCp)<sub>2</sub>TiCl<sub>2</sub>)/methylaluminoxane in toluene at 60 °C, produced highly syndiotactic polystyrene, confirming that Ph<sub>2</sub>Zn-titanocene/MAO are good initiator systems for the stereoregular polymerization of styrene. The syndiotacticity of PS was established by its insolubility in chloroform, benzene or toluene and after continuous extraction in boiling butanone. DSC analysis showed endotherm signals corresponding to the melting temperature (T<sub>m</sub>) of syndiotactic polystyrene.

J. C. W. Chien, Z. Salajka and S. Dong [42] studied the active oxidation state of Ti in the cyclopentadienyltributoxytitanium (CpTi(OBu)<sub>3</sub>)/methylaluminoxane catalyst by electron paramagnetic resonance (EPR) and redox titration. The results, active species concentrations measured by radio labeling techniques, showed that all the catalytic species are trivalent Ti. The syndiospecific species (78 % Ti) is characterized by a sharp EPR resonance that corresponds to a titanium (III) hydride.

Prasit Pattanauwat, Siriprapa Pattanakit and Set Siriwat [161] studied the slurry of styrene with pentamethylcyclopentadienyltitanium trichloride in combine with boron compound and triisobutylaluminum to investigate the effect of catalyst concentration, Al/Ti mole ratio, polymerization temperature ( $T_p$ ) and polymerization time ( $t_p$ ). In addition, soxhlet extractor, Fourier transform infrared (FTIR), differential scanning calorimetry and nuclear magnetic resonance technique were used to measure the properties of polystyrene product.

Polymeric blends of melt processable polymers and liquid crystalline compounds (LCC) have been studied in many researches. The review covers liquid crystalline (LC) blends containing either low molecular weight liquid crystal or high molecular weight liquid crystal. The main reason of blending high molecular weight liquid crystalline compound, liquid crystal polymer (LCP), with other polymers is improved the mechanical properties of matrix polymer. Only few researchers have studied about low molecular weight liquid crystal blends for improving the melt viscosity of the blends.

A. Buckley, A. B. Conciatori and G. W. Calundann [33] investigate the blends of low molecular weight liquid crystalline compound with either polyolefin or polyester. The low molecular weight liquid crystalline compound used has molecular weight less than about 1,000 g/mol. The concentration of low molecular weight liquid crystalline used is present in an amount of from about 0.5-5 % by weight and the melt viscosity of the blend was determined by a capillary rheometer. The melt viscosity of low molecular weight liquid crystalline blends reduced by as much as 25-30 % compared with the pure matrix polymers.

A. Siegmann, A. Dagan and S. Kenig [34] prepared the polymer blends of liquid crystalline aromatic copolyester (based on 6-hydroxy-2-naphthanoic acid (HNA) and p-hydroxybenzoic acid) and an amorphous polyamide (PA) by melted mixing method. The rheological behavior of the blends was very different from pure component and viscosity of blends significantly changed. Only 5 % by weight of LCP in the blend could reduce the viscosity 20-25 times. The tensile mechanical behavior of the blends was very similar to that of polymeric matrix. The blend of two phase morphologies was found to be affected by the LCP compositions. The LCP phase changed gradually with increasing LCP content form ellipsoidal particles to rod-like and fibrillar structure

Y. C. Lin, H. W. Lee and H. H. Winter [41] studied the miscibility and viscoelastic properties of blends of a segmented block copolyester that had the average molecular weight 11,500 g/mol and poly (ethylene terephthalate), PET, that had the average molecular weight 50,000 g/mol. They found that addition of a small quantity of LCP has a dramatic effect on rheology. For example, an addition of 2 wt % LCP reduces the viscosity by about 60 %. This effect is most pronounced for PET of higher molar masses. The melt viscosity decreases exponentially with the LCP content in the range of composition where the blends are miscible. But there was no significant further reduction of viscosity when the LCP content exceeds 50 wt %. The addition of LCP also changes the distribution of the relaxation times of PET and broadens the zero shear viscosity regimes.

Anchana Chuenchaokit [43] studied the effects of thermotropic liquid crystals on properties of polycarbonates (PC). The low molecular weight liquid crystals were cyclohexylbiphenylcyclohexanes (CBC-33) groups that had average molecular weight about 400 g/mol. The blends were prepared by melt mixing at 0.25, 0.5 and 1 % by weight of liquid crystals. The shear viscosity of pure PC and their blends were investigated using a capillary rheometer and the glass transition temperatures ( $T_g$ ) were measured by differential scanning calorimetry. Experimental results showed that the viscosity of the blends with only small weight fraction (1 %) of low molecular weight liquid crystal is about 90 % lower than that of the pure polycarbonates.

Suraphan Powanusorn [16] prepared the blend of low molecular weight liquid crystal with nylon-6, polyethylene, polypropylene (PP), polycarbonate and polyacetal. The low molecular weight liquid crystals had average molecular weight about 400 g/mol. Melt mixing was the preparation method for blending liquid crystal and base polymers together at 0.1, 0.2 and 0.4 % by weight of liquid crystal. The rheological, thermal and mechanical properties of the blends are investigated in order to compare with the base polymer that absence of liquid crystal. The results show that liquid crystal may improve the processability of the base polymer by reducing the melt viscosity while the liquid crystal did not affect the thermal and mechanical properties of the base polymer. The melt viscosity of the blends is about 20 to 80 % lower than that of the base polymer depended on type of polymers at the some shear rate.

Noppawan Motong [44] studied effects of mixing and processing on the viscosity of polycarbonate blends with low molar mass thermotropic liquid crystals, cyclohexylbiphenylcyclohexane. Stirring melt mix was utilized in the first step blending of PC and CBC-33 with content at 0.1, 0.2, 0.4, 0.8 and 1.0 % by weight. Viscosity of the resulting blends were investigated and compared with the base PC. The result showed that 0.2 % by weight of CBC-33 is the suitable concentration because at higher concentration the effects of CBC-33 on the viscosity were less significant.

Light scattering of crystalline polymers and their morphologies have been studied in many researches. The reviews cover light scattering behavior and morphologies of polymers.

Richard S. Stein, A. Misra, T. Yuasa, and F. Khambatta [45] investigated the crystallization kinetics from quantitative measurements of scattered intensities. Because a quantitative comparison of scattered intensities with the predictions indicate the need for theoretical refinement. Quantitative measurements of the variations of scattered intensity with angle may be made with high resolution photometers or by using an optical multichannel analyzer. Such intensity data must be corrected for refraction at sample interfaces as well as for multiple scattering. They found that a quantitative comparison of the theoretically calculated intensity with the experimentally measured leads to two important differences (1) The theoretical intensity is zero at the scattering angle,  $\theta = 0^\circ$  and falls off quite rapidly with increasing  $\theta$  at angles greater than that of the maximum intensity, whereas the experimental intensity is finite at  $\theta = 0^\circ$  and is much greater than the theoretical prediction at large  $\theta$ . (2) The theory predicts that the  $H_v$  intensity should be zero at the azimuthal angle,  $\mu = 0^\circ$  and  $90^\circ$  whereas finite intensities are found experimentally. The differences are ascribed to external and internal disorder. By the

external disorder is associated with phenomena related to difference in the configuration of the spherulitic boundary that arise from incomplete spherulite development, spherulite truncation resulting from impingement and distribution of spherulite sizes. For the internal disorder arises from the volume filling spherulites are not spheres but are truncated and meet at boundaries. So they concluded that quantitative comparisons of measured scattered intensities of light scattering technique with theoretically calculated values are useful for providing information about the crystallization process.

J. Koberstein, T. P. Russell and R. S. Stein [46] studied about technique of Small-Angle Light Scattering (SALS) from spherulites within polymeric solids to compare with theoretical assumption for ideal structure of spherulites. They found that the ideal spherulites differ from their experimental observation in four respects (1) The theory predicts zero intensity at  $\theta = 0^\circ$ ,  $\theta$  is the scattering angle between the incident and scattered ray, while experimentally, finite zero-order scattering is found. (2) The scattering maximum is found to be broader and lower than predicted. (3) Greater intensity is found at large values of  $\theta$  than are predicted. (4) Theory predicts zero intensity at  $\mu = 0^\circ$  and  $90^\circ$ ,  $\mu$  is azimuthal angle, while finite intensity is found. These differences are believed to be due to the disorder of the orientation of optical axes within spherulites and irregular boundaries of spherulites arising from their mutual truncation. And they concluded that this is apparent since spherulite disorder represents a decrease in the degree of nonrandomness of fluctuations.

R. J. Tabar, A. Wasiak, S. D. Hong, T. Yuasa and R. S. Stein [47] studied the effect of the impingement and of growing spherulites on Hv small-angle light scattering patterns. Spherulitic crystallization from the melt usually yields a coherent sample made up of individual structures impinging on and linked to one another by lamellas common to two spherulites. Spherical symmetry is lost when two or more growing spherulites impinge on one another or when crystallization of two different crystal forms occur simultaneously. They found that the impingement produces a lowering of the intensity of the scattering maximum and the diminishing of the overall sharpness of the scattering peak. The extent of these effects increases with area fraction of spherulites. From the imperfect shape of the spherulites due to their impingement also produces the truncation effect. They found that while spherulites grow, the extent of truncation effect on the Hv light scattering pattern increase. Both of the impingement effect and the truncation effect are due to the increasing radii of the spherulites. The effect of truncation is to lower the intensity of the scattering maximum and increase the intensity at small and large angles.

M. Ree, T. Kyu and R. S. Stein [48] studied the melting and crystallization behavior of blends of linear low density polyethylene (LLDPE) with conventional low density polyethylene (LDPE) by using small-angle light scattering technique. They observed that the LLDPE, which is miscible with the LDPE component in the molten state, crystallizes first, forming volume filling spherulites. The LDPE then crystallizes within the performed spherulites. Furthermore the SALS intensity curve changes with composition of the blends that may be interpreted by considering the orientation of crystals within spherulites. It has been observed that the spherulites in the blend have more diffuse boundaries as the LDPE content increases. Moreover, they suggested that the SALS technique is very useful as a complement to DSC for determining



crystallization behavior, cocrystallization or separate crystallization, is this crystallizable blend system.

R. S. Stien, J. Cronauer and H. G. Zachmann [49] studied the crystallization of a single polymer component and polymer blends by using the small-angle light scattering technique. They found that this technique could be a convenient method for quantitatively following spherulitic crystallization. Moreover, it provides information about the number and sizes of spherulites as well as their internal crystallinity. From this technique, they observed that most polymers crystallize by a nucleation and growth mechanism in which spherulites develop as a consequence of the radial growth of branching crystalline lamellae from heterogeneous nuclei. The amorphous component is included within the spherulites. These grow until they imping and become volume filling. The primary crystallization occurs at the expanding interface of the spherulite with the amorphous polymer. Sometime the secondary crystallization may occur within the spherulite.

R. S. Stein and K. Jacob et al. [50] studied light scattering of the crystallization of polymers. They explained that the real time light scattering measurements during polymers crystallization could be interpreted in terms of the number, size and anisotropy of crystallizing species. Such observations have been used to show the lack of ordered regions in amorphous polymers. It is very sensitive for detecting the early stages of crystallization, while the crystals are too small at early stages to affect the angular dependence of scattering. They can appreciably contribute to its intensity, which depends upon their number and size. The subsequent changes in intensity and polarization can be fitted to parameters for a nucleation and growth model. Ultimately, when the dimensions of the growing species become sufficiently large, angularly dependent scattering results, which may be interpreted in terms of their size and state of aggregation. The technique of light scattering may be extended to the study of the crystallization of oriented polymers. It is rapid and may be used to follow the crystallization of films during their processing.

Joo Young Nam, Shigenobu Kadomatsu, Hiromu Saito and Takashi Inoue [51] investigated the change of the crystalline morphology with temperature and the thermal reversibility in linear low density polyethylene by Hv and Vv light scattering using CCD camera system in which the time resolved measurement is possible in millisecond order. They found that the morphological change with time after the temperature drop or jump was found to be very fast in several seconds. And the disordering in the heating process is caused by melting of thermally unstable thin lamellae existing between the thick lamellae, which are already developed at high crystallization temperature. So, the thermal reversibility is attribute to the thermally unstable thin lamellae because these thin lamellae are developed fast at wide temperature range in the cooling process and they melt fast in the heating process at narrow temperature range in which they are developed. Because of the crystalline morphology of LLDPE developed at high temperature cannot be frozen by quenching.

## CHAPTER III

### THEORY

Metallocene compounds are becoming an important class of catalyst for the synthesis of organic molecules and polymers. These complexes also have good potential to act as catalysts or catalyst precursors for a number of organic reactions. The discovery of group 4 metallocene/aluminoxane systems as catalysts for polymerization reactions has opened up a new frontier in the area of organometallic chemistry and polymer synthesis. Metallocene systems are comprised of (1) bicomponents consisting of a metallocene and an aluminoxane and (2) a single component such as  $[\text{Cp}_2\text{MR}]^+[\text{B}(\text{C}_6\text{F}_5)_4]^-$ . The polymerization of monoolefins by metallocene in comparison to conventional Ziegler-Natta systems offers a versatile possibility to polymer synthesis. The broader flexibility of electronic and steric variations in the cyclopentadienyl (Cp) type ligands allows greater maneuvering in the design of catalyst systems. Such modifications govern the polyinsertion reaction leading to regioregular and stereoregular polyolefins.

#### 3.1 Categories of Metallocene Catalyst Systems [52]

Homogeneous catalysts consisting of cyclopentadienyls of titanium with aluminum alkyls were found active for ethylene polymerization [18,53-54]. These systems were investigated to understand the mechanistic aspects of olefin polymerization, which were difficult to comprehend employing titanium tetrachloride based heterogeneous catalysts. A general feature of these homogeneous catalysts is their relatively low activity, viz.,  $1 \times 10^3$ - $4.2 \times 10^3$  g PE/(g Ti.hr.atm). However, the addition of small amounts of water was found to increase the activity of these catalyst systems significantly [55].

Metallocene catalyst systems require a large amount of methylaluminoxane (MAO) for achieving higher productivity. The high cost of the cocatalyst stimulated the search for new families of metallocenes, which can perform in the absence of aluminoxane. In recent years [56], this has led to the synthesis of a number of cationic metallocenes. Attention is now being paid to incorporate metallocene on inorganic supports such as  $\text{MgCl}_2$  and  $\text{SiO}_2$  to control the fluff morphology of the polymer and prevent reactor fouling [57].

##### 3.1.1 Metallocene

Metallocene are a class of compounds in which cyclopentadienyl or substituted cyclopentadienyl ligands are  $\pi$ -bonded to the metal atom. Various types of metallocenes have been synthesized and characterized by physicochemical methods [58-64]. The number of known complexes is so large that it restricts the inclusion of synthetic and characterization aspects of metallocenes in this review. Representative examples of each category of metallocenes are shown in Table 3.2. In recent years [65-78], a great deal of attention has been directed at the synthesis of new metallocenes including a variety of cationic types and metallocenes incorporated on inorganic supports such as  $\gamma$ -alumina,  $\text{MgCl}_2$  and silica [57,79-80].

TABLE 3.1  
Metallocene Catalyst Systems<sup>a</sup>

Catalyst	Cocatalyst	Remark
1. Chlorocyclopentadienyl derivative of titanium: e.g., Cp <sub>2</sub> TiCl <sub>2</sub>	Dialkylaluminum chloride	Active for ethylene but inactive for propylene polymerization
2. Metallocene catalyst systems containing alumoxane compounds		
2.1 Nonstereorigid metallocenes, e.g., Cp <sub>2</sub> MX <sub>2</sub>	Alumoxane	a) High activity for ethylene polymerization b) Active for propylene polymerization (atactic polymer)
2.2 Stereorigid metallocenes, e.g., Et(Ind) <sub>2</sub> MCl <sub>2</sub>	Alumoxane	Active for regio- and stereospecific polymerization of propylene
2.3 Supported metallocene catalysts, e.g., SiO <sub>2</sub> -Et(Ind) <sub>2</sub> MCl <sub>2</sub>	Alumoxane/alkylaluminum	Active for ethylene and propylene polymerization
3. Metallocene catalysts systems containing non alumoxane compounds		
3.1 Ionic metallocenes, e.g., [Cp <sub>2</sub> MR(L)] <sup>+</sup> [BPh <sub>4</sub> ] <sup>-</sup>		Active for ethylene and propylene polymerization

<sup>a</sup>M = Ti, Zr, Hf.

**TABLE 3.2**  
Representative Examples of Metallocenes

---

[A] Nonstereorigid metallocenes:
1) $\text{Cp}_2\text{MCl}_2$ (M = Ti, Zr, Hf)
2) $\text{Cp}_2\text{ZrR}_2$ (R = Me, Ph, $\text{CH}_2\text{Ph}$ , $\text{CH}_2\text{SiMe}_3$ )
3) $(\text{Ind})_2\text{ZrMe}_2$
[B] Nonstereorigid ring-substituted metallocenes:
1) $(\text{Me}_3\text{C}_5)_2\text{MCl}_2$ (M = Ti, Zr, Hf)
2) $(\text{Me}_3\text{SiCp})_2\text{ZrCl}_2$
[C] Stereorigid metallocenes:
1) $\text{Et}(\text{Ind})_2\text{ZrCl}_2$
2) $\text{Et}(\text{Ind})_2\text{ZrMe}_2$
3) $\text{Et}(\text{IndH}_4)_2\text{ZrCl}_2$
[D] Cationic metallocenes:
1) $\text{Cp}_2\text{MR}(\text{L})^+[\text{BPh}_4]^-$ (M = Ti, Zr)
2) $[\text{Et}(\text{Ind})_2\text{ZrMe}]^+[\text{B}(\text{C}_6\text{F}_5)_4]^-$
3) $[\text{Cp}_2\text{ZrMe}]^+[(\text{C}_2\text{B}_9\text{H}_{11})_2\text{M}]^-$ (M = Co)
[E] Supported metallocenes:
1) $\text{Al}_2\text{O}_3\text{-Et}[\text{IndH}_4]_2\text{ZrCl}_2$
2) $\text{MgCl}_2\text{-Cp}_2\text{ZrCl}_2$
3) $\text{SiO}_2\text{-Et}[\text{Ind}]_2\text{ZrCl}_2$

---

### 3.1.2 Aluminoxane

Aluminoxane are synthesized by controlled hydrolysis aluminum alkyls [81-89]. Simple synthetic routes to methylaluminoxanes are not available due to the high reactivity of trimethylaluminum (TMA) with water. Many inorganic hydrated compounds are used as a source of water for preparing aluminoxane from alkylaluminum [90-96]. Hydrating compounds such as  $\text{CuSO}_4 \cdot 5\text{H}_2\text{O}$  and  $\text{Al}_2(\text{SO}_4)_3 \cdot 6\text{H}_2\text{O}$  are employed. Various physicochemical data, such as compositional analysis, molecular weight (MW) determination, mass spectra, X-ray powder Diffraction (XRD), Infrared (IR) and Nuclear Magnetic Resonance (NMR) spectroscopy, are used for the characterization of aluminoxanes [97-102]. In spite of these measurements, the structures of the alkylaluminoxanes are not unambiguously known. Methylaluminoxane is considered to be the oligomeric (cyclic or linear, Figure 3.1) mixture of  $-\text{AlMeO}-$  units [102] containing possibly cluster like or supramolecular aggregates [94,99-100]. In metallocene based catalyst systems, the aluminoxanes appear to have a combination (depending on the nature of the catalyst and the polymerization conditions) of the following functions:

(1) Aluminoxane alkylates the metallocene compound and scavengers the impurity [103].

(2) Aluminoxane interacts with metallocene generate cationic metallocene alkyl species.

The aluminoxane not only produces the cations but also stabilizes them [104-107]. This review has been gaining support due to isolation of the cationic species [108-115]. Resconi et al. [100] proposed that trimethylaluminum is the actual cocatalyst in  $\text{Cp}_2\text{ZrR}_2/\text{MAO}/\text{Me}_3\text{Al}$  systems, while MAO acts as a soluble carrier activator of the ion pair formed upon reaction of the metallocene with trimethylaluminum.

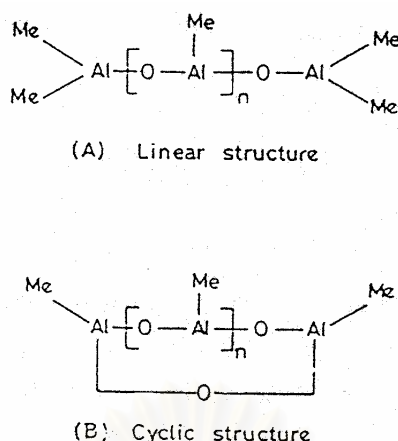


**Figure 3.1** Plausible structure of methylaluminoxane [52]

### 3.2 Cocatalysts and Modifiers

The key factor for the high activity for the metallocene catalyst systems is the cocatalyst methylaluminoxane whose involvement is crucial in the formation of the metallocene active species. Polymerization kinetic profile, stereospecificity and comonomer incorporation as well as the resulting polyolefins molecular weight characteristics are affected not only by the amount of MAO used, but also by the metallocene/MAO ratios. A strong effect on the polymerization kinetic profile was demonstrated for the following:  $\text{Cp}_2\text{ZrCl}_2/\text{MAO}$ ,  $\text{Cp}_2\text{TiEnCl}/\text{AlEtCl}_2$  [116] and  $\text{Cp}_2\text{TiEnCl}/\text{AlMe}(\text{BHT})_2$  [117-118]. Trimethylaluminum, an alkylating agent that is also a scavenger, used with these catalysts.

Zirconocenes in the presence of TMA show limited polymerization activity [116,119], whereas methylaluminoxane increases [120] the activity by a factor of  $10^5$ . Indeed, the influence of different aluminoxane cocatalyst type on the activity of  $\text{Cp}_2\text{ZrMe}_2$  and  $\text{Cp}_2\text{ZrCl}_2$  catalysts is in the following order [121]:

methylaluminoxane > triisobutylaluminoxane (IBAO) > ethylaluminoxane (EAO)

The value of the cocatalyst (MAO)/catalyst ratio is important. An unusually high value of  $5 \times 10^4$  to 1 has been used to achieve high activity in homogeneous catalysis regardless of the  $\pi$ -ligand type. Polymer properties such as molecular weight distribution (MWD) and density are influenced by this ratio for the following metallocene [122-126]:  $\text{CpZrCl}_3$ ,  $\text{Cp}_2\text{ZrCl}_2$ ,  $\text{Cp}_2\text{ZrMe}_2$  and  $(n\text{-MeCp})_2\text{ZrCl}_2$ .

For propylene polymerization, the activity appears to be an increasing function of the  $[\text{Al}]:[\text{Zr}]$  molar ratios up to a point, for  $\text{rac-En}(\text{Ind})_2\text{ZrCl}_2/\text{MAO}$ ,  $\text{rac-En}(4,5,6,7\text{-IndH}_4)_2\text{ZrCl}_2/\text{MAO}$  [127-128] and  $(n\text{-MeCp})_2\text{ZrCl}_2/\text{MAO}$  [124]. Very high  $[\text{Al}]:[\text{Zr}]$  molar ratios are also needed for ethylene polymerization for prochiral  $i\text{-Pr}(\text{Flu})(\text{Cp})\text{ZrCl}_2$  and chiral  $\text{Me}_2\text{Si}(\text{Ind})_2\text{ZrCl}_2$  [129]. In contrast, a lower cocatalyst/catalyst ratio enhances the activity of the monocyclopentadienyl metallocene, namely  $\text{Me}_2\text{Si}(\text{Me}_4\text{Cp})(t\text{-Bu-N})\text{ZrCl}_2$  in ethylene polymerization [130]. The dependence of the catalytic activity on the  $[\text{Al}]:[\text{Zr}]$  ratio has been attributed to the rapid association-dissociation equilibria of MAO involving acid-base and/or electron deficient bridge complexation.

The use of solid reaction product of  $(\text{Me}_5\text{Cp})_2\text{ZrCl}_2$ ,  $(\text{Me}_5\text{Cp})_2\text{ZrMe}_2$  or  $(n\text{-BuCp})_2\text{ZrCl}_2$ , in excess methylaluminumoxane facilitates the reduction of the high cocatalyst/catalyst ratio [131-132]. It was shown that the use of TMA in combination with MAO was effective aside from the fact that replacement of MAO with a substantial amount of TMA minimizes the potential hazards of MAO synthesis. However, the molar ratio of TMA:MAO becomes an additional parameter whose value influences the catalyst activity, polymerization kinetic profile and polyethylene properties, depending on the  $\pi$ -carbocyclic and  $\sigma$ -hydrocarbyl ligands [125] or the level of dilution of TMA with its sterically hindered aryloxy derivative [118]. Similar studies were carried out using chloride-free  $\text{Cp}_2\text{ZrHex}_2$  and  $\text{Ind}_2\text{ZrMe}_2$  systems differing results [133].

Preactivation of metallocene precursor with the methylaluminumoxane also affects catalyst activity and comonomer incorporation, as well as polyolefins microstructures as demonstrated, in propylene homopolymerization and copolymerization (ethylene/propylene or  $\alpha$ -olefin/propylene).

### 3.2.1 Lewis Acids

Lewis acids, in combination with an alkylating agent or a scavenger such as TMA, could be effectively used as cocatalysts with the metallocene catalysts for olefin homopolymerization and copolymerization. The Lewis acids that have been used include  $\text{Me}_2\text{AlF}$  [134],  $[\text{B}(\text{C}_6\text{H}_5)_4]^-$  [135],  $[\text{B}(\text{C}_6\text{F}_5)_3]$  [136],  $[\text{C}_2\text{B}_9\text{H}_{12}]^{2-}$  [137],  $[\text{Ph}_3\text{C}][\text{B}(\text{C}_6\text{F}_5)_4]$  [138-139],  $[\text{R}_2\text{R}'\text{NH}][\text{B}(\text{C}_6\text{H}_5)_4]$  [140] and  $[\text{Ph}_3\text{C}][\text{B}(\text{C}_6\text{F}_4(\text{SiR}_3))]$  [141]. To polymerize ethylene, Lewis acid such as N,N-dimethylanilinium tetrakis(pentafluorophenyl)borate (AFPB) and tris(pentafluorophenyl)boron were used separately or mixed with trimethylaluminum as cocatalyst plus monocyclopentadienyl derivatives and homoleptic hydrocarbyls of titanium and zirconium [142-143]. With AFPB, the catalytic activity was comparable to that shown with MAO, even at low dosage. Likewise, a mixture of varying proportions of trimethylaluminum and  $\text{Me}_2\text{AlF}$  has been used to polymerize olefin without MAO [144].

Ethylene could also be polymerized [145-146] in toluene using  $\text{Cp}^*\text{ZrMe}_2$  reacted with tributylammonium salts of para-substituted tetraarylborates,  $([\text{BuN}_3\text{H}][\text{B}(\text{C}_6\text{H}_4\text{R})_4])$ , where  $\text{R} = \text{H}, \text{Me}, \text{and Et}$ . This is an ionic, base-free zirconocene catalyst that uses neither the pyrophoric alkyl aluminum nor an excess amount of MAO. Generally, noncoordinating anions, such as fluorinated boron together with metallocenes, form ion pairs, which are not stable [147-148] at polymerization temperature above 60 °C. Strong Lewis acid additives [139,149-150] such as  $[\text{Ph}_3\text{C}][\text{B}(\text{C}_6\text{F}_5)_4]$  and  $[\text{B}(\text{C}_6\text{F}_5)_3]$  could be used alkyl aluminum cocatalysts and  $(\text{MeCp})\text{TiCl}_3$  catalyst to polymerize propylene or for ethylene/propylene copolymerization. The resulting polypropylene (PP) is atactic and the copolymer is random having a structure similar to that produced with homogeneous vanadium catalyst system.

### 3.2.2 Miscellaneous Additives

For polymerization and ethylene/1-hexene copolymerization, tetramethyl silicate and silane additives enabled [151] the formation of polyethylenes (PE) with low melt flow rate over a sufficiently high temperature range with a variety of metallocene catalyst systems, namely,  $\text{Cp}_2\text{ZrCl}_2/\text{MAO}$ ,  $\text{Cp}_2\text{ZrMeCl}/\text{MAO}$  and  $\text{Ind}_2\text{ZrCl}_2/\text{MAO}$ . The polymerization could take place at a temperature higher than the melting point of the product, making it possible for a direct introduction of the as polymerized molten polymer into the extruder for palletizing. The solid reaction product of butyl octyl magnesium and silicon or tin tetrachloride was also effective [152-153]. The use of trimethyl boroxine, a scavenger for chain transfer agent, with  $\text{Cp}_2\text{ZrCl}_2$ , prior to the addition of MAO, increased the polypropylene productivity significantly. The effect was different for  $\text{rac-En}(4,5,6,7\text{-IndH}_4)_2\text{ZrCl}_2$  or  $\text{rac-En}(\text{Ind})_2\text{ZrCl}_2$  where the productivity benefit is possible only if the catalyst is pretreated with boroxine [154].

The magnitude of cocatalyst (MAO)/catalyst ratio, as well as the content of the Lewis acid catalyst modifiers, influences the catalyst activity, polymerization kinetic profile and polypropylene microstructure for the  $\text{C}_2$ -symmetric [119,127]  $\text{rac-En}(\text{Ind})_2\text{ZrCl}_2$  and  $\text{rac-En}(\text{IndH}_4)_2\text{ZrCl}_2$  as observed before for the  $\text{C}_{2v}$ -symmetric metallocenes [123-125].

### 3.3 Polystyrene (PS) [169]

Polystyrene is an inexpensive and hard plastic, probably only polyethylene is more common in your everyday life. The outside housing of the computer you are using now is probably made of polystyrene. Model cars and airplanes are made from polystyrene, it also is made in the form of foam packaging and insulation (Styrofoam™ is one brand of polystyrene foam). Clear plastic drinking cups are made of polystyrene. So are a lot of the molded parts on the inside of your car, like the radio knobs. Polystyrene is also used in toys and the housings of things like hairdryers, computers and kitchen appliances.

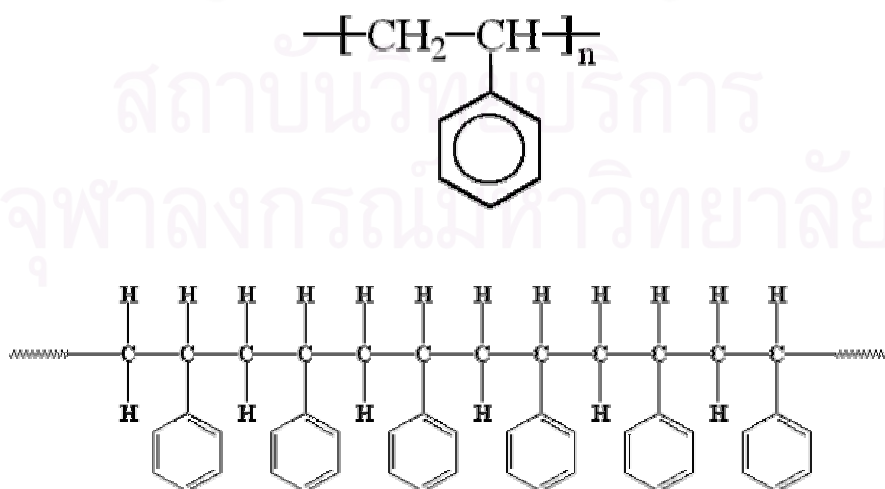
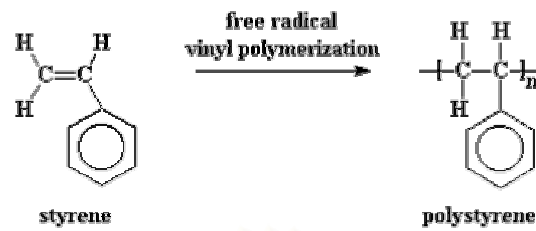


Figure 3.2 Structure of polystyrene

Polystyrene is a vinyl polymer. Structurally, it is a long hydrocarbon chain, with a phenyl group attached to every other carbon atom. Polystyrene is produced by free radical vinyl polymerization, from the monomer styrene.



**Figure 3.3** Free radical polymerization

Polystyrene is also a component of a type of hard rubber called poly (styrene-butadiene-styrene), SBS rubber. It is a thermoplastic elastomer. If take some styrene monomer and polymerize it free radically, but put some polybutadiene rubber in the mix. Polybutadiene has double bonds in it that can polymerize, end up with the polybutadiene copolymerizing with the styrene monomer, to get a type of copolymer called a graft copolymer. This is a polymer with polymer chains growing out of it and which is a different kind of polymer than the backbone chain. In this case, it's a polystyrene chain with chains of polybutadiene growing out of it.

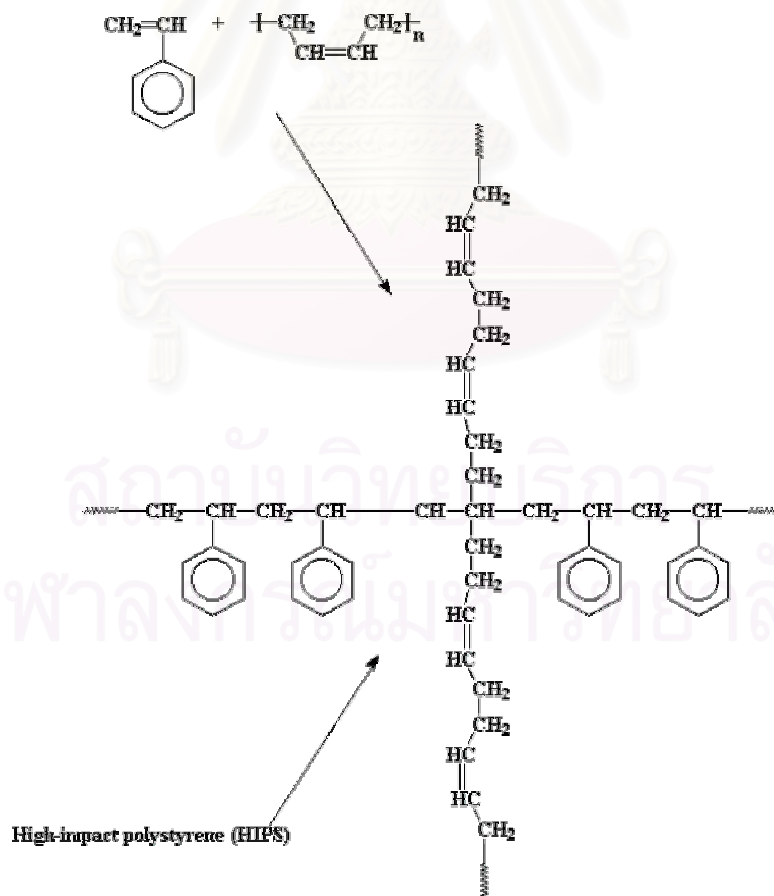


**Figure 3.4** Structure of high-impact polystyrene



These rubbery chains hanging off of the backbone chain do some good things for polystyrene. Polybutadiene and polystyrene homopolymers don't mix, so the polybutadiene branches try as best they can to phase separate and form little globs. But these little globs are always going to be tied to the polystyrene phase. So they have an effect on that polystyrene. They act to absorb energy when the polymer gets hit with something. They give the polymer a resilience that normal polystyrene doesn't have. This makes it stronger, not as brittle and capable of taking harder impacts without breaking than regular polystyrene. This material is called high-impact polystyrene (HIPS) for short.

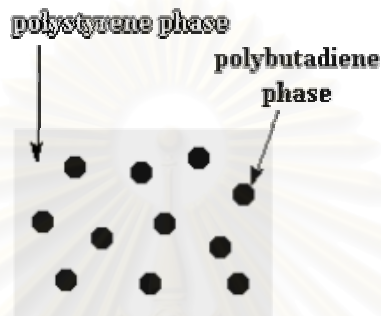


**Figure 3.5** Phase separate of polybutadiene and polystyrene homopolymer

Not all the chains in HIPS are branched like this. There are lot chains of plain polystyrene and plain polybutadiene mixed in there, too. This makes HIPS something and immiscible blend of polystyrene and polybutadiene. But it is the grafted polystyrene-polybutadiene molecules that make the whole system work by binding the two phases (the polystyrene phase and the polybutadiene phase) together. HIPS can be blended with a polymer called poly (phenylene oxide), PPO.

### 3.4 The Polystyrene of the Further

There's a new kind of polystyrene out there, called syndiotactic polystyrene (sPS). It's different because the phenyl groups on the polymer chain are attached to alternating sides of the polymer backbone chain. Normal or atactic polystyrene (aPS) has no order with regard to the side of the chain on which the phenyl groups are attached.

The new syndiotactic polystyrene alongside the old atactic polystyrene in 3-D, sPS has a regular structure, so it can pack into crystal structures. The irregular atactic polystyrene can't.

Syndiotactic polystyrene is a semicrystalline polymer synthesized from styrene monomer using a single-site catalyst, such as metallocene. First synthesized in 1985 by Idemitsu Kosan Co. Ltd. (Tokyo, Japan), the material has been under joint product and process development by Idemitsu and Dow Plastics (Midland, MI) since 1988. Because of its semicrystalline nature, SPS products exhibit performance attributes that are significantly different from those of amorphous styrenic materials. These properties include a high melting point (270 °C), good chemical and moisture resistance and a high degree of dimensional stability, but it's a lot more expensive.

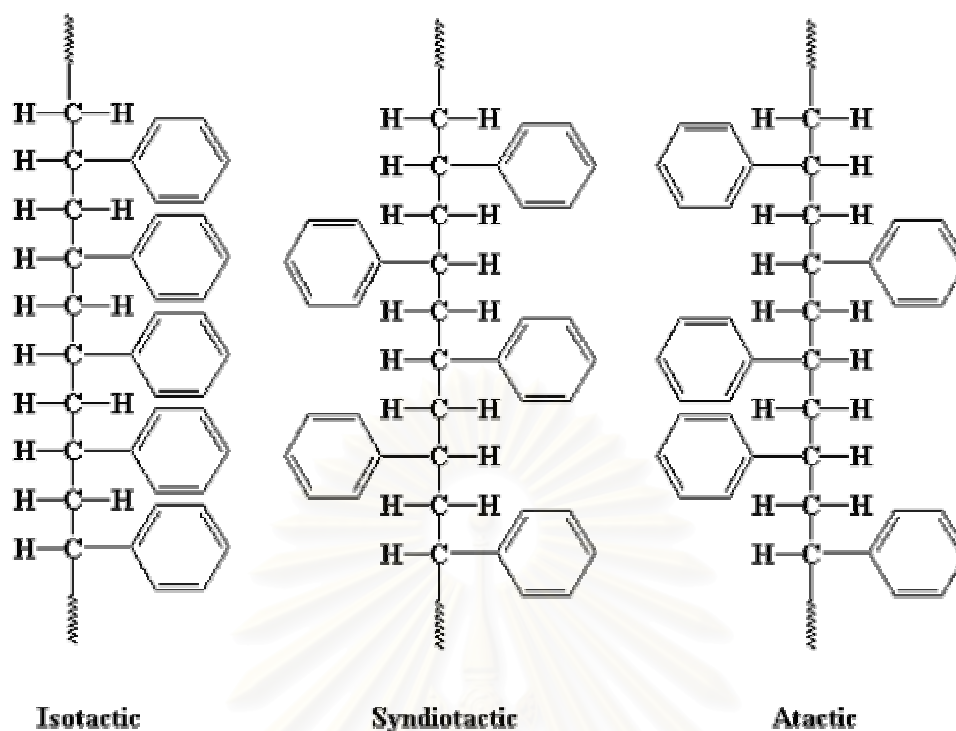


**Figure 3.6** Tacticity of polystyrene

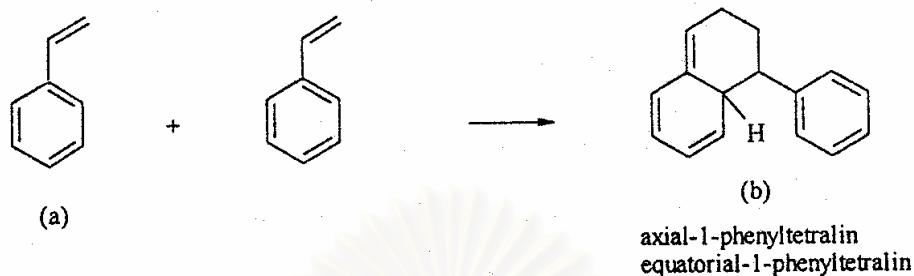
Syndiotactic polystyrene can be differentiated from conventional styrenic polymers on the basis of molecular structure. Atactic or general-purpose, polystyrene is produced with random stereochemistry, resulting in nonspecific placement of the cyclic aromatic portion of the molecule. In contrast, isotactic and syndiotactic polystyrene are made using stereo-specific catalysis techniques that result in highly ordered molecular structures. As SPS cools from the melt, molecules organize and form distinct regions of crystallinity. The rate at which crystallinity develops in SPS can be controlled through the use of comonomers or the addition of nucleating agents.

### 3.5 Styrene Polymerization [155]

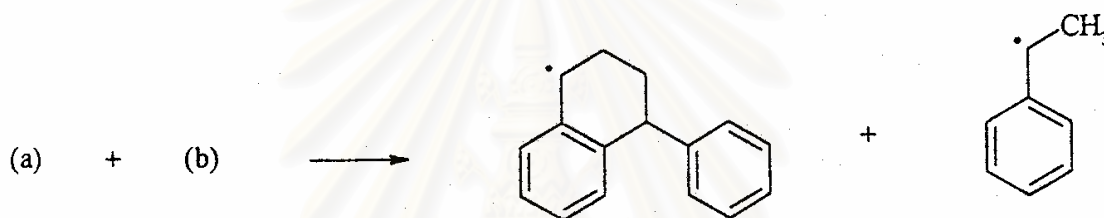
Styrene is slightly polar compared to ethylene and  $\alpha$ -olefins. The lack of a strongly polar functional group allow styrene to undergo highly isospecific polymerization (> 95-98 %) with many of heterogeneous Ziegler-Natta initiators effective for  $\alpha$ -olefins (by Soga et al. in 1988, Pasquon et al. in 1989 and Longo et al. in 1990). Highly syndiotactic polystyrene is obtained using soluble Ziegler-Natta initiators, such as tetrabenzyltitanium, tetrabenzylzirconium and tetraethoxytitanium or cyclopentadienyltitanium trichloride ( $\text{CpTiCl}_3$ ) with methylaluminoxane (by Pellecchia et al. in 1987, Ishihara et al. in 1988 and Zambelli et al. in 1989). Further, there are recent reports of highly syndiospecific polymerization of styrene with heterogeneous initiators based on tetra-*n*-butoxytitanium and methylaluminoxane supported on silica or magnesium hydroxide (by Soga and Monoi in 1990 and Soga and Nakatani in 1990). Styrene can also be homogeneous polymerized. The C-C double bond of styrene can act either as electron-donating or as electron-withdrawing center. Therefore, not only radicals can polymerize styrene but also anionically or cationically or by Ziegler-Natta initiators.

### 3.5.1 Radical Polymerization

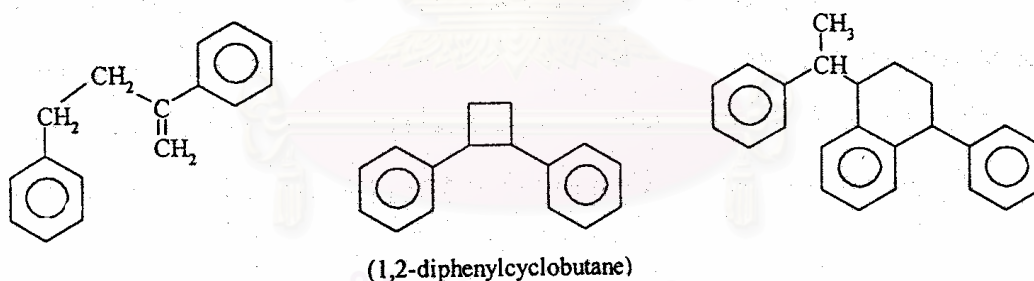
Styrene can be polymerized without a chemical initiator simply by heating. The first step is a Diels-Alder reaction:



Only the axial isomer can react with a further styrene atom, yielding two radicals, which can start a radical polymerization:



Some of the possible dimers and trimers have been identified:



Initiators: The list of initiators available for radical polymerization of styrene is very long. An interesting development is the application of initiators like:

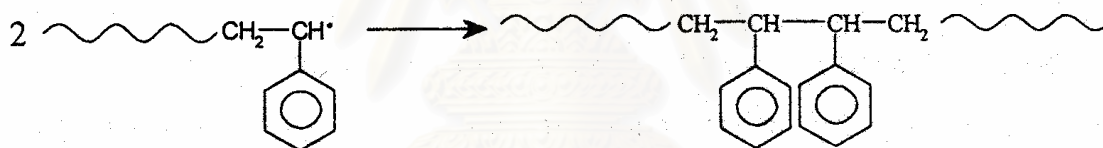


Which decompose to form four radicals. It is even more interesting to have a different half-life for both peroxide groups. These present novel opportunities for changing the molecular weight and its distribution.

**Inhibitors:** During shipping and storage styrene needs an inhibitor. The most efficient inhibitors-quinines, hindered phenols and amines-require traces of oxygen to function. *t*-Butyl-catechol at 15 to 50 ppm is the most common inhibitor for commercial styrene. It is also possible to use nitro phenol, hydroxylamine and nitrogen oxide compounds. To avoid an induction period, the inhibitors have to be removed before polymerization. Traces of metal such as iron or copper and sulfur compounds are the cause of retardation effects.

**Chain transfer:** In styrene polymerization the chain transfer agent can be the solvent, monomer, initiator, polymer or an added chemical agent. As  $C_{tr} = k_p/k_{tr}$  increases, the chain transfer agent becomes more effective. The most important property affected by chain transfer is the molecular weight of the polymer. The transfer to monomer has a value of  $10^{-5}$  which can be neglected. However, since the transfer constant to the Diels-Alder dimer equatorial 1-phenyltetralin is about 118 at 80 °C, this may cause experimental error. Any transfer to polymer would lead to branched structures in the final product. Although this reaction has been investigated to some extent, there is no conclusive evidence that it is an important reaction. The most important aspect of chain transfer is the control of molecular weight by the adequate use of added transfer agent. Mercaptanes are by far the most widely used chemicals for this purpose.

**Termination:** The free radical polymerization of styrene is terminated almost exclusively by the combination of two growing chain.



Termination is diffusion controlled at all temperature below 150 °C. Increasing viscosity leads to a reduction in the termination rate. However, the resulting Trommsdorff effect is comparably small for polystyrene.

**Processing:** Free radical polystyrene can be synthesized either by bulk, solution, suspension or emulsion techniques.

The bulk process needs pure styrene, it is very simple and yields polymer with high clarity. Due to its poor control, this process is not used commercially. In solution polymerization styrene is diluted with solvent, which makes temperature control easier. However, solvents normally reduce the molecular weight and polymerization rate. Both processes can be carried out either in batch or continuously. The advantages are more uniform products and low volatile levels. The main disadvantage is the transportation of highly viscous finished product.

Suspension polymerization is still an important mode of polystyrene production, although it has lost ground to continuous solution polymerization. The polymerization system contains monomer suspended in water, stabilizing agents and initiators to speed polymerization. The easy heat and removal of the finished polymer count as advantages. Contamination with stabilizing agents is considered a disadvantage.

Emulsion polymerization requires water as a carrier with emulsifying agents. It yields extremely small particles. Advantages are rapid reactions and excellent heat control. Disadvantages are the contamination of polymer with the emulsifier, water, its deficit in clarity and the limitation to batch processing. However, this type of processing is important for ABS polymers.

### 3.5.2 Anionic Polymerization

The phenyl group of styrene is able to act as an electron-donating or an electron-withdrawing center. This situation allows the growing end of the polymer to be either a carbenium ion or a carbanion. It also makes it possible to polymerize styrene by Ziegler-Natta catalysts.

**Initiation:** A highly purified monomer is reacted with a storage base. Although several initiators are known, organolithium compounds are the most studied and probably the best understood initiators.

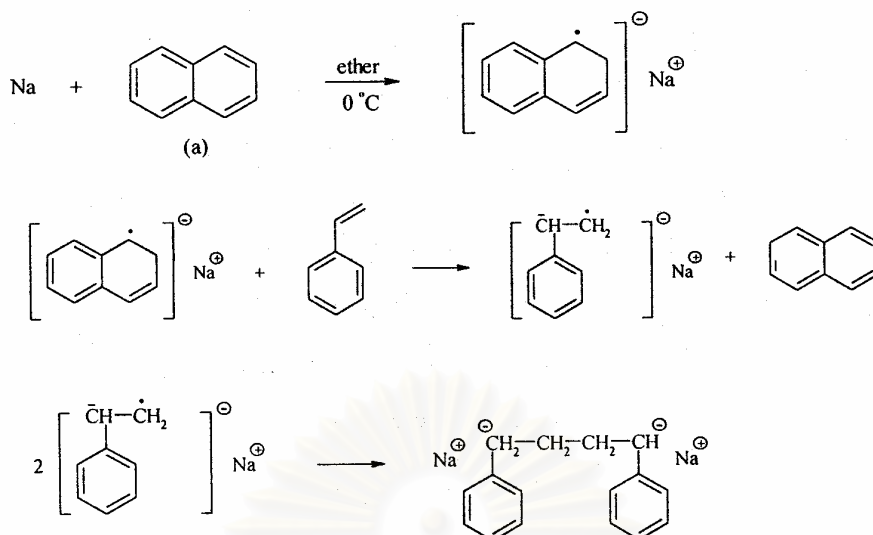


**Propagation:** The anionic chain end then propagates the chain by adding another monomer molecule.

The ideal polymerization of this type obeys the following equation:

$$R_p = k_p[C^*][M]$$

Where  $C^*$  represents the molar concentration of active chain ends. The rate constant is strongly affected by the solvent. In addition to solvent, the counterion affects the rate of polymerization. The effect of the counterions is often explained on the basis of their sizes. For the growing end of poly(styryllithium), an association of two growing chains has been discussed. This complex dissociates if polar solvents such as THF and ethyl ether are added, resulting in an increase in the polymerization rate. Instead of using a monofunctional initiator, it is possible to use a bifunctional anionic initiator. One of the best described systems involves the reaction between metal and naphthalene, forming a radical anion that transfers this character to the monomer, the two radical anions combine quickly to form a dianion.



### 3.5.3 Cationic Polymerization

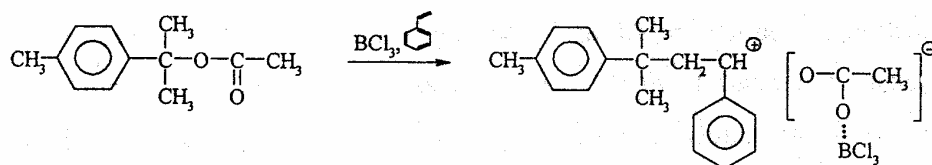
The commercial use of cationic polymerization of styrene is practically nonexistent at this time because of low temperature needed, uncontrollable molecular weight and residual acidic initiator. However, since numerous basic papers are published on this topic it is discussed here briefly. The initiators of a cationic polymerization of styrene can be carried out in the presence of strong acids like: protonic acids like perchloric, hydrochloric or sulfuric acid or Lewis acids. Additionally, alumina, silica and molecular sieves were used to initiate cationic polymerization.

Cationic polymerization of styrene in the presence of salts such as  $(n\text{-Bu})_4\text{N}^+\text{ClO}_4^-$  has been shown to accelerate the polymerization rate compared to the rate for salt-free polymerization. This result is explained on the basis of the following reaction:

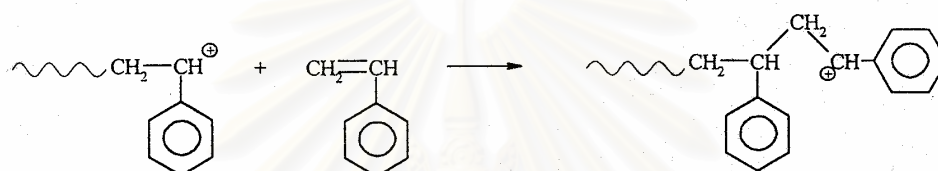


Interesting effects were observed if cationic polymerization was carried out under electric field. Depending on the solvent, the degree of ion separation is decreased under the influence of the electrical field. However, if toluene is applied, the effect is small due to the low  $\epsilon$  value of the solvent. In the range of intermediate values of  $\epsilon$  (dichloroethane) the highest changes in the rate are observed. In nitrobenzene, a solvent with high  $\epsilon$  values, the ion separation is almost complete. Therefore, application of an external field does not affect the free ion concentration and the rate.

Normally, molecular weight is difficult to control in cationic polymerization of styrene. This is not only because of transfer to polymer and solvent but also of transfer to monomer. Friedal-Crafts reactions during growth with aromatic solvents significantly decrease the molecular weight.



Addition of further monomer results in an increase in molecular weight. The danger of termination by indane formation seems to be reduced by adding the monomer in small portions.



### 3.5.4 Coordination Polymerization

Styrene can be polymerized to stereoregular by coordination catalysts. Highly isotactic polystyrene (iPS) is prepared using catalysts obtained from the reaction between  $\text{TiCl}_4/\text{AlEt}_3$  and  $\text{TiCl}_3/\text{Al}(\text{i-Bu})_3$  mixture. Optimal conditions for isotactic structures are 0 to 10 °C, with aging for at least 10 min but no longer than 30 min. Furthermore, the Al/Ti ratio has to be 3:1 for the formation of isotactic polystyrene. A mixture of methylaluminoxane and tetrabenzyltitanium was used as catalyst.

## 3.6 Polymer Morphology

Generally, there are two morphologies of polymers, amorphous and crystalline. The former is a physical state characterized by almost complete lack of order among the molecules. The crystalline refers to the situation where polymer molecules are oriented or aligned. Because polymers for all practical purposes never achieve 100 % crystallinity, it is more practical to categorize their morphologies as amorphous and semicrystalline.

### 3.6.1 The Amorphous State

Some polymers do not crystallize at all. Therefore they remain in an amorphous state throughout the solidification. The amorphous state is characteristic of those polymers in the solid state that, for reasons of structure, exhibit no tendency toward crystallinity. In the amorphous state, the polymer resembles as a glass. We can imagine the amorphous state of polymers like a bowl of cooked spaghetti. The major difference between the solid and liquid amorphous states is that with the former, molecular motion is restricted to very short-range vibrations and rotations, whereas in the molten state there is considerable segmental motion or conformational freedom arising from rotation about chemical bonds. The molten state has been likened on a

molecular scale to a can of worms, all intertwined and wriggling about, except that the average worm would be extremely long relative to its cross-sectional area. When an amorphous polymer achieves a certain degree of rotational freedom, it can be deformed. If there is sufficient freedom, the polymer flows then the molecules begin to move past one another. At low temperatures amorphous polymers are glassy, hard and brittle. As the temperature is raised, they go through the glass-rubber transition characterized by the glass transition temperature ( $T_g$ ).

### 3.6.2 Glass Transition Temperature

One of the most important characteristics of the amorphous state is the behavior of a polymer during its transition from solid to liquid. If an amorphous glass is heated, the kinetic energy of the molecules increases. Motion is still restricted, however, to short-range vibrations and rotations so long as the polymer retains its glasslike structure. As temperature is increased further, there comes a point where a decided change takes place, the polymer loses its glasslike properties and assumes those more commonly identified with a rubber. The temperature at which this takes place is called the glass transition temperature. If heating is continued, the polymer will eventually lose its elastomeric properties and melt to a flowable liquid. The glass transition temperature is defined as the temperature at which the polymer softens because of the onset of long-range coordinated molecular motion. The amorphous parts of semicrystalline polymers also experience glass transition at a certain  $T_g$ .

The importance of the glass transition temperature cannot be overemphasized. It is one of the fundamental characteristics as it relates to polymer properties and processing. The transition is accompanied by more long-range molecular motion, greater rotational freedom and consequently more segmental motion of the chains. It is estimated that between 20 and 50 chain atoms are involved in this segmental movement at the  $T_g$ . Clearly for this increased motion to take place, the space between the atoms (the free volume) must increase, which gives rise to an increase in the specific volume. The temperature at which this change in specific volume takes place, usually observed by dilatometry (volume measurement), may be used as a measure of  $T_g$ . Other changes of a macroscopic nature occur at the glass transition. There is an enthalpy change, which may be measured by calorimetry. The modulus or stiffness, decreases appreciably, the decrease readily detected by mechanical measurements. Refractive index and thermal conductivity change.

### 3.6.3 The Crystalline Polymer

Polymers crystallized in the bulk state are never totally crystalline, a consequence of their long chain nature and subsequent entanglements. The melting temperature ( $T_m$ ) of the polymer, is always higher than the glass transition temperature,  $T_g$ . Thus the polymer may be either hard and rigid or flexible. For example, ordinary polyethylene that has a  $T_g$  of about  $-80\text{ }^\circ\text{C}$  and a melting temperature of about  $+139\text{ }^\circ\text{C}$ . At room temperature it forms a leathery product as a result. Factors that control the  $T_m$  include polarity, hydrogen bonding and packing capability.



The development of crystallinity in polymers depends on the regularity of structure in the polymer, the tacticity of the polymer. The different possible spatial arrangements are called the tacticity of the polymer. If the R groups on successive pseudochiral carbons all have the same configuration, the polymer is called isotactic. When the pseudochiral centers alternate in configuration from one repeating unit to the next, the polymer is called syndiotactic. If the pseudochiral centers do not have any particular order, but in fact are statistical arrangements, the polymer is said to be atactic.

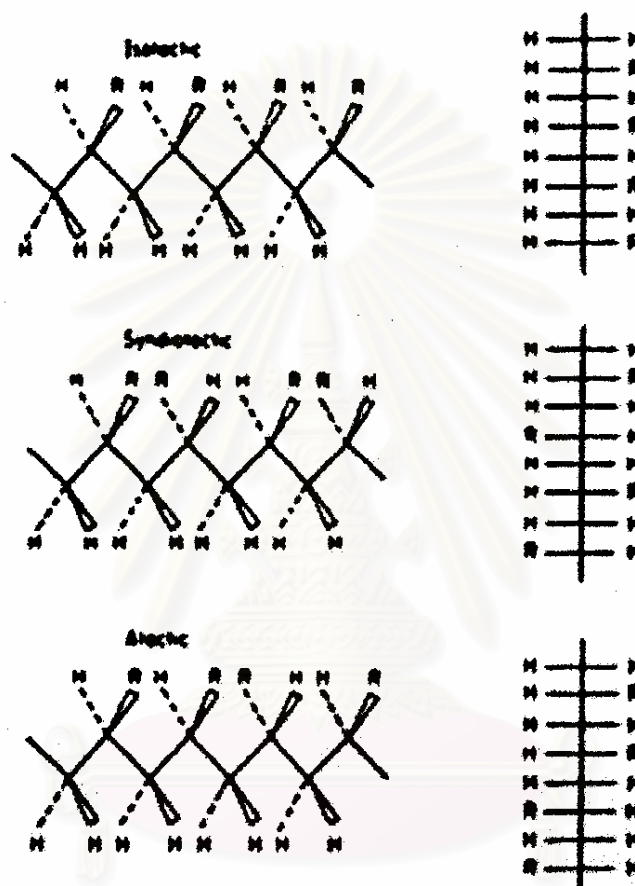


**Figure 3.7** Three different configurations of a mono-substituted polyethylene [163]

Thus isotactic and syndiotactic structures are both crystallizable, because of their regularity along the chain but their unit cells and melting temperatures are not the same. On the other hand, atactic polymers are usually completely amorphous unless the side group is so small or so polar as to permit some crystallinity.

Nonregularity of structure first decreases the melting temperature and finally prevents crystallinity. Mers of incorrect tacticity tend to destroy crystallinity. Thus statistical copolymers are generally amorphous. Blends of isotactic and atactic polymers show reduced crystallinity, with only the isotactic portion crystallizing. Furthermore, the long chain nature and the subsequent entanglements prevent total crystallization.

Crystalline polymers constitute many of the plastics and fibers of commerce. Polyethylene is used in films to cover dry-cleaned clothes and as water and solvent containers. Polypropylene makes a highly extensible rope, finding particularly important applications in the marine industry. Polyamides and polyesters are used as both plastics and fibers. Their use in clothing is world famous, cellulose, mentioned above, is used in clothing in both its native state and its regenerated state.

### 3.7 Melting Phenomena

The melting of polymers may be observed by any of several experiments. For linear or branched polymer, the melting causes the samples to become liquid and flows. First of all, simple liquid behavior may not be immediately apparent because of the polymer has high viscosity. If the polymer is cross-linked, it may not flow at all. It must also be noted that amorphous polymers soften at their glass transition temperature, which is emphatically not a melting temperature. If the sample does not contain colorants, it is usually hazy in the crystalline state because of the difference in refractive index between the amorphous and crystalline portions. On melting, the sample becomes clear or more transparent.

Ideally, the melting temperature, should give a discontinuity in the volume, with a concomitant sharp melting point. In fact, because of the very small size of the crystallites in bulk crystallized polymers, most polymers melt over a range of several degrees. The melting temperature is usually taken as the temperature at which the last trace of crystallinity disappears. This is the temperature at which the largest and/or most perfect crystals are melting.

### 3.8 Thermal Properties

The existence of a polymeric system as a rigid glassy liquid, a mobile liquid, a microcrystalline solid or a liquid crystalline mesophase depends on the temperature and the chemical structure of the polymer. Changes from a microcrystalline state to a liquid crystalline or isotropic liquid state take place at the equilibrium melting temperature.

$T_m$  and  $T_g$  of crystallizable polymers vary widely with a change in the chemical structure. The presence of amide and aromatic groups in the chain raise  $T_m$  and  $T_g$ . The morphology of a thermoplastic crystallizable homopolymer at a particular usage temperature depends on  $T_m$ , which is in turn dependent on the intermolecular forces. If the usage temperature is greater than  $T_m$  for a crystallizable polymer, only a rubbery liquid morphology will be realized. At temperatures below  $T_m$  but above  $T_g$  such a material will be partially crystalline, when crystallized quiescently, with rubbery interlayers. Below  $T_g$ , the interlayers between crystalline will be glassy.

In various kind of the polymers, the melting points refer to the melting of crystal form with the highest  $T_m$ . Changes from one form to another at easily attained temperatures and pressures can be reversible or involve melting of one form and crystallization of the other.

Some polymers with few chain irregularities, although intrinsically crystallizable, can be easily super cooled, without appreciable crystallizable, into a glassy amorphous state upon rapid cooling from the melt to a temperature below  $T_g$ . Polymers showing this type of behavior usually contain rings in the main of side chains. Examples are poly (ethylene terephthalate) and various polymers that form liquid crystalline mesophases. These supercooled materials can be crystallized by heating to a temperature where the polymer is below  $T_m$  but above  $T_g$ . Sufficient time for the various portions of the chains to adopt the conformation necessary for crystallization is then supplied.

### 3.9 Structure of Crystalline Polymers

Very early studies on bulk materials showed that some polymers were partly crystalline. X-ray line broadening indicated that the crystals were either very imperfect or very small. Because of the known high molecular weight, the polymer chain was calculated to be even longer than the crystallites. Hence it was reasoned that they passed in and out of many crystallites and many unit cells. These findings led to the fringed micelle model.



**Figure 3.8** The fringed micelle model [163]

According to the fringed micelle model, the crystallites are about  $100 \text{ \AA}$  long. The disordered regions separating the crystallites are amorphous. The chains wander from the amorphous region through a crystallite and back into the amorphous region. The chains are long enough to pass through several crystallites, binding them together.

The fringed micelle model was used with great success to explain a wide range of behaviour in semicrystalline plastics and also in fibers. The amorphous regions, if glassy, yielded a stiff plastic. However, if they were above  $T_g$ , then they were rubbery and were held together by the hard crystallites. This model explains the leathery behaviour of ordinary polyethylene plastics. The greater tensile strength of polyethylene over that of low molecular weight hydrocarbon waxes was attributed to amorphous chains wandering from crystallite to crystallite, holding them together by primary bonds. However, the exact stiffness of the plastic was related to the degree of crystallinity or fraction of the polymer that was crystallized.

## 3.10 Crystal Structure in Polymers

### 3.10.1 Crystallization from Dilute Solution

#### 3.10.1.1 Polymer Single Crystals

Although the formation of single crystals of polymers was observed during polymerization many years ago, such crystals could not be produced from polymer solution because of molecular entanglement. In several laboratories, the phenomenon of growth has been reported for so many polymers, including polyethylene, polypropylene and other poly ( $\alpha$ -olefins), that it appears to be quite general and universal.

All the structures described as polymer single crystals have the same general appearance, being composed of thin, flat platelets (lamellae) about  $100 \text{ \AA}$  thick and often many micrometers in lateral dimensions. They are usually thickened by the spiral growth of additional lamellae from screw dislocations. A typical lamellae crystal is shown in Figure 3.9.



**Figure 3.9** Electron micrograph of a single crystal of nylon-6 grown by precipitation from dilute glycerine solution [163]

The size, shape and regularity of the crystals depend on their growth conditions, such as solvent, temperature and growth rate being important. The thickness of the lamellae depends on crystallization temperature ( $T_c$ ) and any subsequent annealing treatment. Electron-diffraction measurements indicated that the polymer chains are oriented very nearly normal to the plane of the lamellae. Since the molecules in the polymers are at least  $1000 \text{ \AA}$  long and the lamellae are only about  $100 \text{ \AA}$  thick, the only reasonable description is that the chains are folded, for example, the molecules of polyethylene can fold in such a way that only about five chain carbon atoms are involved in the fold itself.

Many single crystals of essentially linear polyethylene show secondary structural features, including corrugations as shown in Figure 3.10 and pleats as shown in Figure 3.11.



**Figure 3.10** Optical micrograph showing corrugations in single crystal of linear polyethylene grown from a solution in perchloroethylene [163]

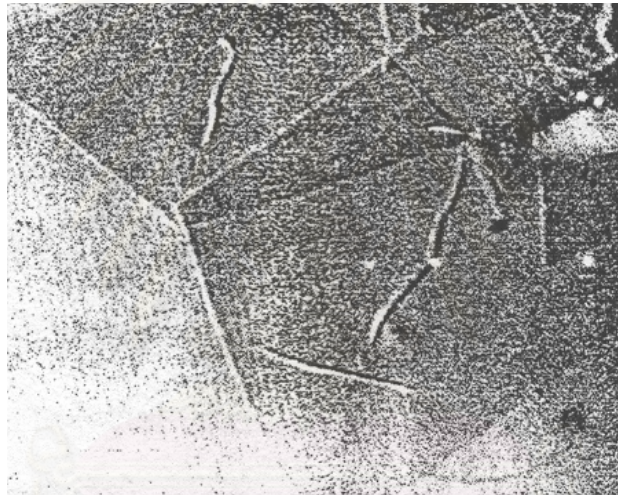


**Figure 3.11** Electron micrograph showing pleats in a crystal of linear polyethylene grown from a solution in perchloroethylene [163]

Both these features result from the fact that many crystals of polyethylene grow in the form of hollow pyramids. When solvent is removed during the preparation of the crystals for microscopy, surface-tension forces cause the pyramids to collapse.

#### 3.10.1.2 The Folded Chain Model

This led to the folded chain model, shown in Figure 3.12.

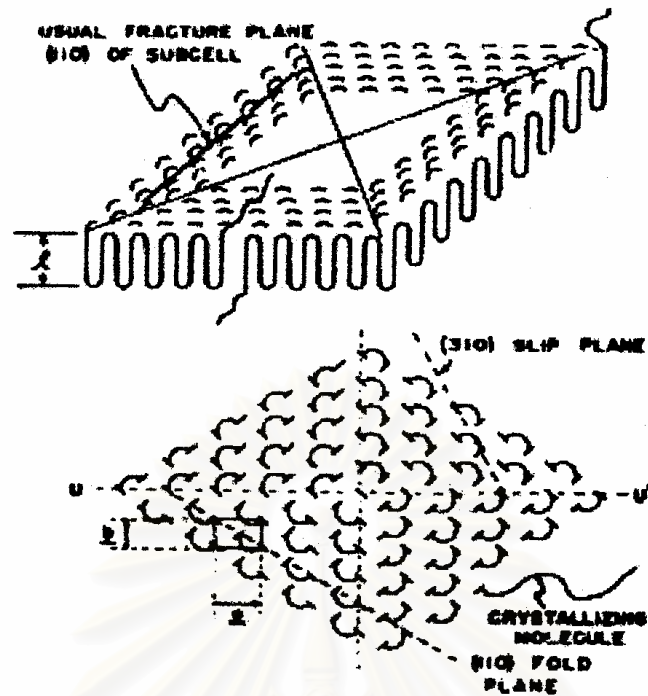


**Figure 3.12** Schematic view of a polyethylene single crystal exhibiting adjacent reentry [163]

Ideally, the molecules fold back and forth with hairpin turns building a lamellar structure by regular folding. The chain folding is perpendicular to the plane of the lamellar. While adjacent reentry has been generally confirmed by small-angle neutron scattering and infrared studies for single crystals. For many polymers, the single crystals are not simple flat structures. The crystals often occur in the form of hollow pyramids, which collapse on drying. If the polymer solution is slightly more concentrated, or if the crystallization rate is increased, the polymers will crystallize in the form of various twins, spirals and dendritic structures, which are multilayered.

### 3.10.1.3 The Switchboard Model

In the switchboard model, the chains do not have a reentry into the lamellae by regular folding, but rather reentry more or less randomly. Both the perfectly folded chain and switchboard models represent limiting cases. Real system may combine elements of both.

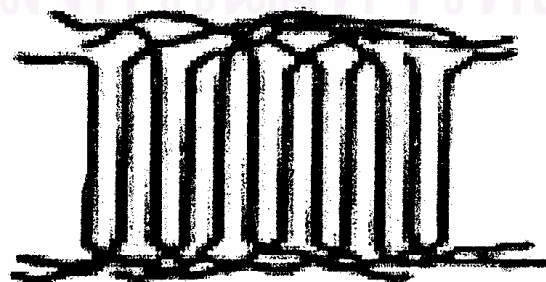


**Figure 3.13** Switchboard Model [163]

### 3.10.2 Crystallization from the Melt

#### 3.10.2.1 Spherulitic Morphology

When polymer samples are crystallized from the bulk of an unstained melt, the most obvious of the observed structures are the spherulites. Spherulites are sphere-shaped crystalline structure that form in the bulk. Usually the spherulites are really spherical in shape only during the initial stages of crystallization. During the latter stages of crystallization, the spherulites impinge on their neighbors. When the spherulites are nucleated simultaneously, the boundaries between them are straight. However, when the spherulites have been nucleated at different times, so that they are different in size when impinging on one another, their boundaries form hyperbolas. Finally, the spherulites form structures that pervade the entire mass of the material.

Electron microscopy examination of the spherulitic structure shows that the spherulites are composed of individual lamellar crystalline plates. The lamellar structures sometimes resemble staircases, being composed of nearly parallel lamellae of equal thickness.

The growth and structure of spherulites may also be studied by small-angle light scattering (SALS). The sample is placed between polarizers, a laser light beam is passed through and the resultant scattered beam is photographed. Two types of scattering patterns are obtained, depending on polarization condition. When the polarization of the incident beam and that of the analyzer are both vertical, it is called a Vv type of pattern. When the incident radiation is vertical in polarization but the analyzer is horizontal (polarizers crossed), an Hv pattern is obtained.



**Figure 3.14** Different types of light scattering patterns are obtained from spherulitic polyethylene using (a) Vv and (b) Hv polarization [164]

These patterns arise from the spherulitic structure of the polymer, which is optically anisotropic, with the radial and tangential refractive indices being different.

A model of the spherulite structure is illustrated in Figure 3.15.

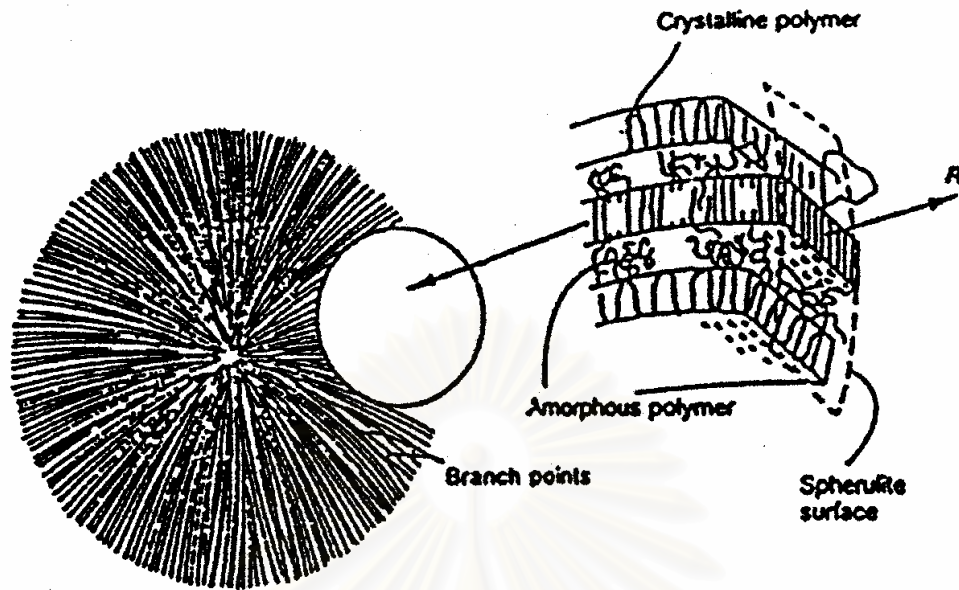


**Figure 3.15** Model of spherulitic structure [163]

The chain direction in the bulk crystallized lamellae is perpendicular to the broad plane of the structure, just like the dilute solution crystallized material. The spherulite lamellae also contain low-angle branch points, where new lamellar structures are initiated. The new lamellae tend to keep the spacing between the crystallites constant. While the lamellar structures in the spherulites are the analogue of the single crystals. In between the lamellar structures lies amorphous material. This portion is rich in components such as atactic polymers, low molecular weight material or impurities of various kinds.

The individual lamellae in the spherulites are bonded together by tie molecules, which lie partly in one crystallite and partly in another. Sometimes these tie molecules are actually in the form of what are called intercrystalline links, which are long, threadlike crystalline structures. These intercrystalline links are thought to be important in the development of the great toughness characteristic of semicrystalline polymers. They serve to tie the entire structure together by crystalline regions and/or primary chain bonds.

### 3.10.2.2 Mechanism of Spherulite Formation

On cooling from the melt, the first structure that forms is the single crystal. These rapidly degenerate into sheaf like structures during the early stages of the growth of polymer spherulites. These sheaf like structures have been variously called axialites or hedrites. These transitional, multilayered structures represent an intermediate stage in the formation of spherulites.



### 3.10.2.3 Spherulites in Polymer Blends

There are two cases to be considered. Either the two polymers composing the blend may be miscible and form one phase in the melt or they are immiscible and form two phase. If the glass transition of the non-crystallizing component is lower than that of the crystallizing component (i.e., its melt viscosity will be lower, other things being equal), then the spherulites will actually grow faster, although the system is diluted. The crystallization behavior is quite different if the two polymers are immiscible in the melt. On spherulite formation, the droplets, which are non-crystallizing, become ordered within the growing arms of the crystallizing component.

### 3.10.2.4 Effect of Crystallinity on Glass Transition Temperature

Semicrystalline polymers such as polyethylene or polypropylene types also exhibit glass transitions, though only in the amorphous portions of these polymers. The  $T_g$  is often increased in temperature by the molecular-motion restricting crystallites. Sometimes  $T_g$  appears to be masked, especially for high crystalline polymers.

Many semicrystalline polymers appear to possess two glass temperatures (1) a lower one,  $T_g$  (L), which refers to the completely amorphous state and which should be used in all correlations with chemical structure and (2) an upper value,  $T_g$  (U), which occurs in the semicrystalline material and varies with extent of crystallinity and morphology.

## 3.11 Introduction to Plastics Additives [17]

Plastics are chemicals that can be formed into useful shapes. Stated another way, plastics are organic materials that have a visual appearance appropriate to the intended function and that perform this function safely for the life of the product at a competitive cost.

Polymer additives fall into three general functional classes (1) those which are essential for fabrication of parts (2) those which improve properties and (3) those which correct problems caused by other additives.

Polymers differ from all other chemicals because of their relatively long chains and high molecular weights. Plastics are polymers that have been modified for commercial use by the use of additives.

## 3.12 Functions of Additives

Plastics additives serve three different and important functions. First, additives are required in order to process or fabricate many polymers. Polyvinyl chloride (PVC), polypropylene, poly(ethylene-carbon monoxide) (E/CO) and polyoxymethylene (POM) have thermal stability limitations that force the producers to find and utilize stabilizers that allow melt processing without loss of properties. Even room temperature storage requires that some polymers be stabilized from the effects of the oxygen in air.

Some plastics and monomers will not wet reinforcing glass fibers, and wetting agents must be used in order to process the mixture into a useful plastic. These additives are usually put onto the glass by the glass manufacturer. Sometimes, the plastic compounder adds his own wetting agent or coupling agent (there is a big difference) to gain a competitive advantage. This illustrates the second type of additive, those used for property enhancement. In the above example, a wetting agent may be necessary to process the plastic, but a coupling agent can be added as an enhancement to provide long-term durability.

Fillers improve the flexural modulus and deflection temperature under load (DTUL). Color, objectionable odor, surface gloss and other properties can be improved by additives of this second category. Polymers having elastomeric or rubbery-like properties improve impact resistance. Fibers can do a bit of both. Flame retardants enhance the safety properties of a plastic and make it more valuable. Additives of this second type pay for themselves by giving more performance value than the cost of the additive.

The third type or class of additive corrects the flaws of the first two classes. Plasticizers are required to fabricate flexible PVC, lubricants are required for unplasticized PVC. Some of these additives provide food for the growth of microorganisms such as bacteria and fungi. A further additive is needed to correct this flaw, created by required additives. Mineral fillers reduce impact while increasing modulus. Impact modifiers are used to correct these flaws. Coupling agents along with decoupling agents (often wetting agents are used for this purpose) are used to correct these flaws also.

A lubricant is an additive whose characteristics permit it to assist the internal rotation of a polymer chain under strain. In other terms, it adds to the free volume associated with that segment of the polymer.

A plasticizer is also an additive that promotes movement of chains and segments of an at least a partly amorphous polymer. Normally, however, plasticizers are used in more than trace amounts and are expected to provide significant changes in observable properties (e.g., increased flexibility and extensibility). In addition, the addition of plasticizer provides improved processability and may be selected partly on that basis.

Mechanistic differences between the action of plasticizers and lubricants are suggested by the difference in the levels at which they are used. Recent views of the mechanism of a plasticization center on the equilibrium replacement of dipolar, dispersion and hydrogen bond interactions between polymer chains (the forces inhibiting internal rotation) by similar interactions between the polymer and functional groups on the plasticizer molecule. The remainder of the plasticizer molecule supplies substantial free molar volume (i.e., has a weak interaction with its neighbors). A plasticizer is often considered a nonvolatile solvent. In this context, a lubricant becomes an analog of a surfactant. The distinction is that a lubricant has a balance of polarity that makes it very mobile in the polymer phase. Its function is to repeat its facilitation of internal rotation at different sites on the polymer. This is not to say that a plasticizer is completely bound to one segment or domain, merely that its balance of polarity is consistent with lower mobility in the polymer phase than that of

a lubricant. In summary, a lubricant provides a plasticizer function at a series of particular sites on the polymer, sites that are under strain from processing, therefore, function at a low additive level. The effect of deforming strain is to increase polarization, polar groups on the polymer become more polar. The lubricant must be selected to prefer the polarity of the strained section over those at rest.

### **3.13 Liquid Crystal**

#### **3.13.1 The History of Liquid Crystal [156]**

The discovery of liquid crystals has been approximately occurred 150 years ago, although its significance was not fully realized until over a hundred years later. Around the middle of the last century, Virchow, Mettenheimer and Valentin found from their research that the nerve fiber formed a film substance when left in water that exhibited a strange behavior when it was viewed by polarized light. They did not realize this as a different phase, but they are attributed with the first observation of liquid crystal. Later, in 1877, Otto Lehmann used a polarizing microscope with hot stage to investigate the phase transitions of various substances. He found that one substance would change from a clear liquid to a cloudy liquid before crystalline but thought that this was simply an imperfect phase transition from liquid to crystalline. In 1888 Reinitzer conducted similar experiments and was the first to suggest that cloudy fluid was a new phase of matter. He has consequently been given the credit for the discovery of the liquid crystalline phase. Up till 1890 all the investigated liquid crystalline substances had been naturally occurred and it was the first synthetic liquid crystal, *p*-azoxyanisole, was produced by Gatterman and Ritschke. Subsequently, more liquid crystals were synthesized and it is now possible to produce liquid crystals with specific predetermined material properties.

In the beginning of this century George Freidel conducted many experiments on liquid crystals and firstly explained the orienting effect when applied electric fields in the presence of defects in liquid crystals. In 1922, he proposed a classification of liquid crystals based upon the different molecular orderings of each substance. It was between 1922 and the World War II that Oseen and Zocher developed a mathematical basis for the study of liquid crystals. After the war started, many scientists believed that the important features of liquid crystals had completely been discovered and it was not until the 1950's that work by Brown in America. Gray and Frank in England and Chistiakoff in the Soviet Union led to a revival of interest in liquid crystals. Maier and Saupe formulated a microscopic theory of liquid crystals, Frank, Leslie and Ericksen developed continuum theories for static and dynamic systems, in 1968 scientists from Radio Corporation of America first demonstrated a liquid crystal display. The interest in liquid crystals has grown ever since.

#### **3.13.2 Introduction to Liquid Crystal [157]**

Polymer liquid crystals (PLCs) are a class of materials that combine the properties of polymers with those of liquid crystal. These hybrids show the same mesophases characteristic of ordinary liquid crystals, while still retained the useful and versatile properties of polymers.

Differences from normally flexible polymers, characteristics of the display liquid crystals have rod-like or disk-like elements called mesogens incorporated into their chains. The placement of the mesogens plays a large role in determining the type of PLCs that is formed. Main chain polymer liquid crystals or MC-PLCs are formed when the mesogens are themselves part of the main chain of a polymer. Conversely, side chain polymer liquid crystals or SC-PLCs are formed when the mesogens are connected as side chains to the polymer by a flexible bridge called the spacer.

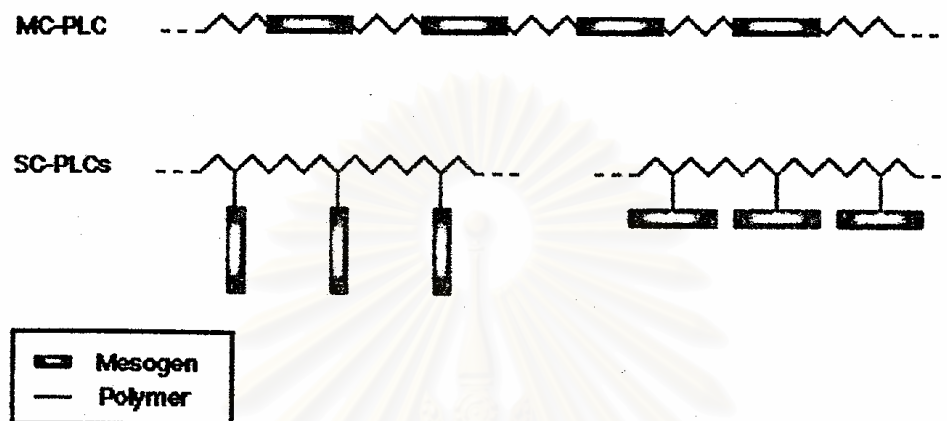


Figure 3.16 The structure of MC-PLCs and SC-PLCs [157]

Other factors influencing the mesomorphic behavior of polymers include the presence of long flexible spacers, a low molecular weight and regular alternation of rigid and flexible units along the main chain.

### 3.13.3 Main Chain Polymer Liquid Crystals

Main chain polymer liquid crystals are formed when rigid elements are incorporated into the backbone of normally flexible polymers, these interact usually occur through a condensation reaction. These stiff regions along the chain allow the polymer to orient in a manner similar to ordinary liquid crystals and thus display liquid crystal characteristics. There are two distinct groups of MC-PLCs, differentiated by the manner in which the stiff regions are formed. The first group of main chain polymer liquid crystals is characterized by stiff, rod-like monomers. The monomers are typically made up of several aromatic rings, which provide the necessary size. The following figure shows an example of his kind of MC-PLC.

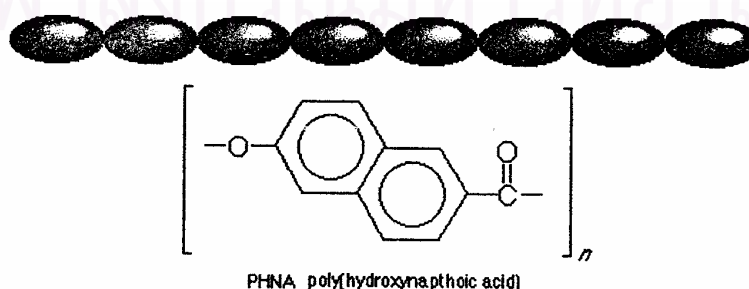
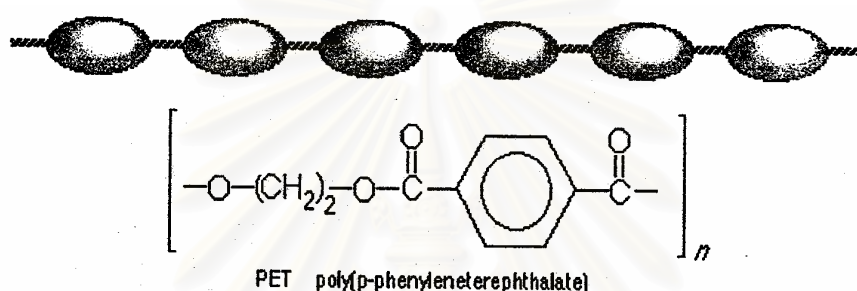


Figure 3.17 The structure of MC-PLC [157]

The second and more prevalent group of main chain polymer liquid crystals is different because it incorporates a mesogen directly into the chain. The mesogen acts just like the stiff areas in the first group. Generally, the mesogenic units are made up of two or more aromatic rings that provide the necessary restriction on movement that allow the polymer to display liquid crystal properties. The stiffness is necessary for liquid crystallinity results from restrictions on rotation caused by steric hindrance and resonance this gives the polymer its stiffness. Otherwise, the molecules are not rod-like enough to display the characteristics of liquid crystals. This group is different from the first in that the mesogens are separated or decoupled by a flexible bridge called a spacer. Decoupling of the mesogens provides for independent movement of the molecules, which facilitates proper alignment. The following is a figure of this type of main chain polymers liquid crystals. Notice the flexible spacer (methylene groups) and the stiff mesogens (aromatic ring and double bonds).



**Figure 3.18** The structure of MC-PLC [157]

It is difficult to create polymer liquid crystals that show mesogenic behavior over temperature ranges, which are convenient to work with. In fact, many times the temperature of the liquid crystalline behavior is actually above the point where the polymer begins to decompose. This problem can be avoided in one or more of the following ways. The first method of lowering polymer melting temperatures involves the arrangement of the monomers in the chain. If the molecules are put together in random orientation (head-to-tail, head-to-head, etc.), interactions between successive chains are minimized. This allows for a lower melting temperature.



**Figure 3.19** The random orientation of monomers in the polymer chain [157]

Another method to bring the temperature down to a useful range involves copolymerization. If a random copolymer can be created, the regularity of the chains is greatly reduced. This will help to minimize the interactions between the chains by breaking up the symmetry, which in turn will lower polymer melting temperature. The following figure shows how the irregularity of polymer substitute can lead to decreased interactions.

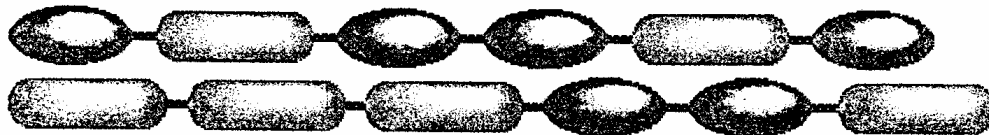


**Figure 3.20** The irregularity of polymer substitute in polymer chain [157]

Finally, defects can be introduced into the chain structure, which lower the polymer melting temperature. This method creates 120 degree (kinks) in the chain that disrupt the ability for neighboring polymers to line up. Unfortunately, this also decreases the effective persistence length so too many kinks can destroy any liquid crystal behavior.



**Figure 3.21** 120-degree kinks in the polymer chain [157]

#### 3.13.4 Side Chain Polymer Liquid Crystals

It has been demonstrated that main chain polymer liquid crystals often cannot show mesogenic behavior over a wide temperature range. Side chain polymer liquid crystals are able to expand this scale. These materials are formed when mesogenic units are attached to the polymer as side chains that interact through an addition reaction.

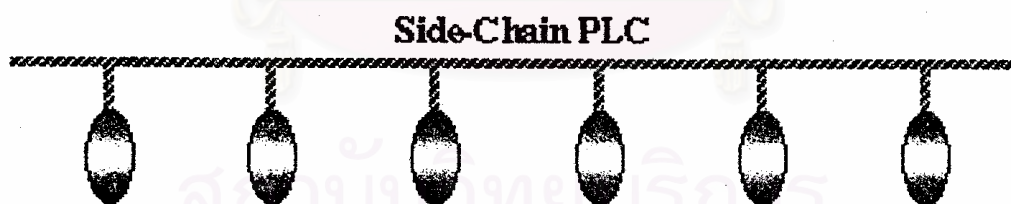


**Figure 3.22** The structure of SC-PLCs [157]

Side chain polymer liquid crystals have three major structural components, the backbone, the spacer and the mesogen. The versatility of SC-PLCs arises because these structures can be varied in a number of ways.

The backbone of a side chain polymer liquid crystal is the element that the side chains are attached to. The structure of the backbone can be very important in determining if the polymer shows liquid crystal behavior. Polymers with rigid backbones typically have high glass transition temperatures and thus liquid crystal behavior is often difficult to observe. In order to lower this temperature, the polymer backbone can be made more flexible.

Perhaps the most important part of a side chain polymer liquid crystal is the mesogen. It is the alignment of these groups that causes the liquid crystal behavior. Usually, the mesogen is made up of a rigid core of two or more aromatic rings joined together by a functional group. The following figure is a typical repeating unit in a side chain polymer liquid crystal. Notice the spacer of methylene (-CH<sub>2</sub>-) units and the mesogen of aromatic rings.

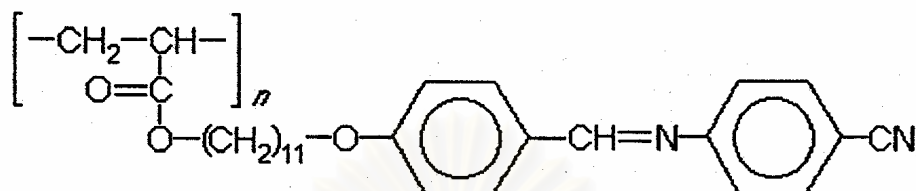


**Figure 3.23** The spacer of methylene units and the mesogen of aromatic rings [157]

Like their main chain counterparts, mesogens attached as side groups on the backbone of side chain polymer liquid crystals are able to orient because the spacer allows for independent movement. Notice in the following figure that even though the polymer may be in a tangled conformation, orientation of the mesogen is still possible because of the decoupling action of the spacer.



**Figure 3.24** The tangle conformation and orientation of the mesogens [157]

The structure of the spacer is an important determining factor in side chain polymer liquid crystals. Generally, the spacer consists of two to four methylene groups attached together in a line. Accordingly, the spacer lengths has a profound effect on the temperature and type of phase transitions. Usually, the glass transition temperature decreases with increasing spacer length. Short spacers lead to nematic phases, while longer spacers lead to smectic phases.

### 3.13.5 Type of Liquid Crystal [158]

Liquid crystals can be classified into two main categories:

1. Thermotropic liquid crystals
2. Lyotropic liquid crystals

These two types of liquid crystals are distinguished by the mechanisms that drive their self organization, but they are also similar in many ways.

Thermotropic liquid crystals are occurred in most liquid crystals and they are defined by the fact that the transitions to the liquid crystalline state are induced thermally. That is, one can arrive at the liquid crystalline state by raising the temperature of a solid and/or lowering the temperature of a liquid. Thermotropic liquid crystals can be classified into two types:

1. Enantiotropic liquid crystals, which can be changed into the liquid crystal state from either lowering the temperature of a liquid or raising of the temperature of a solid.
2. Monotropic liquid crystals, which can only be changed into the liquid crystal state from either an increase in the temperature of a solid or a decrease in the temperature of a liquid, but not both.

In general, thermotropic mesophases occur because of anisotropic dispersion forces between the molecules and because of packing interactions.

Lyotropic liquid crystal transitions occur with the influence of solvents, not by a change in temperature. Lyotropic mesophases occur as a result of solvent induced aggregation of the constituent mesogens into micellar structures. Lyotropic mesogens are typically amphiphilic, meaning that they are composed of both lyophilic (solvent-attracting) and lyophobic (solvent-repelling) parts. This causes them to form into micellar structure in the presence of a solvent, since the lyophobic ends will stay together as the lyophilic ends extend outward toward the solution. As the concentration of the solution is increased and the solution is cooled, the micelles increase in size and eventually coalesce. This separates the newly formed liquid crystalline state from the solvent.

### **3.13.6 Liquid Crystal Phases**

Friedel was able to distinguish clearly three different types of mesophase:

1. Smectic phase
2. Nematic phase
3. Cholesteric phase

Smectic phase begin from the word smectic that is derived from the Greek word “soap”, ironically the slippery substance found out the bottom of a soap dish is actually a type of smectic liquid crystal. The smectic phase is the most ordered state, where all the mesogens are arranged in a parallel and lateral order. Although this state is rare and is only observed for thermotropic polymers. In this phase the liquid crystal is turbid and the viscosity is rather high.



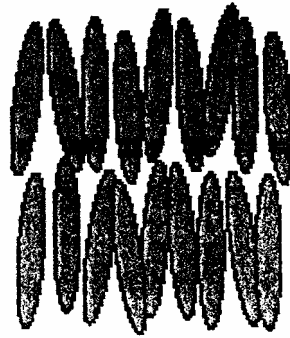


**Figure 3.25** The structure of smectic phase [156]

Nematic phase, the molecules having no positional order but tend to point in the same direction characterize this phase. It is observed that the mesogens are arranged in parallel order but do not have lateral order. Also aromatic polyamides (aramid) form a nematic order when mixed in a heavy concentration of solution. In this phase the liquid crystal is turbid but the viscosity is decrease, the molecules can move because it is mobile state.

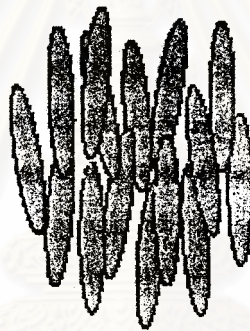


**Figure 3.26** The structure of nematic phase [156]

Cholesteric phase occurs when the mesogens are arranged parallel to each other, but the directions vary from one layer to the next. In this phase the liquid crystal is turbid but the viscosity is decrease, the molecules can move because it is mobile state, exhibiting some unique optical characteristics, quite different form those of the smectic and nematic phases. The majority of compounds exhibiting this type of mesophase are derived from cholesterol or other sterol systems.

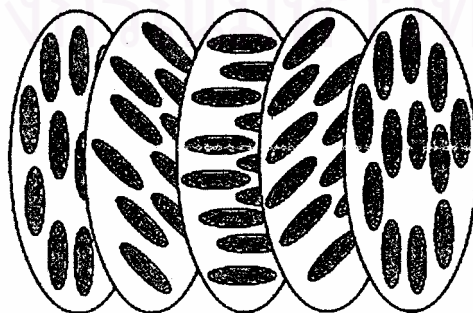


**Figure 3.27** The structure of choresteric phase [156]

### 3.13.7 Mesophasic Transition Temperature [159]

The various transitions that liquid crystal undergo as the temperature increases from the most ordered to the least ordered states, can be shown.

Crystal  $\longrightarrow$  Smectic  $\longrightarrow$  Nematic  $\longrightarrow$  Isotropic

The temperature that liquid crystals change from crystal to the smectic phase is called “crystalline melting temperature”.

The temperature that liquid crystals change from smectic phase to nematic phase is called “S-N transition temperature”.

The temperature that liquid crystal change from nematic phase to isotropic liquid is called “clearing temperature”.

The example of mesophasic transition temperature of low molecular weight liquid crystal used in this study, cyclohexylbiphenylcyclohexane (CBC-33), is shown below.

Crystal  $\xrightarrow{158\text{ }^{\circ}\text{C}}$  Smectic  $\xrightarrow{223\text{ }^{\circ}\text{C}}$  Nematic  $\xrightarrow{327\text{ }^{\circ}\text{C}}$  Isotropic

### 3.13.8 Application of Liquid Crystals [157]

Liquid crystal technology has had a major effect in many areas of science and engineering, as well as device technology. Applications for this special kind of material are still being discovered and continued to provide effective solutions to many different problems.

1. Liquid crystal displays (LCD) is the most common application of liquid crystal technology. This field has grown into a multi-billion dollar industry and many significant scientific and engineering discoveries have been made.

2. Liquid crystal thermometers demonstrated earlier, chiral nematic (cholesteric) liquid crystal reflects light with a wavelength equal to the pitch. Because the pitch and the color reflected also is dependent upon temperature. Liquid crystals make it possible to accurately gauge temperature just by looking at the color of the thermometer. By mixing different compounds, a device for practically any temperature range can be built.

3. Optical imaging is an application of liquid crystals that is only now being explored, is optical imaging and recording. In this technology, a liquid crystal cell is placed between two layers of photoconductor. Light is applied to the photoconductor, which increases the material's conductivity. This causes an electric field to develop in the liquid crystal corresponding to the intensity of the light. The electric pattern can be transmitted by an electrode, which enables the image to be recorded. This technology is still being developed and is one of the most promising areas of liquid crystal research.

4. High strength fibers is an application of polymer liquid crystals that has been successfully developed for industry, is the area of high strength fibers. Kevlar, which is used to make such things as helmets and bulletproof vests, is just one example of the use of polymer liquid crystals in applications calling for strong, lightweight materials. Ordinary polymers have never been able to demonstrate the stiffness necessary to compete against traditional materials like steel. It has been observed that polymers with long straight chains are significantly stronger than their tangled counterparts. Main chain liquid crystal polymers are well suited to ordering processes. For example, the polymer can be oriented in the desired liquid crystal phase and then quenched to create a highly ordered, strong solid. As these technologies continue to develop, an increasing variety of new materials with strong and lightweight properties will become available.

5. Other applications of liquid crystal have a multitude of other uses. They are used for nondestructive mechanical testing of materials under stress. This technique is also used for the visualization of radio frequency (RF) waves in wave guides. They are used in medical applications where, for example, transient pressure transmitted by a walking foot on the ground is measured. Low molar mass (LMM) liquid crystals have applications including erasable optical disks, full color, electronic slides, for computer aided drawing (CAD) and light modulators for color electronic imaging.

### 3.13.9 Structural Considerations of Low Molecular Weight Liquid Crystal Systems [160]

#### 1. Aromatic Systems

Looking back to the period before the 1970s, the great majority of liquid crystal materials were aromatic in character and of general structure.

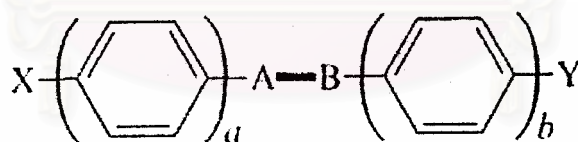


**Figure 3.28** The general structure of aromatic system [160]

Where 1. X and Y represent a range of terminal substituents such as alkyl, alkoxy and cyano.

2. A-B represents a linking unit in the core structure, e.g., CH=N, N=N, N=NO and CO.O

3. a and b have small integral values.

It was quickly realized that any substituent X or Y that does not broaden the molecule too much is superior to an H at the end of the molecule and that groups such as cyano and alkoxy are more favorable than others such as alkyl or halogen in promoting high  $T_{N-1}$  values. At typical nematic terminal group efficiency order is CN > OCH<sub>3</sub> > NO<sub>2</sub> > Cl > Br > N(CH<sub>3</sub>)<sub>2</sub> > CH<sub>3</sub> > H. The nature of the central linkage is also of great importance and linking units containing multiple bonds that maintain the rigidity and linearity of the molecules are most satisfactory in preserving high  $T_{N-1}$

values. Thus in simply systems in Figure 3.28 with  $a$  and  $b = 1$ , the  $-\text{CH}_2-\text{CH}_2-$  flexible unit is a poor one and gives rise to vary weak or nonexistent nematic tendencies. The ester function contains no multiple bonds in the chain of atoms actually linking the rings, but conjugative interactions within the ester function and with the rings lead to some double bond character and a stiffer structure than might be expected. Esters are in fact fairly planer systems and quite strongly nematogenic. A typical central group nematic efficiency order is  $\text{trans } -\text{CH}=\text{CH} > \text{N}=\text{NO} > \text{CH}=\text{NO} > \text{C}=\text{C} > \text{N}=\text{N} > \text{CO.O} > \text{none}$ .

## 2. Alicyclic Systems

The fairly low  $T_{\text{N-1}}$  values of the cyanobiphenyls gave little scope for structure modification by lateral substitution of the molecules, although this was possible in the case of the related terphenyl systems, used as high  $T_{\text{N-1}}$  additives.

The first major development of the biphenyl class of mesogen came therefore with the preparation of the cyclohexane analogs of structure in Figure 3.29 where  $a$  may be 1 in the cyclohexane ring compounds.

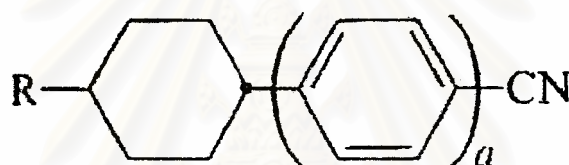


**Figure 3.29** The general structure of alicyclic system [160]

However, the cyclohexane ring compounds also had higher  $T_{\text{N-1}}$  values than the biphenyl analogs, e.g.,  $\text{R} = \text{C}_5\text{H}_{11}$  have  $T_{\text{N-1}}$  values of biphenyl  $35^\circ\text{C}$  but  $T_{\text{N-1}}$  values of cyclohexane ring  $55^\circ\text{C}$ . This disadvantageous effect of the cyclohexane ring at high temperatures may be due to the flexibility of the ring and its ability to adopt skewed or twisted conformations that are higher in energy and less conducive to nematic order. With regard to polymers, the advantages of disadvantages of using cyclohexane ring would also depend on  $T_{\text{N-1}}$  values. However, there are other features of using cyclohexane rings that may be important. The viscosity of low molecular weight liquid crystal systems is lowered e.g., in cyanobiphenyl analogs that  $\text{R} = \text{C}_5\text{H}_{11}$  the viscosity at  $20^\circ\text{C}$  in nematic phase  $32\text{ cP}$  but in cyclohexane rings analogs have the viscosity at  $20^\circ\text{C}$  in nematic phase  $21\text{ cP}$ .

## 3. Cholesteric Systems

Since the cholesteric phase is a spontaneously twisted analog of the nematic phase, it is not surprising that molecular structural changes affect the transition temperatures of cholesteric and nematic phases in the same way. Consequently, the above generalizations about structure change in relation to  $T_{\text{N-1}}$  values apply to  $T_{\text{Ch-1}}$  values.

Only the pitch of the twist and its sense need therefore be considered additionally. Twist sense is very sensitive to structure change and for cholesterogens derived from sterols such as cholesterol. However, for commercially useful cholesterogens we do not usually want to have the presence of a bulky and often UV-sensitive steryl skeleton and most of the important low molecular weight materials are simply chiral analogs of nematogens, the chirality being introduced by having a chiral centre in a terminally situated alkyl or alkoxy group.

Turning therefore to twisting power, this decreases as the chiral center is moved away from the ring system, i.e., as  $n$  is increased in a structure such as Figure 3.30. Practically speaking, the best value of  $n$  to use is 1. This achieves a good tightness of the pitch without involving the very great reduction in  $T_{N-1}$  values that arises with  $n = 0$ .

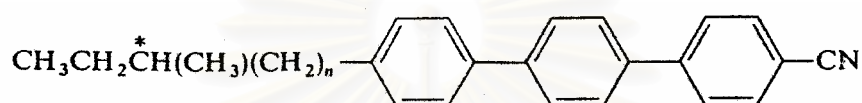


**Figure 3.30** The structure of cholesteric system [160]

#### 4. Smectic Systems

In low molecular weight liquid crystal systems of commercial interest one usually wished to avoid smectic properties. This is not always the case, however, for latent smectic properties can be valuable for increasing the sensitivity of the color response of cholesteric phase to temperature.

Although correlated smectic phases can be envisaged for liquid crystal main chain polymers, these structures would be so akin to solids that it is doubtful, if like correlated low molecular weight smectics, these would be of commercial interest. With liquid crystal side chain polymers it is hard to envisage long-range correlation of the smectic ordering of the side chain groups that would not be interfered with by the polymer backbone.

#### 5. Diskogens

Diskogens has centered recently around compound consisting of flat, disk-shaped molecules that can pack together to form flexible columns. These columns than constitute a diskotic liquid crystal phase, quite distinct from smectic or nematic liquid crystal phases and having a negative sign of the optic axis.

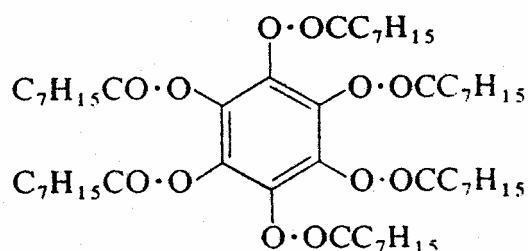


**Figure 3.31** The structure of diskogens system [160]

The relevance of such diskotic phases to polymer systems, liquid crystal main chain or liquid crystal side chain polymers is hard to judge. Presumably a fairly straight polymer backbone with a sufficient density of lateral functions radiating outward could constitute a columnar structure, but whether this approximates closely enough to a stacking of individual disk-shaped molecules cannot easily be judged.

### **3.14 Polymer Blends**

Polymer blends are the mixtures of at least two or more polymers. The mixing of two or more existing polymers may obtain the new properties of the blend. By using these techniques the designed properties can be explored without synthesizing the new polymer, which have the designed properties. The results of blending polymers have many advantages, for example, lower cost than synthesizing the desired properties of new polymer. The new properties can also be under controlled. There are many methods to mix each polymer together, such as by using heat (melt mixing), by using solvent (solution casting, freeze drying) or by in situ reaction, etc.

#### **3.14.1 Melt Mixing**

Melt mixing of thermoplastics polymer is performed by mixing the polymers in the molten state under shear in various mixing equipments. The method is popular in the preparation of polymer blends on the large commercial scale because of its simplicity, speed of mixing and the advantage of being free from foreign components (e.g. solvents) in the resulted blends. A number of are available for laboratory scale mixing such as internal mixer, electrically heated two roll mill, extruder and rotational rheometer.

The advantages of this method are the most similar to the industrial practice. The commercial compounding or adding additives into base polymers are applied by melt mixing. So the investigations of polymer blends by melt mixing method are the most practical methods in industrial applications.

#### **3.14.2 Solvent Casting**

This method group is performed by dissolving polymers in the some solvent. The solution is then cast on a glass plate into thin films and the removal of solvent from the films is performed by evaporating the solvent out at ambient or elevated temperature. To remove traces of solvents from the casting polymer films, the condition of high temperature is invariably needed and protection of polymer in case of degradation is essential. The inert gas or lower down the pressure (vacuum) is typically used. In the vacuum conditions, the vapor pressure can be reduced and thus allows the solvents to evaporate more easily. However, too fast evaporation rate of solvent will result in the bubble in the final films produced.

Solvent casting is the simplest mixing method available and is widely practiced in academic studies, usually when the experiments need a very small quantity of polymers.

### 3.14.3 Freeze Drying

In the freeze drying processes, the solution of the two polymers is quenched down immediately to a very low temperature and the solution is frozen. Solvent is then removed from the frozen solution by sublimation at a very low temperature. Dilute solutions must be used and the solution volume must have as large surface area as possible for good heat transfer.

An Advantage of this method is that the resulted blend will be independent of the solvent, if the single phase solution is freezed rapidly enough. However, there are many limitations of this method. Freeze drying method seems to work best with solvents having high symmetry, i.e. benzene, naphthalene, etc. The powdery form of the blend after solvent removal is usually not very useful and further shaping must be performed. While not complex, freeze drying does require a good vacuum system for low – boiling solvents and it is not a fast blending method. After solvent removal, the blend is in the powdery form, which usually needs further shaping. The advantage of this method is the simplicity. However, this method needs a good fume trap, vacuum line for the sublimation solvent and it takes time to complete the sublimation process.

### 3.14.4 Emulsions

The advantages of the emulsion polymer mixing are the easy handling and all the other advantages as the solvent casting. The mixing or casting of the film requires neither expensive equipment nor high temperature. However, emulsions of polymers are an advantage technique and not always applicable to all monomers.

### 3.14.5 Reactive Blend

Co-crosslinking and interpenetrating polymer networks (IPN) formations are the special methods for forming blends. The idea of these methods is to enforce degree of miscibility by reactions between the polymer chains. Other methods involve the polymerization of a monomer in the presence of a polymer and the introduction of interface graft copolymer onto the polymer chains.

## 3.15 Light Scattering Theory

The phenomenon of light scattering is encountered widely in every life. For example, light scattering by airborne dust particles causes a beam of light coming through a window to be seen as a shaft of light, the poor visibility in a fog results from light scattering by airborne water droplets and laser beams are visible due to scattering of the radiation by atmospheric particles. Also, light scattering by gas molecules in the atmosphere gives rise to the blue color of the sky and the spectacular colors that can sometimes be seen at sunrise and sunset. There are all examples of static light scattering since the time-averaged intensity of scattered light is observed.

In general, interaction of electromagnetic radiation with a molecule results in scattering of the radiation, Scattering results from interaction of the molecule with the oscillating electric field of the radiation, which forces the electrons to move in one direction and the nuclei to move in the opposite direction. Thus a dipole is induced in the molecules, which for isotropic scatterers is parallel to and oscillates with, the

electric field. Since an oscillating dipole is a source of electromagnetic radiation, the molecules emit light, the scattered light, in all directions. Almost all of the scattered radiation has the same wavelength (and frequency) as the incident radiation and results from elastic scattering that is zero energy change. Additionally, a small amount of the scattered radiation has a higher or lower, wavelength than the incident radiation and arises from inelastic scattering that is non-zero energy change. Inelastically scattered light carries information relating to bond vibrations and is the basis of Raman spectroscopy, a technique that increasingly is being used in studies of polymer structure and polymer deformation micromechanics.

The scattering of light from crystalline polymeric films has been studied for long time. This scattering arises principally from orientation fluctuations among aggregates of crystals. The scattering patterns are complex, especially with polarized light and oriented samples. This technique described involved photometric measurement of the scattered intensity as a function of sample and scattering angle. The photographic technique like the photographic X-ray diffraction except that a laser is used as a radiation source as a substitute for an X-ray tube. A typical photographic light scattering apparatus is shown in Figure 3.32.

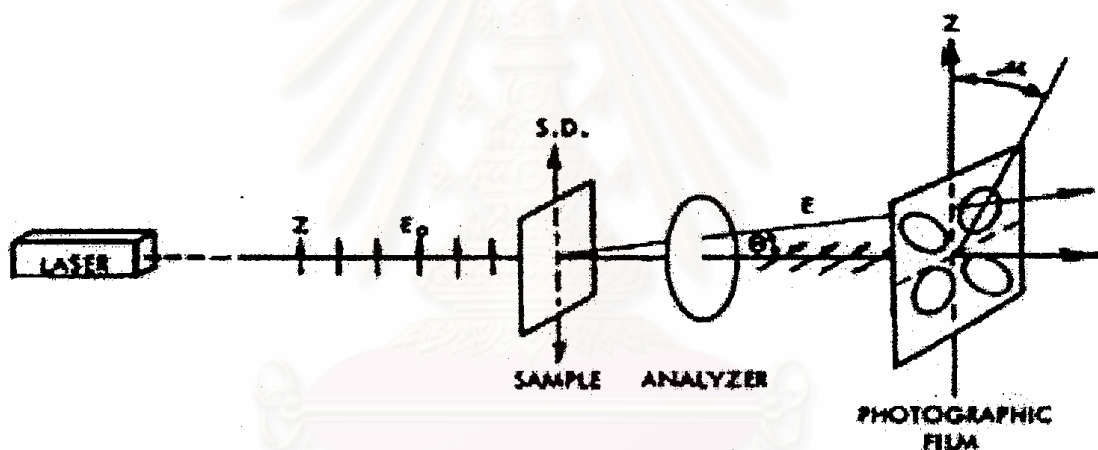
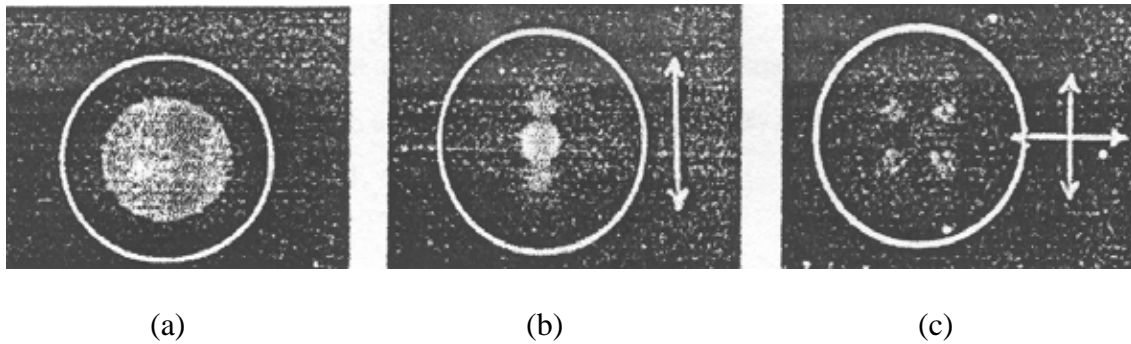


**Figure 3.32** A typical photographic light scattering apparatus [165]

The intensity depends upon the scattering angle  $\theta$  between the incident and scattered ray and the azimuthal angle  $\mu$ . The range of  $\theta$  that may be recorded in a picture depends upon the sample to film distance,  $d$  since  $\tan \theta = (x/d)$ , where  $x$  is the distance from the center of the photographic film to the point where the intensity is recorded.

Some typical scattering patterns from an unoriented medium density polyethylene is presented in Figure 3.33.



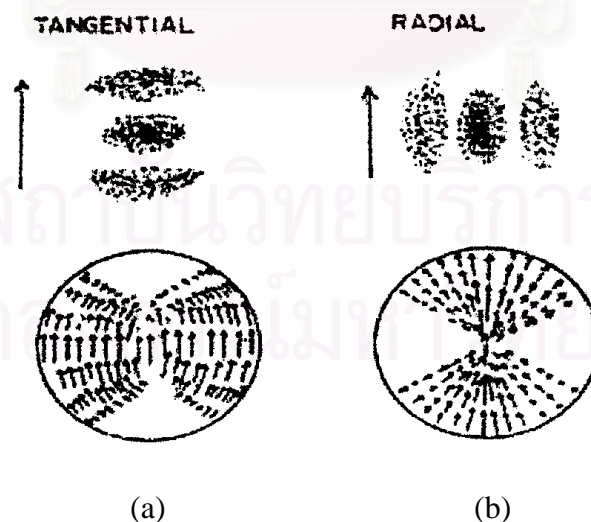


(a) (b) (c)  
**Figure 3.33** Typical light scattering photographs for (a) unpolarized light (b) Vv polarization and (c) Hv polarization [164]

Two types of polarized patterns are (1) Vv patterns obtained when the polarizer in the incident beam and the polarizer (or known as analyzer) in the scattering beam are both vertical and (2) Hv patterns where the polarizer is vertical and the analyzer is horizontal. It is observed that the Vv scattering patterns are elongation in the direction of polarization. An anisotropic scattering pattern of this sort is usually interpreted in terms of an oriented scattering object. This cannot be the case with an unoriented polyethylene sample, particularly since the direction of extension of the scattering pattern is dependent upon the direction of polarization. Consequently, the interpretation may be made in terms of an anisotropic but unoriented arrangement of principal polarizability directions.

Polyethylene crystallites are known to be arranged in spherical aggregates called spherulites with different radial and tangential refractive indexes. This optical anisotropy is a consequence of the arrangement of the anisotropic crystalline within the spherulites.

There are two idealized cases illustrated in Figure 3.34.



(a) (b)  
**Figure 3.34** The arrangement of induced dipoles and the expected Vv scattering patterns for spherulites (a) only polarizable tangentially (b) only polarizable rapidly [164]

For case (a), it is assumed that the electrons within the spherulite may only be displaced in a tangential direction. It is apparent that for vertically polarized light, dipoles are induced in only the equatorial regions of the spherulite. The scattering pattern, which is most elongated in the direction of smallest extension of the spherulite, is extended in the vertical direction. In case (b), where the electrons may move only along the radii of the spherulite, the induced dipoles are principally in the polar regions and the scattering pattern is extended horizontally. For isotropic spherulites, radial and tangential motion of the electrons is equally easy and induced dipoles are uniformly arranged throughout the spherulite. The scattering pattern will be the sum of those for cases (a) and (b) and will have circular symmetry. The observed extension of the  $V_v$  scattering pattern in the polarization direction corresponds to case (a) and indicates that it is the tangential component of polarizability, which gives rise to scattering. The low intensity of scattering in the direction perpendicular to polarization observed in  $V_v$  polarization pattern indicates that the radial polarizability contribution is negligible. This probably arises because of destructive interference among adjacent spherulites.

The cloverleaf type pattern obtained with crossed polaroids may also be understood in terms of spherulite anisotropy. For vertical polarization of the incident light, the induced dipoles are distributed as in case (a). If these are viewed through a horizontally oriented analyzer, the large dipoles along the equator will be oriented perpendicularly to the analyzer and will not contribute to the scattered light by the analyzer. It will be the dipoles in planes of the spherulite oriented at 45 degree to both the polarizer and analyzer that will make the maximum contribution to scattering. The arrangement of these is indicated in Figure 3.30. The cloverleaf arrangement of these is apparent.

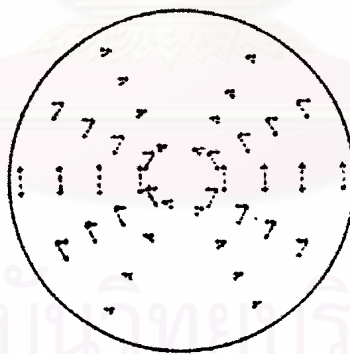


**Figure 3.35** The arrangement of induced dipoles in a tangentially polarizable spherulite which will contribute to  $H_v$  scattering [164]

It is also apparent that in isotropic spherulites, the induced dipole will be oriented in the direction of polarization of the incident light and no scattered light will be transmitted through an analyzer perpendicular to polarizer. Consequently, the  $H_v$  component of scattering for isotropic spherulites will be zero.

## CHAPTER IV

### EXPERIMENT

In the present study of the influence of homogeneous half-metallocene catalyst system with dimethyl anilinium tetrakis (pentafluoro phenyl) borate as cocatalyst on styrene polymerization and crystallinity of polymer blends between syndiotactic polystyrene and additives were performed, the experiments were divided into four parts.

- (i) Styrene monomer preparation
- (ii) Styrene polymerization with the homogeneous half-metallocene catalyst system
- (iii) Blend polymer between syndiotactic polystyrene and additives
- (iv) Characterization of all polystyrene products (pure and blend polymers) and additives

The details of the experiment were explained in the following.

#### 4.1 Chemicals

The chemicals used in this experiment were normal analytical grade, but only critical materials were specified as follows.

1. Ultra high purity argon gas (Ar, 99.999 % vol.) was purchased from Thai Industrial Gas Co., Ltd. and further purified by passing through columns packed with molecular sieve 3 °A, BASF Catalyst R3-11G, sodium hydroxide (NaOH) and phosphorus pentoxide (P<sub>2</sub>O<sub>5</sub>) to remove traces of oxygen gas and moisture.
2. Toluene was donated from EXSOL Chemical Ltd., Thailand. This solvent was dried over dehydrated CaCl<sub>2</sub> and distilled over sodium/benzophenone under argon atmosphere before use.
3. Styrene monomer purchased from Fluka Chemie A.G., Switzerland was distilled form sodium under vacuum just before use.
4. Methyl ethyl ketone (MEK) purchased form Carlo Erba, Italy was used without further treatment.
5. Methanol (CH<sub>3</sub>OH) obtained from Carlo Erba, Italy was used as received.
6. Pentamethylcyclopentadienyltitanium trichloride (Cp\*TiCl<sub>3</sub>) obtained from Japan was used without further purification.
7. Dimethyl anilinium tetrakis (pentafluoro phenyl) borate [PhNMe<sub>2</sub>H]<sup>+</sup> [B(C<sub>6</sub>F<sub>5</sub>)<sub>4</sub>]<sup>-</sup> obtained from Japan was used without further purification.
8. Triisobutylaluminum (TIBA) purchased from Fluka Chemie A.G., Switzerland was used without further purification.
9. Cyclohexylbiphenylcyclohexane (CBC-33) purchased from Merck Co., Ltd., Germany was used as received.
10. Glycerol monostearate (GMS) obtained from Rikevita Ltd., Malaysia was used as received.

## 4.2 Equipments

All equipments, used in syndiotactic polymerization of styrene and polymer blend, were listed as follows:

### 4.2.1 Schlenk Line

Schlenk line consists of vacuum and argon lines. The vacuum line was equipped with the solvent trap and pump, respectively. The argon line was connected to the trap and the mercury bubbler that was a manometer tube and contains enough mercury to provide a seal from the atmosphere when argon line is evacuated. The schlenk line was shown in Figure 4.1.

### 4.2.2 Schlenk Tube

A tube with a ground glass joint and a side arm which was three way glass valve as shown in Figure 4.2. Sizes of the Schlenk tubes were 50, 100 and 200 ml used to prepare catalysts and collect materials, which were sensitive to oxygen gas and moisture.

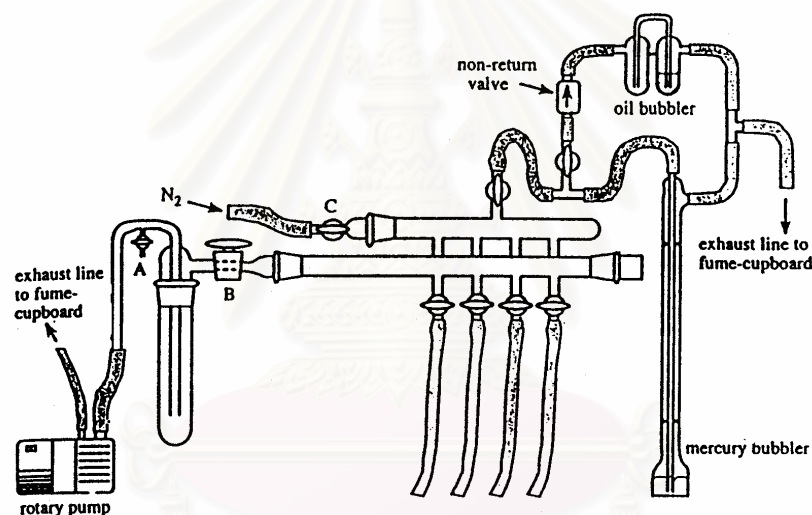


Figure 4.1 Schlenk line

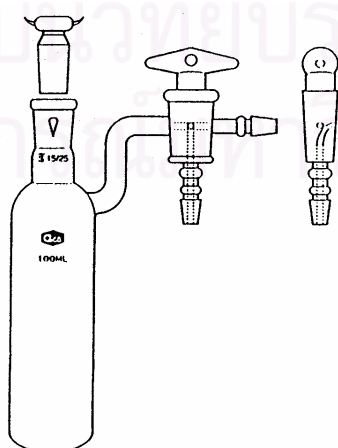


Figure 4.2 Schlenk tube

### 4.2.3 Glove Box

Glove box was equipment for storage and prepare the chemicals under inert gas atmosphere to avoid oxygen gas and moisture.

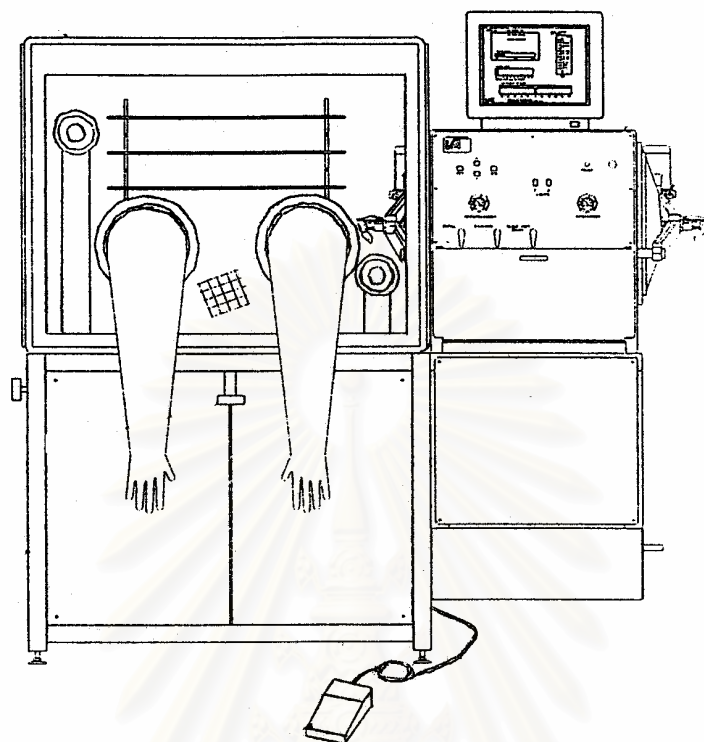


Figure 4.3 Glove box

### 4.2.4 Vacuum Pump

The vacuum pump model 195 from Labconco Corporation was used. A pressure of  $10^{-1}$  to  $10^{-3}$  mmHg was adequate for the vacuum supply to the vacuum line in the Schlenk line.

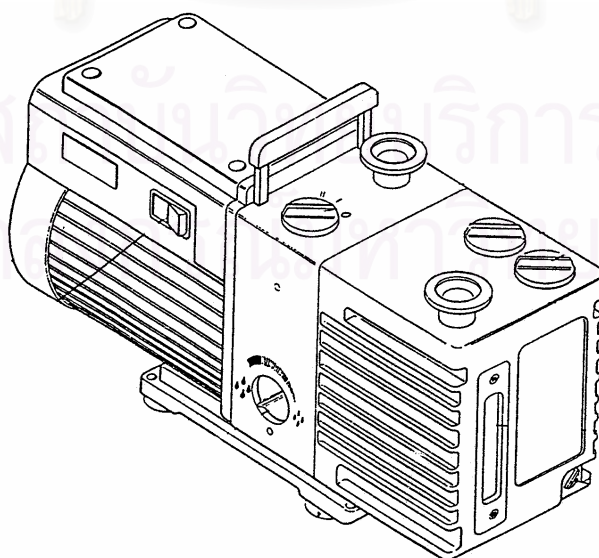
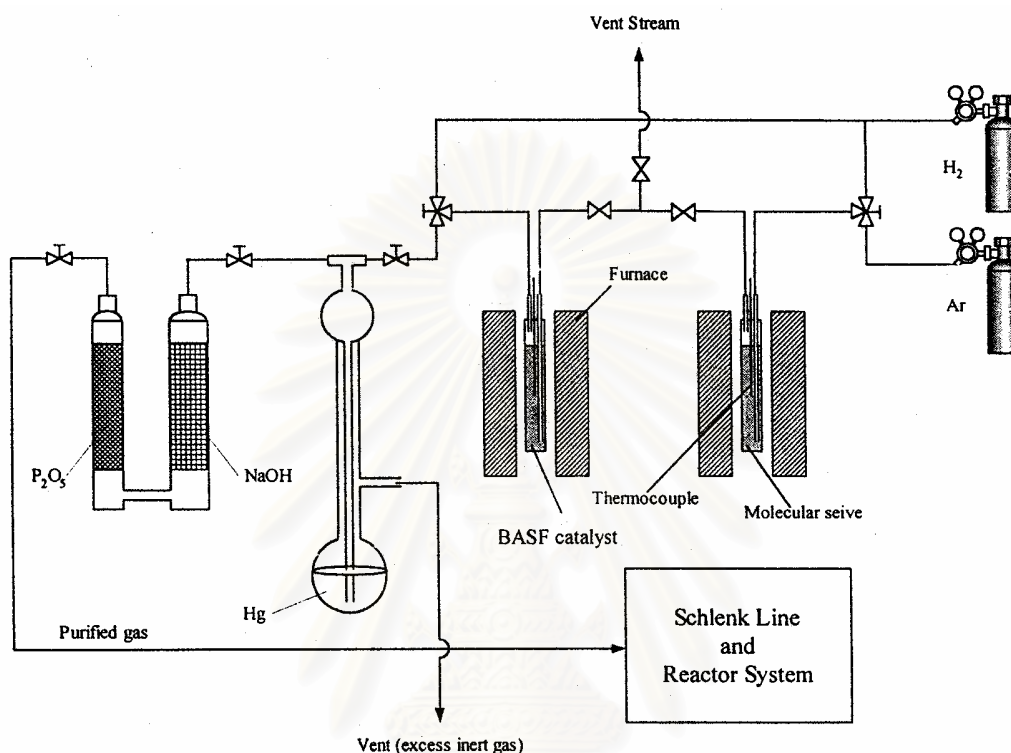


Figure 4.4 Vacuum pump

### 4.2.5 Inert Gas Supply

The inert gas, argon, was passed through columns of BASF Catalyst R3-11G as oxygen scavenger and molecular sieve 3 A to remove moisture. The BASF catalyst was regenerated by treatment with hydrogen at 300 °C overnight before flowing the argon gas through all of the above columns. The inert gas supply system is shown in Figure 4.5.



**Figure 4.5** Inert gas supply system

### 4.2.6 Glass Reactor

The polymerization reactor was a 250 ml three-neck flask. The reactor was equipped with several fittings for injection and argon lines.

### 4.2.7 Magnetic Stirrer and Hot Plate

The magnetic stirrer and hot plate model RCT basic from IKA Labortechnik were used.

### 4.2.8 Digital Hot Plate Stirrer

A Cole-Parmer digital hot plate stirrer was used for melt mixing the polymers with additives. This hot plate stirrer is programmable. All functions can be set from digital panel and display their status on LCD. The plate temperature, stirrer speed and time are controllable.

### 4.2.9 Cooling System

There were two cooling systems, one was used for the solvent distillation for condensing the freshly evaporated solvent and the other one was for cooling the system of the polymerization reactor due to the rapid rate of polymerization that is the exothermic reaction.

#### 4.2.10 Syringe, Needle and Septum

The syringe use in the experiment had a volume of 50, 20, 10, 2 and 1 cc and needle were No. 15, 20 and 22, respectively. The septum was a silicone rod. It was used to prevent the surrounding air from entering into glass bottle by blocking at the needle end. Solvent, catalyst, cocatalyst, scavenger and monomer were transferred to a glass bottle by using needles.

### 4.3 Characterization Instruments

The instruments used to characterize all polystyrene products (pure and blend polymers) and additives were specified in the following:

#### 4.3.1 Soxhlet Extractor

Soxhlet extractor was used for determining syndiotactic index (S.I.). Polystyrene product was weighed in cellulose thimble about 0.1 g and then was extracted with methyl ethyl ketone (MEK) for 10 hours in atmosphere. The residual polymer was dried at room temperature. The fraction of the whole polymer unextracted and multiply by 100 was taken as a % syndiotactic index (% S.I.) according to the equation.

$$\% \text{ S.I.} = (\text{Insoluble Weight of PS} / \text{Total Weight of PS}) \times 100$$

#### 4.3.2 Differential Scanning Calorimetry (DSC)

The glass transition temperature (T<sub>g</sub>), crystalline temperature (T<sub>c</sub>) and melting temperature (T<sub>m</sub>) of polymer were determined by a Perkin-Elmer DSC 7 at Central Instrument Facility (CIF), Mahidol University. The analyses were performed at heating rate 20 °C/min in the temperature range 50-300 °C. The heating cycle was run twice. The first scan, samples were heated and then cooled to room temperature. The second scan, sample were reheated at the same rate, both the results of the first and second scan were reported. In general, the first scan was influenced by the mechanical and thermal history (annealing) of samples but the second scan was influenced by the heat energy for endothermic and exothermic reaction within DSC instrument.

#### 4.3.3 Scanning Electron Microscope (SEM)

SEM observation with a JSM-5410LV Scanning Microscope at Scientific and Technological Research Equipment Centre (STREC), Chulalongkorn University was employed to investigate the morphology of all polystyrene products and additives. The samples for SEM analysis were coated with gold particles by ion sputtering device to provide electrical contact to the specimen.

#### 4.3.4 Small-Angle Light Scattering (SALS)

This experiment was performed using the static light scattering apparatus at Polymer Engineering Research Laboratory (PEL), Department of Chemical Engineering, Chulalongkorn University. The equipment is schematically shown in Figure 4.6.

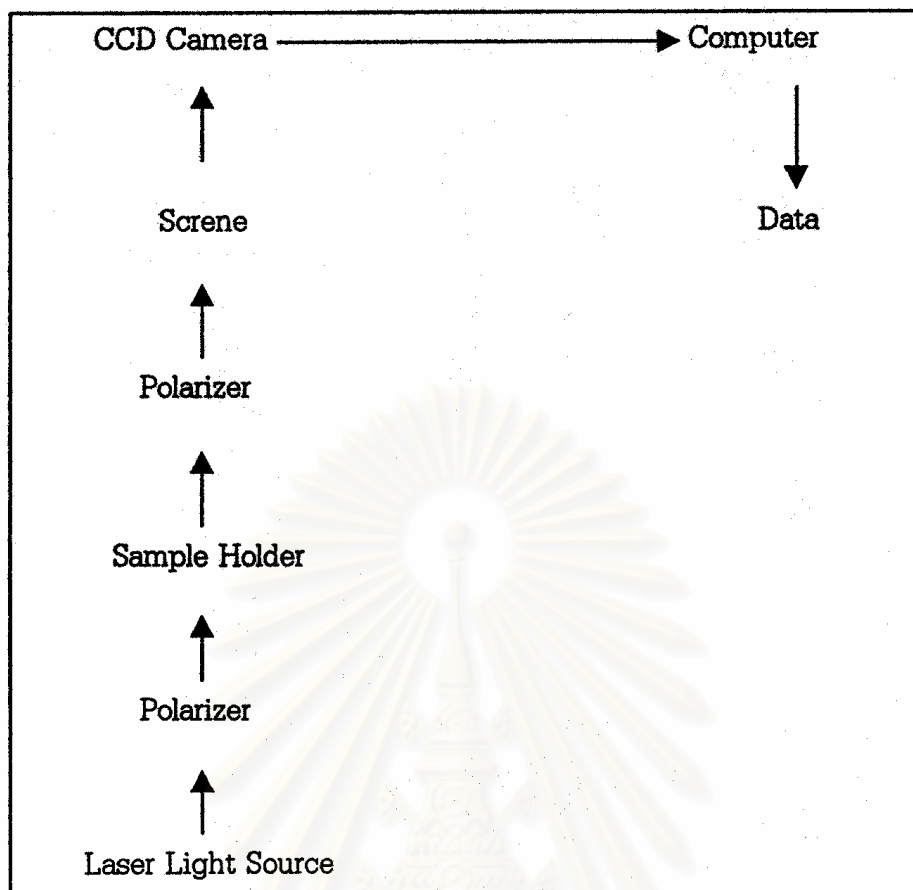


**Figure 4.6** A schematic diagram of static light scattering equipment

A He/Ne laser ( $\lambda = 632.8 \text{ nm}$ ) is used as an incident light source. Samples were placed inside a holder, which was mounted between two polarizers where the polarization direction of the polarizer near the incident light was vertical and the other was horizontal. Light scattering photographs were detected by CCD Camera with exposure times 2 seconds and the illumination of laser light source was set at no.3 (gain 3), no.5 (gain 5) and no.7 (gain 7) by using the computer program which was connected to the apparatus. Then these photographs were transferred to analyze using the computer.

#### 4.3.5 Wide-Angle X-ray Diffraction (WAXD)

X-ray Diffractometer (XRD) observation with a Philips Expert PW3710 BASED HT10 at the Metallurgy and Materials Science Research Institute (MMRI), Chulalongkorn University was used for determining crystallinity of all polystyrene products and additives. The X-ray diffraction experiments were performed consisting of rotating tube anode (Cu) generator and wide-angle powder goniometer fitted with a high temperature attachment. The generator was operated at 40 kV and 30 mA. The X-ray diffraction patterns were obtained at room temperature for all polystyrene products and additives and at higher temperature (700 °C under vacuum atmosphere) for only polystyrene products. The X-ray diffraction profiles were recorded in the  $2\theta$  range 5-30 ° at a scan rate 0.04 ° (2 $\theta$ )/s.



## 4.4 Polymerization Procedure

### 4.4.1 Preparation of Catalyst

$Cp^*TiCl_3$  approximately 5.8 mg was dissolved in 10 ml toluene under argon atmosphere in glove box. The catalyst solution was stirred until the catalyst was completely soluble. The solution was used as a catalyst for styrene polymerization with dimethyl anilinium tetrakis (pentafluoro phenyl) borate cocatalyst.

### 4.4.2 Preparation of Cocatalyst

$[PhNMe_2H]^+[B(C_6F_5)_4]^-$  approximately 16 mg was dissolved in 10 ml toluene under argon atmosphere in glove box. The cocatalyst solution was stirred until the cocatalyst was completely soluble.

### 4.4.3 Preparation of Styrene Monomer

Styrene monomer was extracted with NaOH solution (5 % w/w) and distilled water, then distilled over sodium under vacuum atmosphere before use.

### 4.4.4 Styrene Polymerization

A 250 ml glass reactor equipped with a mechanical stirrer was charged with 3.69 ml of toluene, 3.00 ml of catalyst solution, 3.00 ml of cocatalyst solution and 0.31 ml TIBA under argon atmosphere, respectively. The solution mixture was stirred for 15 minutes, the polymerization reaction was initiated by injecting the 10.00 ml styrene monomer, which was distilled at 50 °C. After polymerization times, the termination reaction was quenched by adding methanol and 10 % HCl in methanol. The polystyrene was immediately by filtration and washed with methanol several times and dried at room temperature.

This study of styrene polymerization emphasized on the effect of polymerization time, the conditions [161] for styrene polymerization by using homogeneous half-metallocene catalyst system.

$[Cp^*TiCl_3]$	=	$3 \times 10^{-4}$ mol/l
$[[PhNMe_2H]^+[B(C_6F_5)_4]^-]$	=	$3 \times 10^{-4}$ mol/l
[TIBA]	=	0.06 mol/l
[Styrene]	=	4.35 mol/l
B/Ti mole ratio	=	1
$Al_{TIBA}/Ti$ mole ratio	=	200
Toluene	=	10.00 ml
Polymerization Temperature ( $T_p$ )	=	60 °C
Polymerization Time ( $t_p$ )	=	1.0, 1.5 and 2.0 hr

## 4.5 Blend Polymer between Syndiotactic Polystyrenes and Additives

The blend of syndiotactic polystyrenes and additives were prepared by using a digital hot plate stirrer at the composition 1.0 % (w/w). sPS and GMS or CBC-33 were weighed corresponding to the desired compositions. Each sample was placed on cover slip and placed on the digital hot plate stirrer. The hot plate was set at 280 °C and mixed together in order to have a uniform mixture. After that the sample was heated to melt again at 280 °C for 1 minute, then cooled to annealing at 220 °C for 10 minutes and finally quenched to room temperature.

## 4.6 Characterization of All Polystyrene Products

### 4.6.1 Catalytic Activity

The term of catalytic activity in this study is expressed in gram of polystyrene produced by 1 mmol of titanium during 1.0 hour of polymerization time (g PS/mmol Ti.hr).

### 4.6.2 Stereospecificity

The syndiotacticity of polystyrene can be determined in a number of ways. The most widely used method involved extracting the polymer in a Soxhlet extraction with a boiling solvent. For syndiotactic polystyrene, boiling methyl ethyl ketone (MEK) was commonly used. The fraction of the whole polystyrene unextracted x 100 was a % syndiotactic index (% S.I.).

### 4.6.3 Glass Transition, Crystalline and Melting Temperature

Differential scanning calorimetry was an instrument designed to measure the thermal properties especially glass transition, crystalline and melting temperature. The T<sub>g</sub>, T<sub>c</sub> and T<sub>m</sub> of polystyrene products were determined the critical point of DSC curve.

### 4.6.4 Morphology

The morphology of the obtained polystyrene was observed with scanning electron microscopy.

### 4.6.5 Light Scattering

The light scatterings of the polystyrene products were observed with small-angle light scattering.

### 4.6.6 Crystalline Structure

The polystyrene products were analyzed for their lattice structures using wide-angle X-ray diffraction.

## CHAPTER V

### RESULTS AND DISCUSSION

#### 5.1 Polymerization of Styrene with Pentamethylcyclopentadienyltitanium Trichloride ( $Cp^*TiCl_3$ ) as Catalyst

##### 5.1.1 The Effect of Polymerization Time on Catalytic Activity

The effect of various polymerization times on styrene polymerization using  $Cp^*TiCl_3$  as catalyst, dimethyl anilinium tetrakis (pentafluoro phenyl) borate  $[PhNMe_2H]^+[B(C_6F_5)_4]^-$  as cocatalyst and triisobutylaluminum (TIBA) as scavenger was investigated. The polymerization conditions were conducted in toluene (total volume 20.00 ml),  $[Cp^*TiCl_3]$   $3 \times 10^{-4}$  mol/l,  $[PhNMe_2H]^+[B(C_6F_5)_4]^-$   $3 \times 10^{-4}$  mol/l, [TIBA] 0.06 mol/l, [styrene] 4.35 mol/l, Al/Ti 200 and polymerization temperature at 60 °C with three different polymerization time viz., 1.0, 1.5 and 2.0 hr. The experimental results and the relationship of polymerization time, % yield of polystyrene and catalytic activity of polystyrene produced are shown in Table 5.1, Figure 5.1 and Figure 5.2, respectively. As shown in Figure 5.1, % yield of polystyrene rapidly increases at the early polymerization time and then it begins to a slight increase with an increase in polymerization time in the length between 1.5 and 2.0 hr. According to a slight increase of % PS yield after 1.5 hr, it was expected that the carbocation active species formed by the reaction of  $Cp^*TiCl_3$  and  $[PhNMe_2H]^+[B(C_6F_5)_4]^-$  were shielded with the produced polystyrene. Hence, the polymerization time about 1.0 hr is the sufficient suitable time for the styrene polymerization. From Figure 5.2, the catalytic activity shows a tendency to decrease with increasing polymerization time. The maximum catalytic activity is achieved at polymerization time as 1.0 hr and then the catalytic activity gradually decreases at higher polymerization time may concern with steric effect of the produced polymer for the styrene polymerization [162].

**Table 5.1** % Yield and catalytic activity of polystyrene produced at different polymerization times <sup>a</sup>

Polymerization Time (hr)	% Yield (-)		Catalytic Activity (g PS/mmol Ti.hr)	
	Before Extraction	After Extraction	Before Extraction	After Extraction
1.0	30.05	26.01	454	393
1.5	42.94	39.26	432	395
2.0	50.01	46.56	378	352

<sup>a</sup> Polymerization conditions:  $[Cp^*TiCl_3] = [PhNMe_2H]^+[B(C_6F_5)_4]^- = 3 \times 10^{-4}$  mol/l, [styrene] = 4.35 mol/l, Al/Ti = 200,  $T_p = 60$  °C and total volume = 20.00 ml

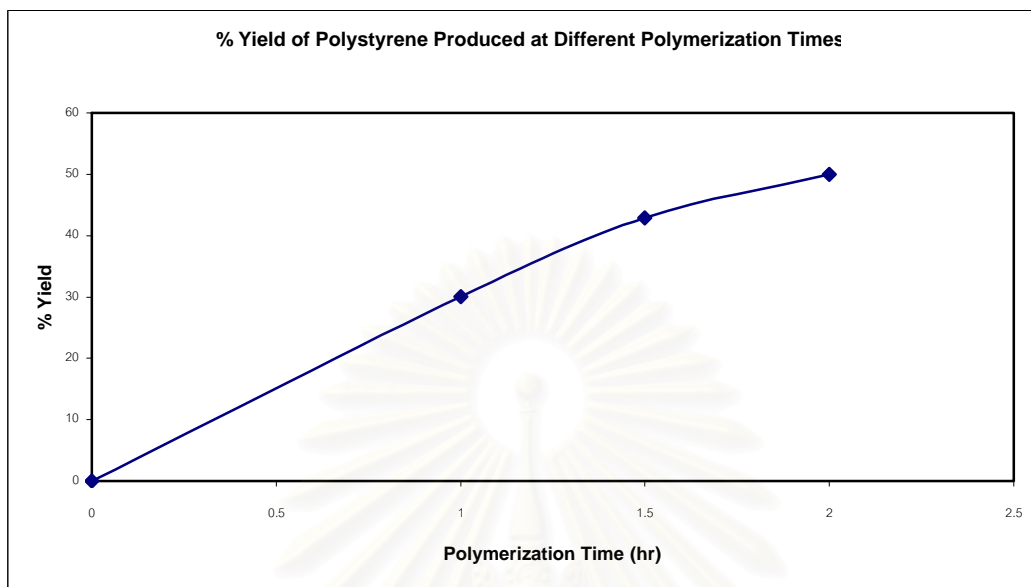


**Figure 5.1** % Yield of polystyrene produced at different polymerization times

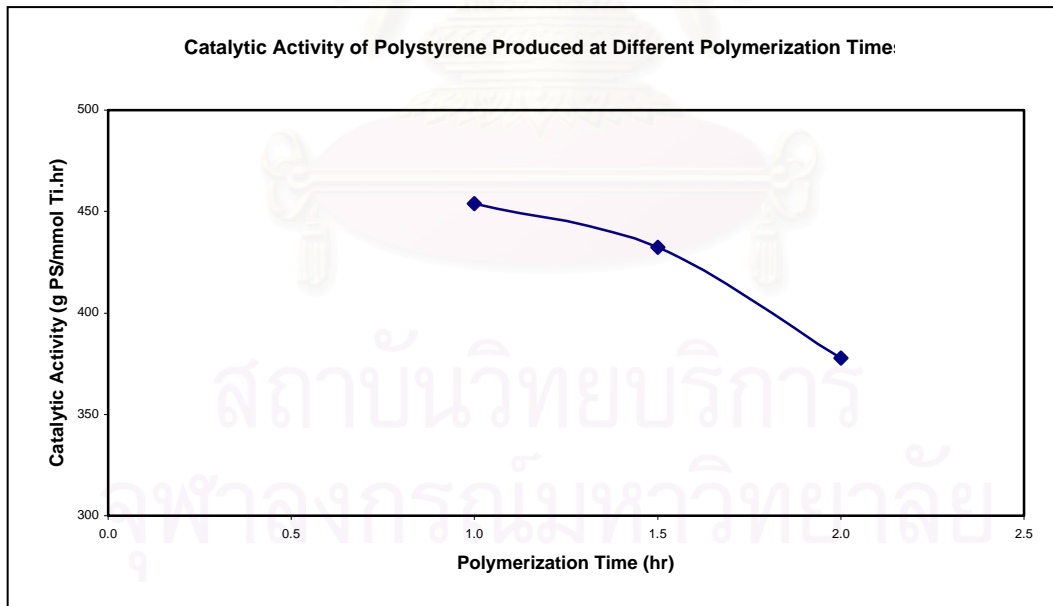


**Figure 5.2** Catalytic activity of polystyrene produced at different polymerization times

## 5.2 Characterization of All Polystyrene Products (Pure and Blend polymers) and Additives

### 5.2.1 Stereospecificity

The polystyrene product was extracted in the boiling methyl ethyl ketone by soxhlet extraction for 10 hours to investigate their syndiotacticity. Analysis of the syndiotactic index (S.I.) was calculated from the weight fraction of boiling MEK-insoluble part. The testing of syndiotacticity of polystyrene products with various polymerization times was presented in Table 5.2 and Figure 5.3.

**Table 5.2** % Syndiotactic index (% S.I.) of polystyrene products at various polymerization times <sup>a</sup>

Polymerization Time (hr)	Weight of Polystyrene Product		% Syndiotactic Index (% S.I.)
	Before Extracted (g)	After Extracted (g)	
1.0	0.0997	0.0863	86.56
1.5	0.1005	0.0919	91.44
2.0	0.1002	0.0933	93.11

<sup>a</sup> Polymerization conditions:  $[Cp^*TiCl_3] = [[PhNMe_2H]^+[B(C_6F_5)_4]^-] = 3 \times 10^{-4}$  mol/l,  $[styrene] = 4.35$  mol/l, Al/Ti = 200,  $T_p = 60$  °C and total volume = 20.00 ml

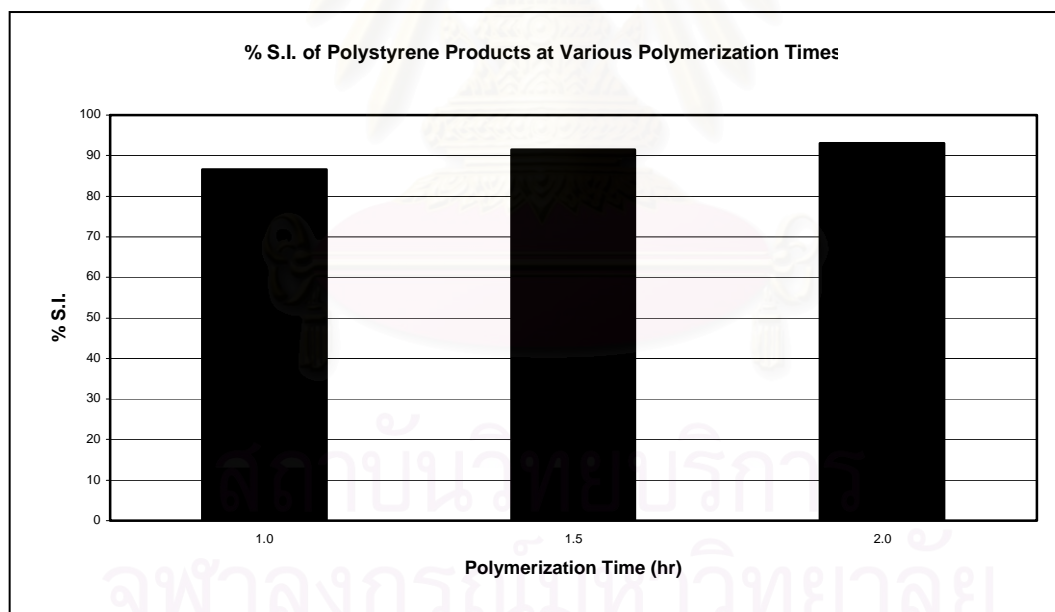


**Figure 5.3** % S.I. of polystyrene products at various polymerization times

The Figure 5.3 clearly showed that the syndiotacticity of polystyrene obtained with various polymerization times had the slight difference in every polymerization time. The results show that the increase in polymerization time from 1.0 to 2.0 hr leads to an increment of syndiotacticity of polystyrene.

### 5.2.2 Glass Transition, Crystalline and Melting Temperature

The glass transition, crystalline and melting temperature of all resulting polystyrene products and additives were evaluated by differential scanning calorimetry between +50 °C and +300 °C at 20 °C/min at a heat/cool/heat cycle. The heating cycle was run twice. The first scan, samples were heated and then cooled to room temperature. The second scan, sample were reheated at the same rate, both the results of the first and second scan were reported. In general, the first scan was influenced by the mechanical and thermal history (annealing) of samples but the second scan was influenced by the heat energy for endothermic and exothermic reaction within DSC instrument. The results of various effects, such as polymerization time and chemical that using in polymer blend on all temperatures of produced polymer are demonstrated in Table 5.3.

**Table 5.3** Glass transition, crystalline and melting temperature of the obtained polymer

Type of Polymer	Tg <sub>1</sub> (°C)	Tg <sub>2</sub> (°C)	Tc (°C)	Tm <sub>1</sub> (°C)	Tm <sub>21</sub> (°C)	Tm <sub>22</sub> (°C)
sPS 1.0 hr	90.17	89.47	224.00	254.81	241.00	254.51
sPS 1.0 hr / GMS	90.36	90.41	220.44	247.72	233.90	248.99
sPS 1.0 hr / CBC-33	90.34	90.40	209.57	250.59	237.00	250.58
sPS 1.5 hr	90.02	89.14	227.46	257.95	245.50	256.23
sPS 1.5 hr / GMS	90.28	90.09	223.37	251.33	238.10	253.16
sPS 1.5 hr / CBC-33	91.67	91.09	209.68	252.62	244.20	253.85
sPS 2.0 hr	90.00	91.68	228.24	257.15	245.90	257.22
sPS 2.0 hr / GMS	90.01	92.16	222.40	251.32	240.50	254.66
sPS 2.0 hr / CBC-33	92.19	92.08	220.58	253.81	237.70	254.30

From the above Table, all of the obtained polystyrene using the Cp\*TiCl<sub>3</sub>/[PhNMe<sub>2</sub>H]<sup>+</sup>[B(C<sub>6</sub>F<sub>5</sub>)<sub>4</sub>]/TIBA catalyst system presented glass transition, crystallization and melting temperature of pure polymers with various polymerization times, could summarized as follow:

From DSC curves, the value of Tg of sPS 1.0 hr at the first scan (Tg<sub>1</sub>) changed from 90.17 °C to 90.36 °C (different +0.19 °C) and changed to 90.34 °C (different +0.17 °C) for blend with GMS and CBC-33, respectively, whereas at the second scan (Tg<sub>2</sub>) changed from 89.47 °C to 90.41 °C (different +0.94 °C) and changed to 90.40 °C (different +0.93 °C) for blend with GMS and CBC-33, respectively. The value of Tg<sub>1</sub> of sPS 1.5 hr changed from 90.02 °C to 90.28 °C (different +0.26 °C) and changed to 91.67 °C (different +1.65 °C) for blend with GMS and CBC-33, respectively, whereas the value of Tg<sub>2</sub> changed from 89.14 °C to 90.09 °C (different +0.95 °C) and changed to 91.09 °C (different +1.95 °C) for blend with GMS and CBC-33, respectively. The value of Tg<sub>1</sub> of sPS 2.0 hr changed from 90.00 °C to 90.01 °C (different +0.01 °C) and changed to 92.19 °C (different +2.19 °C) for blend with GMS and CBC-33, respectively, whereas the value of Tg<sub>2</sub> changed from 91.68 °C to 92.16 °C (different +0.48 °C) and changed to 92.08 °C (different +0.40 °C) for blend with GMS and CBC-33, respectively. From Tg of all resulting polystyrene products, the addition of low molar mass liquid crystal and commercial lubricant to base polymer by affected the slight increasing of Tg (0.01-2.19 °C) in polymer blends that

contrasted with the fact that the blend  $T_g$  should be lower than  $T_g$  of PS because of both values of  $T_g$  of GMS and CBC-33 lesser than sPS. Thus the additive addition did not effect the value of  $T_g$  if the additive added was as low as 1.0 % w/w. Furthermore, the addition with GMS might not found the value of  $T_g$  or the peak of  $T_g$  was not clear. In addition to the peak of polymer blend at about 63 °C came GMS and the peaks at about 155 and 205 °C came from CBC-33 might not be found due to the amount of additive was very little (1.0 % w/w) in all the experiments.

The value of  $T_c$  of sPS 1.0 hr changed from 224.00 °C to 220.44 °C (different -3.56 °C) and changed to 209.57 °C (different -14.43 °C) for blend with GMS and CBC-33, respectively. The value of  $T_c$  of sPS 1.5 hr changed from 227.46 °C to 223.37 °C (different -4.09 °C) and changed to 209.68 °C (different -17.78 °C) for blend with GMS and CBC-33, respectively. The value of  $T_c$  of sPS 2.0 hr changed from 228.24 °C to 222.40 °C (different -5.84 °C) and changed to 220.58 °C (different -7.66 °C) for blend with GMS and CBC-33, respectively. From  $T_c$  of all resulting polystyrene products, the addition of low molar mass liquid crystal and commercial lubricant to base polymer by affected the reducing of  $T_c$  (3.56-17.78 °C) in polymer blends because the solid crystal phase of blend polymer more stable than the phase of pure polymer. The addition with GMS had effect in reducing  $T_c$  lesser than CBC-33. Furthermore, the reduction of  $T_c$  of sPS was characteristic that opposite with isotactic polypropylene (iPP) [174] due to the differential in stereochemistry of both polymers.

At the first scan in DSC curves, it could be found the single of melting temperature ( $T_{m1}$ ). The value of  $T_{m1}$  of sPS 1.0 hr changed from 254.81 °C to 247.72 °C (different -7.09 °C) and changed to 250.59 °C (different -4.22 °C) for blend with GMS and CBC-33, respectively. The value of  $T_{m1}$  of sPS 1.5 hr changed from 257.95 °C to 251.33 °C (different -6.62 °C) and changed to 252.62 °C (different -5.33 °C) for blend with GMS and CBC-33, respectively. The value of  $T_{m1}$  of sPS 2.0 hr changed from 245.90 °C to 240.50 °C (different -5.40 °C) and changed to 237.70 °C (different -8.20 °C) for blend with GMS and CBC-33, respectively. At the second scan, could found the double of melting temperature ( $T_{m21}$  and  $T_{m22}$ ). The value of  $T_{m21}$  of sPS 1.0 hr changed from 241.00 °C to 233.90 °C (different -7.10 °C) and changed to 237.00 °C (different -4.00 °C) for blend with GMS and CBC-33, respectively, whereas the value of  $T_{m22}$  changed from 254.51 °C to 248.99 °C (different -5.52 °C) and changed to 250.58 °C (different -3.93 °C) for blend with GMS and CBC-33, respectively. The value of  $T_{m21}$  of sPS 1.5 hr changed from 245.50 °C to 238.10 °C (different -7.40 °C) and changed to 244.20 °C (different -1.30 °C) for blend with GMS and CBC-33, respectively, whereas the value of  $T_{m22}$  changed from 256.23 °C to 253.16 °C (different -3.07 °C) and changed to 253.85 °C (different -2.38 °C) for blend with GMS and CBC-33, respectively. The value of  $T_{m21}$  of sPS 2.0 hr changed from 245.90 °C to 240.50 °C (different -5.40 °C) and changed to 237.70 °C (different -8.20 °C) for blend with GMS and CBC-33, respectively, whereas the value of  $T_{m22}$  changed from 257.22 °C to 254.66 °C (different -2.56 °C) and changed to 254.30 °C (different -2.92 °C) for blend with GMS and CBC-33, respectively. Overall  $T_m$  of the resulting polystyrene products indicated the crystallinity of material. From the first scan, the single of melting temperature was seen that the addition of low molar mass liquid crystal and commercial lubricant to base polymer by affected the reducing of  $T_{m1}$  (4.22-8.2 °C), whereas the second scan, the double of melting temperatures were seen that the addition of additives by affected the reducing of  $T_{m21}$  (1.30-8.20 °C) and  $T_{m22}$  (2.38-5.22 °C). From  $T_m$  of all resulting polystyrene products, the addition with

GMS blend have slightly lower  $T_m$  than CBC-33, but stay within the same quantity due to the amount of additive was very little (1.0 % w/w) in all experiments. It indicated that the solid crystal phase of polymer blend with GMS began to melt before the polymer blend with CBC-33 and the GMS addition disturbed the occurrence of the solid crystal phase more than the addition of CBC-33. The main reason of reduction of  $T_m$  when polymer had additive was the increasing of the molecular mobility of the blends when added with low concentration. GMS could also improve the mobility of the blend but in lesser extent and the effect did not increase at higher concentration. On the other hand, the more LC added, the higher the mobility [167,170]. So we expected to  $T_m$  might be reduce due to the molecule could move or separate easily.

The almost all values of  $T_g$  of blend polymers were constant, but  $T_c$  and  $T_m$  of blend were reduced when compared with pure polymers. This phenomenon indicated that the polymer blends, which contained additives were improved in their process ability, modification of polymers could enhance the molecular mobility of melt mixed blends and improved the blends melt flow properties.

**Table 5.4** Melting enthalpy and % crystallinity of the obtained polymer

Type of Polymer	$\Delta H_{f1}$ (J/g)	$\Delta H_{f2}$ (J/g)	$\Delta H_c$ (J/g)	% Crystallinity (-)
sPS 1.0 hr	28.51	24.35	24.63	45.94
sPS 1.0 hr / GMS	33.16	33.17	31.53	63.22
sPS 1.0 hr / CBC-33	35.71	31.32	37.61	59.69
sPS 1.5 hr	30.27	30.10	30.40	56.79
sPS 1.5 hr / GMS	33.46	32.25	32.70	61.46
sPS 1.5 hr / CBC-33	30.70	30.67	32.47	58.45
sPS 2.0 hr	31.33	31.51	21.28	59.45
sPS 2.0 hr / GMS	31.62	31.59	27.91	60.21
sPS 2.0 hr / CBC-33	31.34	32.26	30.08	61.48

The normalized crystallinity of sPS ( $\chi_c$ ) is given by the following equation [168]:

$$\chi_c = [(\Delta H_f / \Delta H_f^0) / \omega] \times 100$$

where  $\Delta H_f$  = the melting enthalpy of the blend  
 $\Delta H_f^0$  = the melting enthalpy of 100 % crystalline sPS (53 J/g)  
 $\omega$  = the weight fraction of sPS in the blend

At the first heat scan in DSC curves, the value of  $\Delta H_{f1}$  of sPS 1.0 hr changed from 28.51 J/g to 33.16 J/g (different +4.65 J/g) and changed to 35.71 J/g (different +7.20 J/g) for blend with GMS and CBC-33, respectively, whereas at the heat second scan, the value of  $\Delta H_{f2}$  changed from 24.35 J/g to 33.17 J/g (different +8.82 J/g) and changed to 31.32 J/g (different +6.97 J/g) for blend with GMS and CBC-33, respectively. The value of  $\Delta H_{f1}$  of sPS 1.5 hr changed from 30.27 J/g to 33.46 J/g (different +3.19 J/g) and changed to 30.70 J/g (different +0.43 J/g) for blend with GMS and CBC-33, respectively, whereas the value of  $\Delta H_{f2}$  changed from 30.10 J/g to 32.25 J/g (different +2.15 J/g) and changed to 30.67 J/g (different +0.57 J/g) for blend



with GMS and CBC-33, respectively. The value of  $\Delta H_{f1}$  of sPS 2.0 hr changed from 31.33 J/g to 31.62 J/g (different +0.29 J/g) and changed to 31.34 J/g (different +0.01 J/g) for blend with GMS and CBC-33, respectively, whereas the value of  $\Delta H_{f2}$  changed from 31.51 J/g to 31.59 J/g (different +1.49 J/g) and changed to 32.26 J/g (different +2.16 J/g) for blend with GMS and CBC-33, respectively. At the cool scan, the value of  $\Delta H_c$  of sPS 1.0 hr changed from 24.63 J/g to 31.53 J/g (different +6.90 J/g) and changed to 37.61 J/g (different +12.98 J/g) for blend with GMS and CBC-33, respectively. The value of  $\Delta H_c$  of sPS 1.5 hr changed from 30.40 J/g to 32.70 J/g (different +2.30 J/g) and changed to 32.47 J/g (different +2.07 J/g) for blend with GMS and CBC-33, respectively. The value of  $\Delta H_c$  of sPS 2.0 hr changed from 21.28 J/g to 27.91 J/g (different +6.63 J/g) and changed to 30.08 J/g (different +8.80 J/g) for blend with GMS and CBC-33, respectively. From  $\Delta H_f$  and  $\Delta H_c$  of all resulting polystyrene products, the addition of low molar mass liquid crystal and commercial lubricant to base polymer by affected the increasing of  $\Delta H_f$  (0.01-8.82 J/g) and  $\Delta H_c$  (2.07-12.98) in polymer blends, meaning that % crystallinity ( $\% \chi_c$ ) of blend polymer are higher than pure polymer. The increase in normalized crystallinity of sPS in the blends was probably due to the penetration of additives into sPS domain enhanced by the molecular mobility of melt mixed blends and improved the blends melt flow properties [167,170]. In the fact, each the value of  $\Delta H$  at scan in DSC might have the equal value or same value but in the experiment did not, the reason that each the value of  $\Delta H$  at scan not same value because the choiceness of the length for area under curve, which could occur the error of % crystallinity. Out side of the melting enthalpy for decompose crystalline ( $\Delta H_f$ ) was nearly with the melting enthalpy for construct crystalline ( $\Delta H_c$ ) it indicated that measurement was accurate and the additives addition affect to increasing  $\Delta H_f$  and  $\Delta H_c$  in the same values, although the other polymers were used in the experiment.

### 5.2.3 Morphology

The additives and all polystyrene products in this study was observed by scanning electron microscope to determine its morphology as exhibited in Figure 5.4, Figure 5.5 and Figure 5.6-5.17, respectively. All morphologies of pure polymers showed slight differences, it indicated that all pure polymers with the different polymerization time had closely the same chemical. In addition, the SEM images of polystyrene after extraction showed similar. Therefore, extraction could be removed atactic part in polystyrene, also improved the morphology of polystyrene.

จุฬาลงกรณ์มหาวิทยาลัย

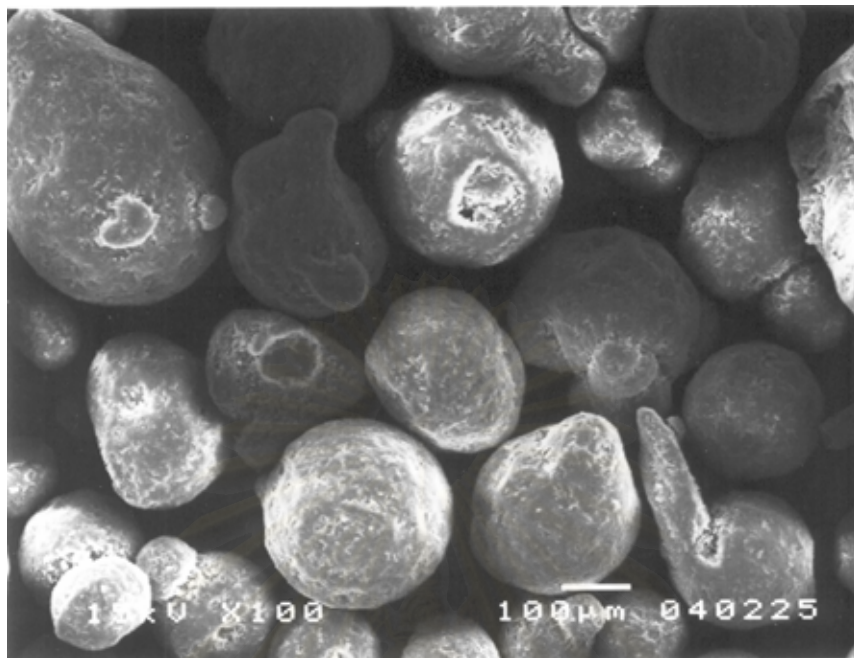


**Figure 5.4** SEM image of GMS



**Figure 5.5** SEM image of CBC-33

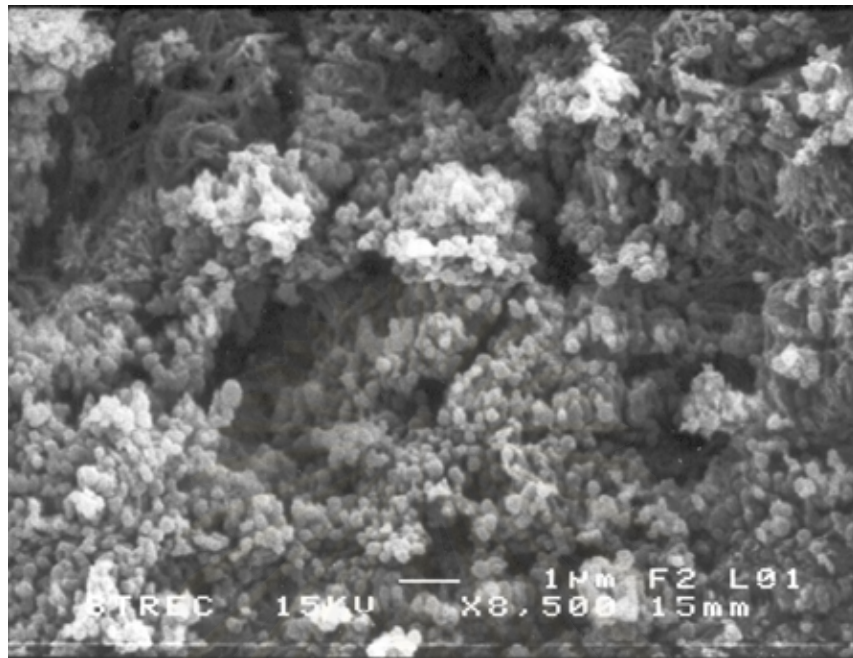


**Figure 5.6** SEM image of polystyrene 1.0 hr (before extracted)

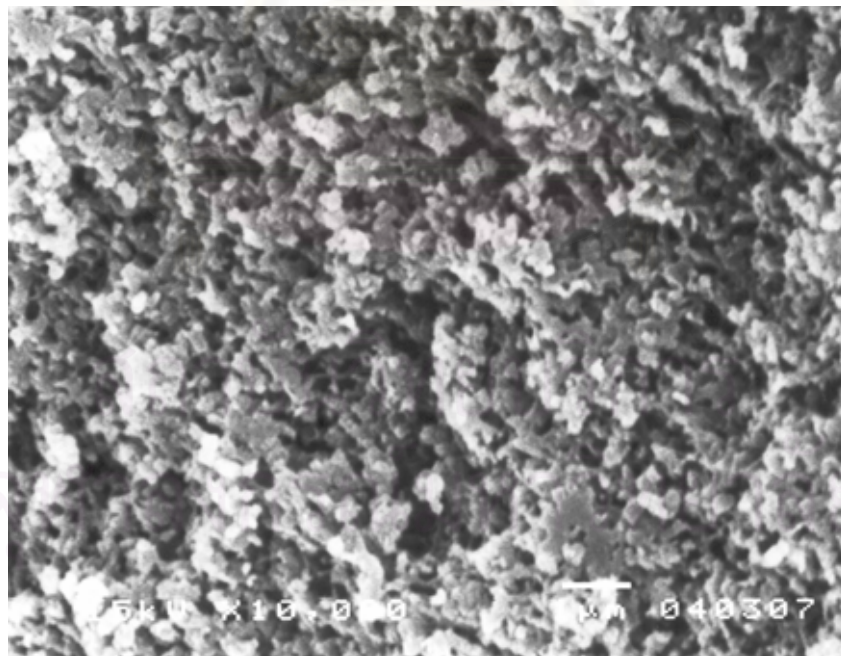


**Figure 5.7** SEM image of polystyrene 1.0 hr (after extracted)

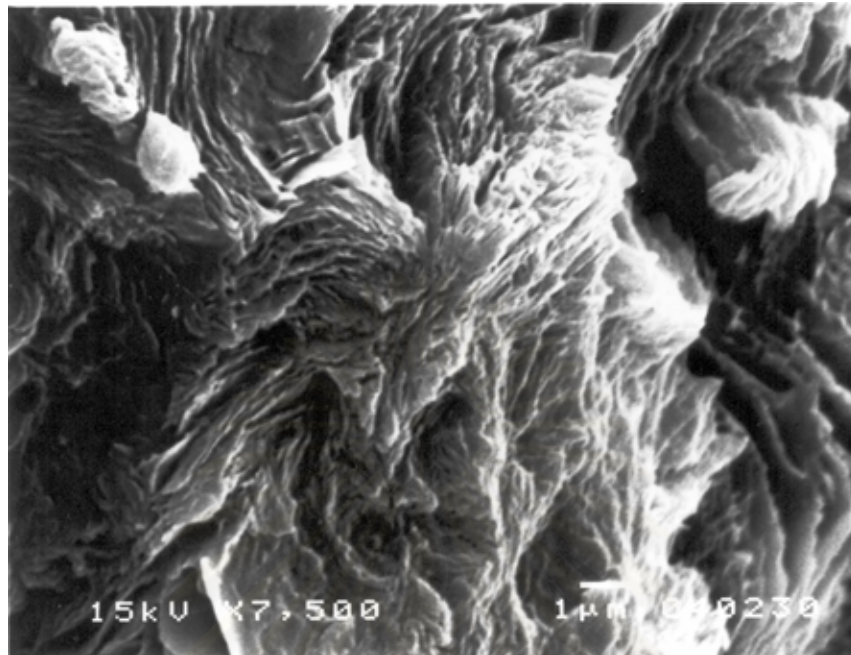


**Figure 5.8** SEM image of polystyrene 1.0 hr blended with GMS

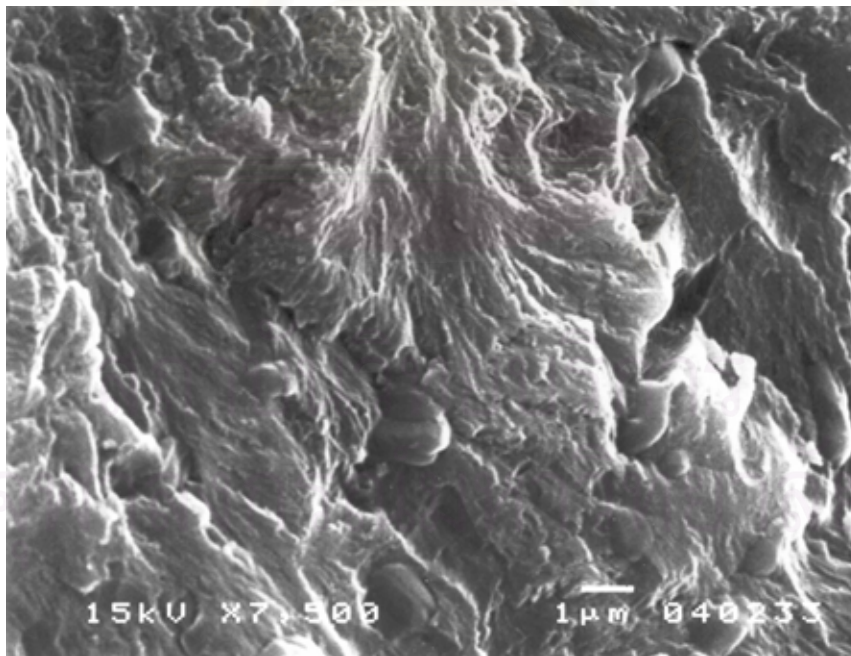


**Figure 5.9** SEM image of polystyrene 1.0 hr blend with CBC-33

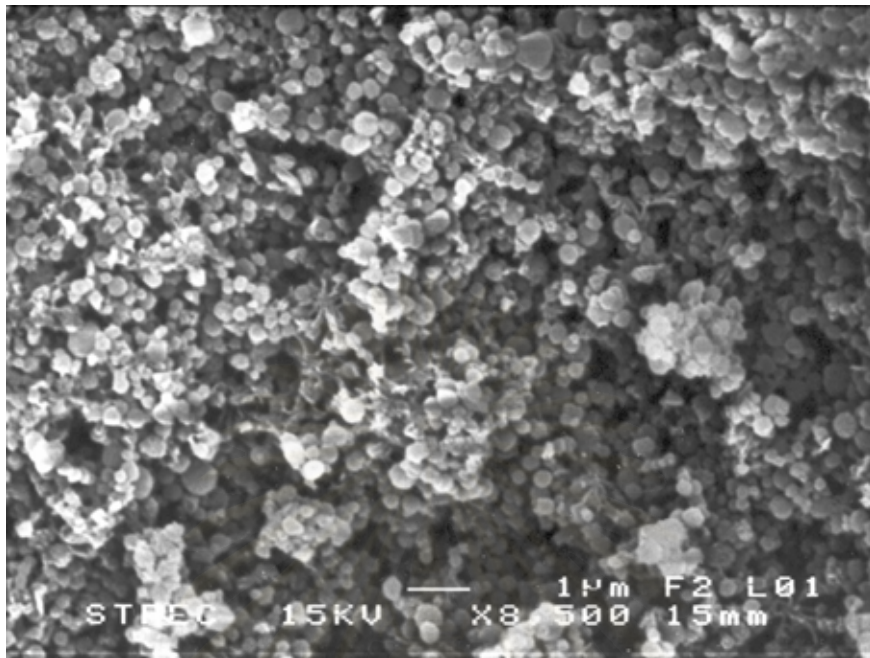


**Figure 5.10** SEM image of polystyrene 1.5 hr (before extracted)

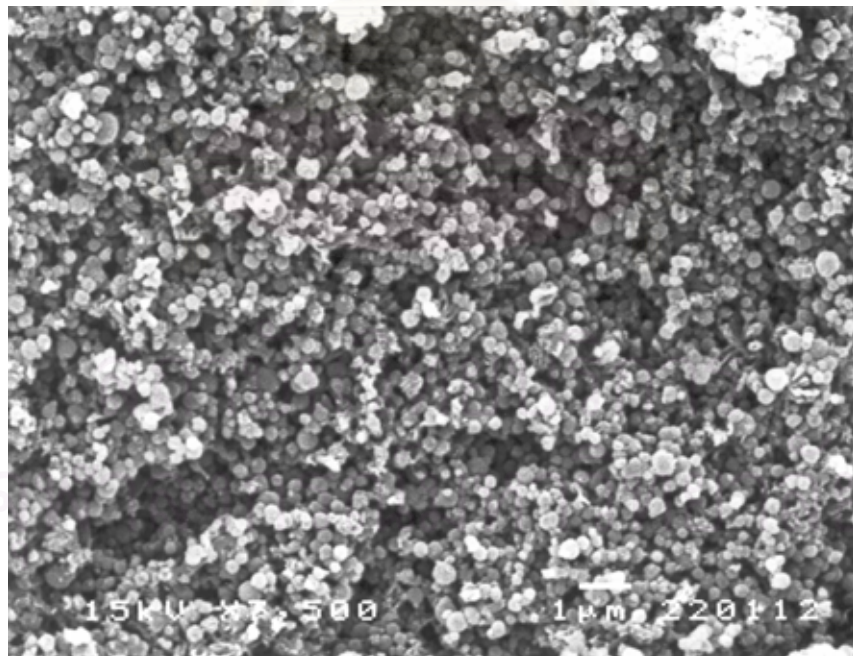


**Figure 5.11** SEM image of polystyrene 1.5 hr (after extracted)

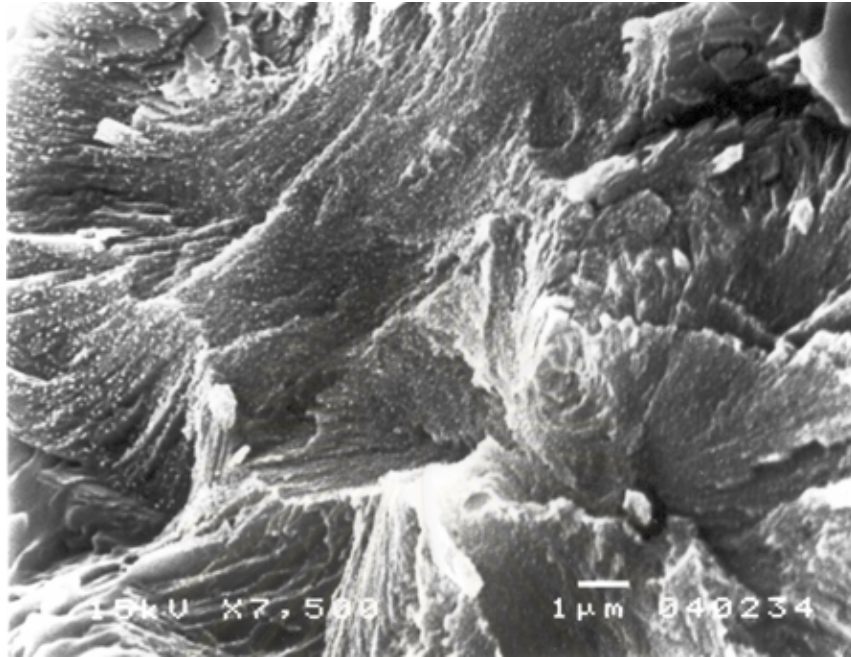


**Figure 5.12** SEM image of polystyrene 1.5 hr blend with GMS

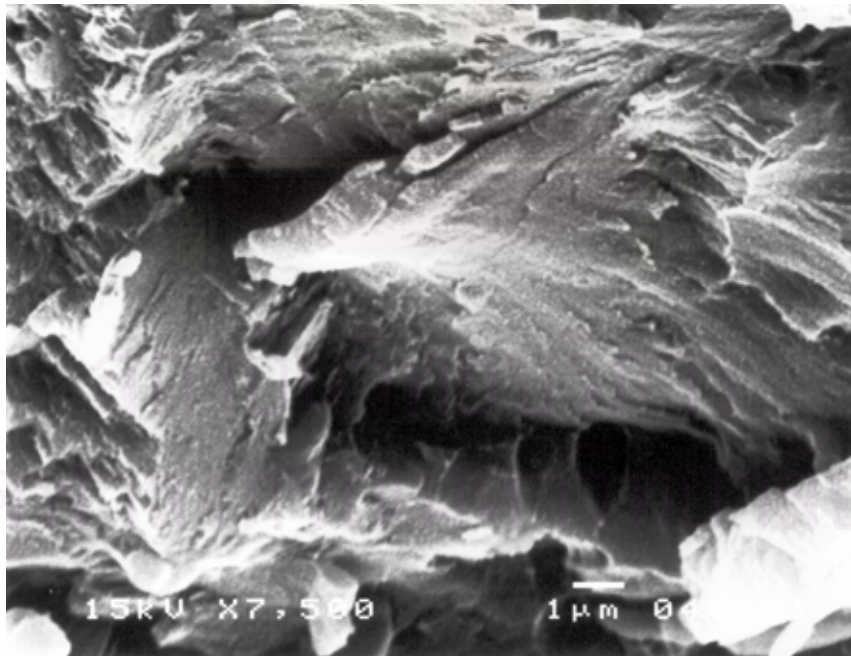


**Figure 5.13** SEM image of polystyrene 1.5 hr blend with CBC-33

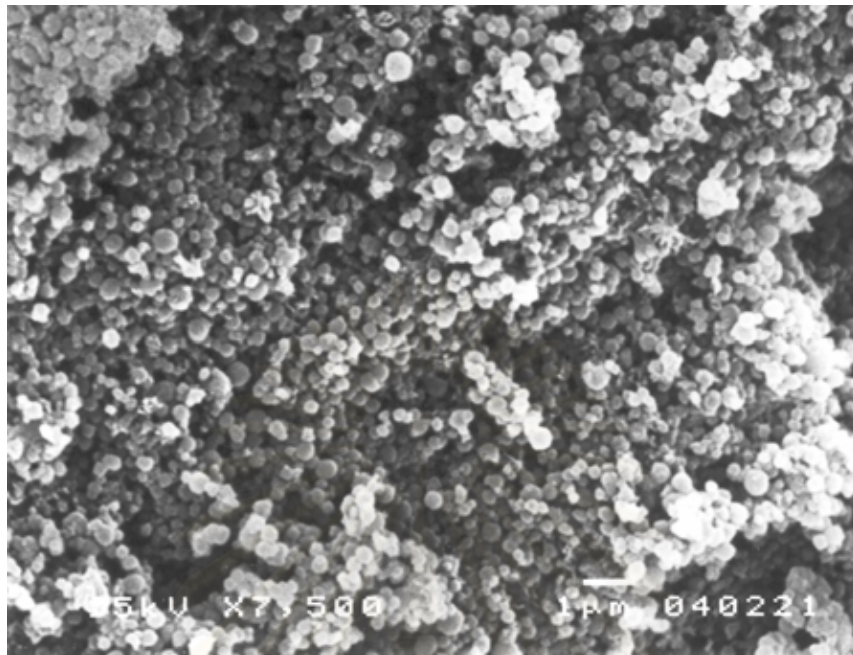


**Figure 5.14** SEM image of polystyrene 2.0 hr (before extracted)

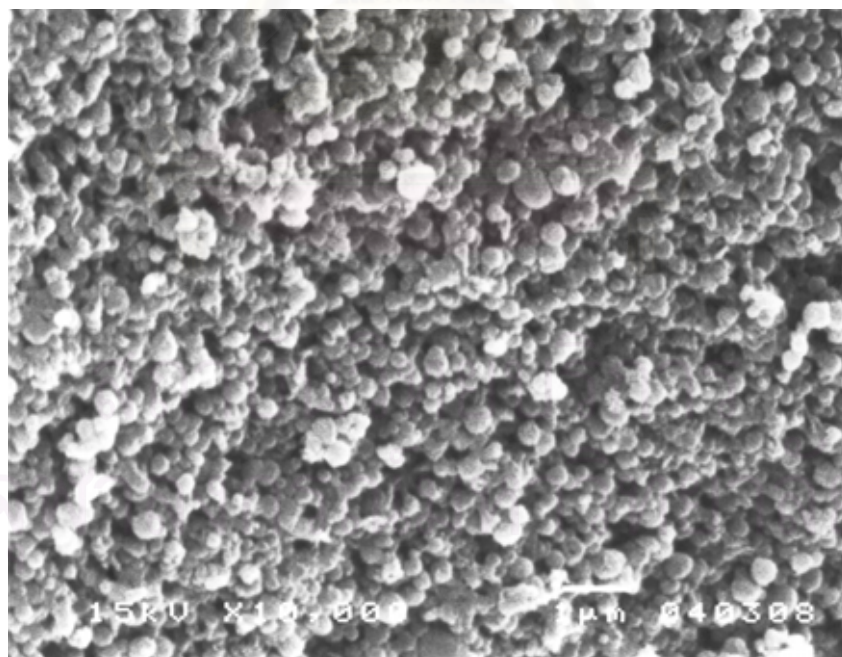


**Figure 5.15** SEM image of polystyrene 2.0 hr (after extracted)

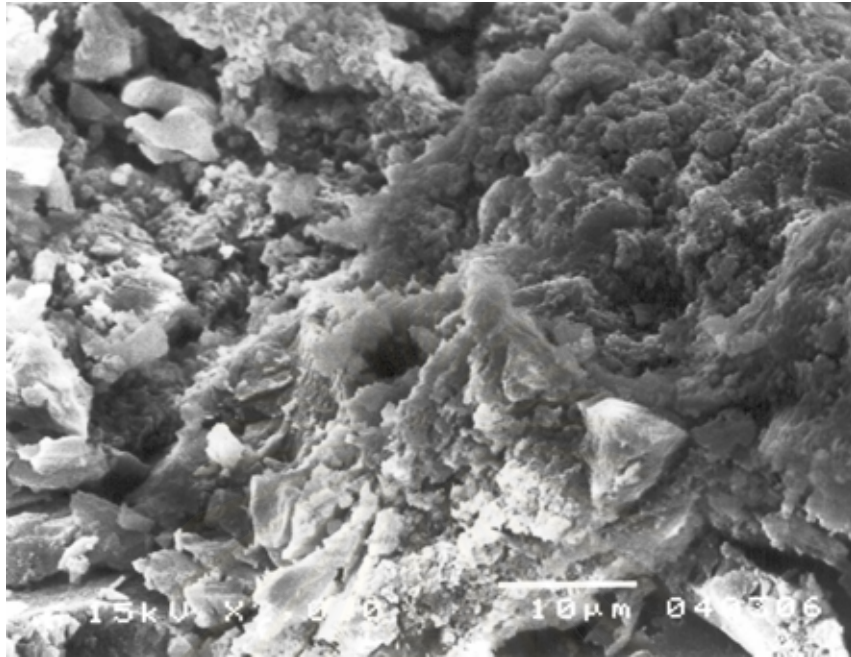


**Figure 5.16** SEM image of polystyrene 2.0 hr blend with GMS

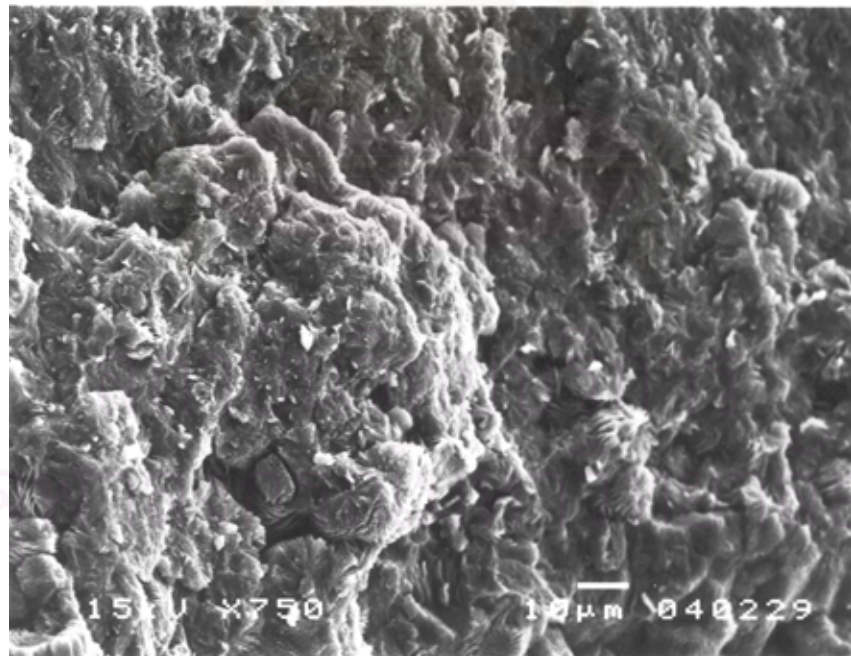


**Figure 5.17** SEM image of polystyrene 2.0 hr blend with CBC-33

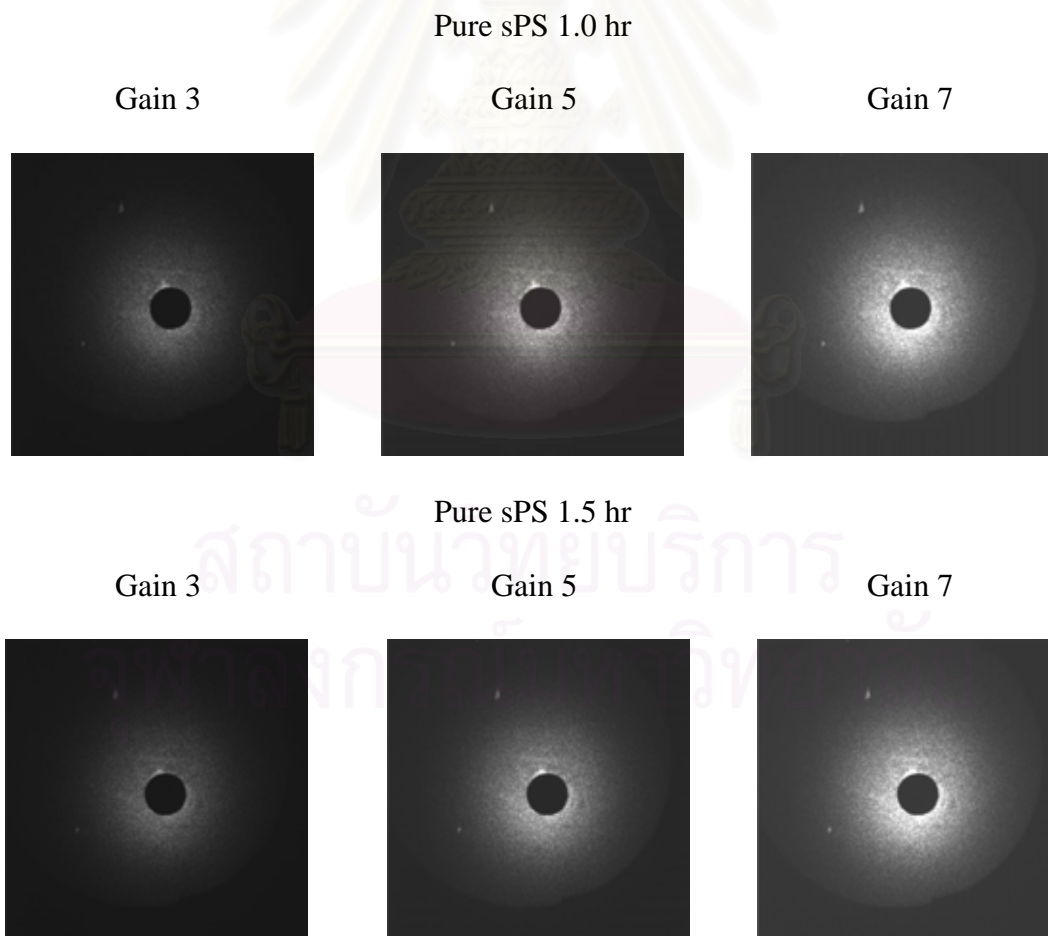


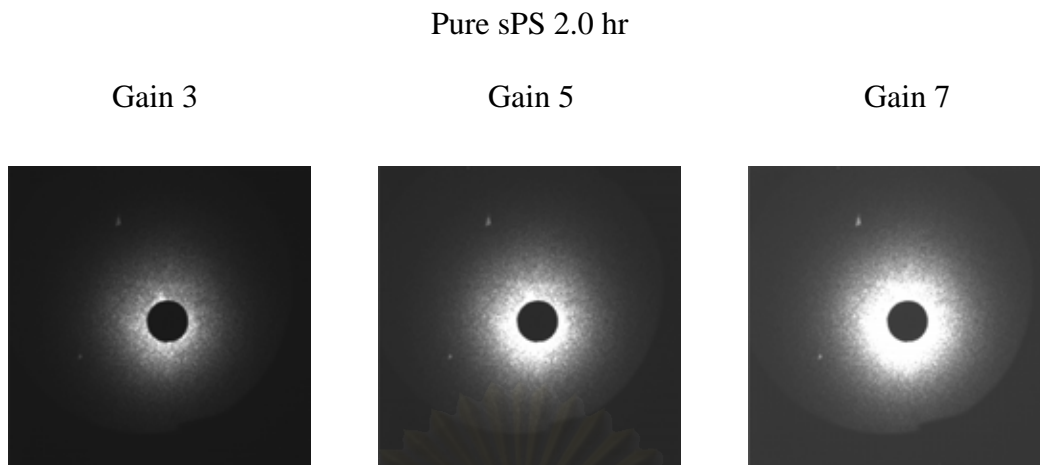
## 5.2.4 Light Scattering Measurement

There are two parts of the results from light scattering experiment, scattered light photographs and digital intensity data.

### 5.2.4.1 Scattered Light Photographs

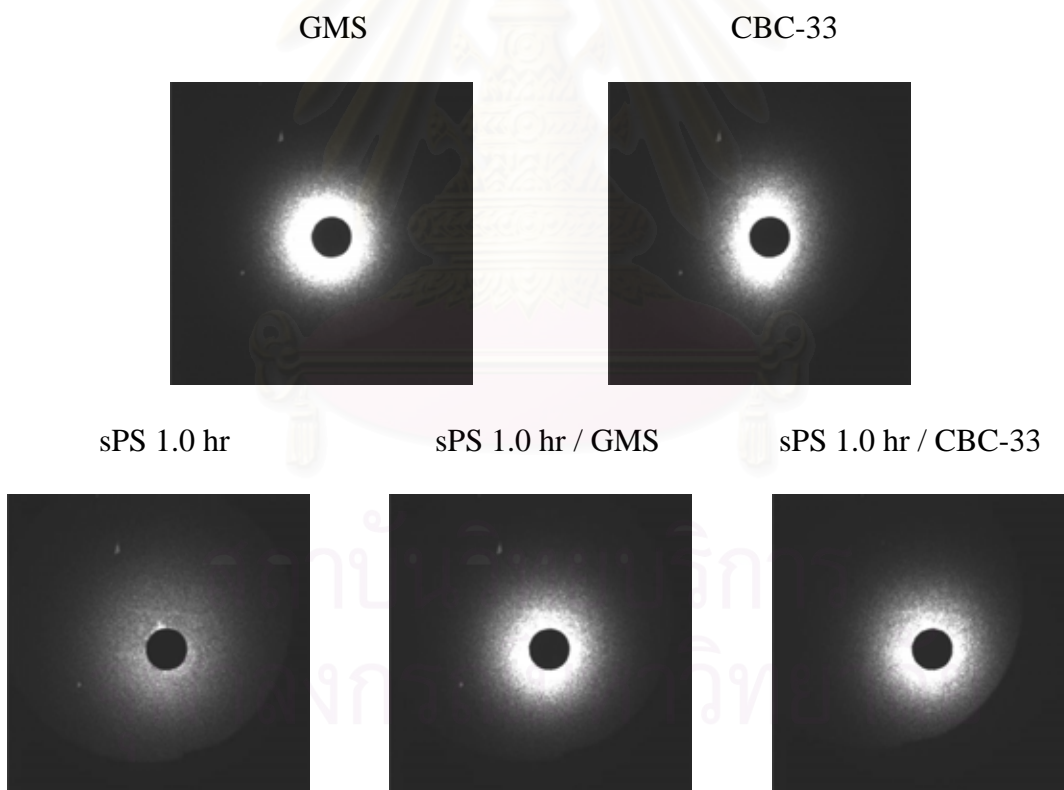
Light scattering behaviors of the system of polymer blends between syndiotactic polystyrenes with additives were investigated by using the modified Small-Angle Light Scattering (SALS) apparatus with the illumination of light no.3 (gain 3), no.5 (gain 5) and no.7 (gain 7). This apparatus will show the scattered light photographs that are both the single image and successive images. Furthermore it can provide digital intensity data at every angle of scattering. This modification is different from the original apparatus, which use only the photographic into the computer. Unlike the modified apparatus, the original apparatus can measure intensity at some angle of scattering. Therefore there are many information from the modified apparatus. Figure 5.18 shows scattered light photographs of three pure components. Form the result of light scattering behavior, the best results is no.5 (gain 5) because some images from no.3 (gain 3) are very darkness and some images from no.7 (gain 7) are very brightness.





**Figure 5.18** Scattered light photographs of pure sPS 1.0, 1.5 and 2.0 hr that vary intensity of light

Figure 5.19 shows scattered light photographs of pure components and the blends at 1 % by weight from no.5 (gain 5), the result of light scattering behavior is between two types of pure component.



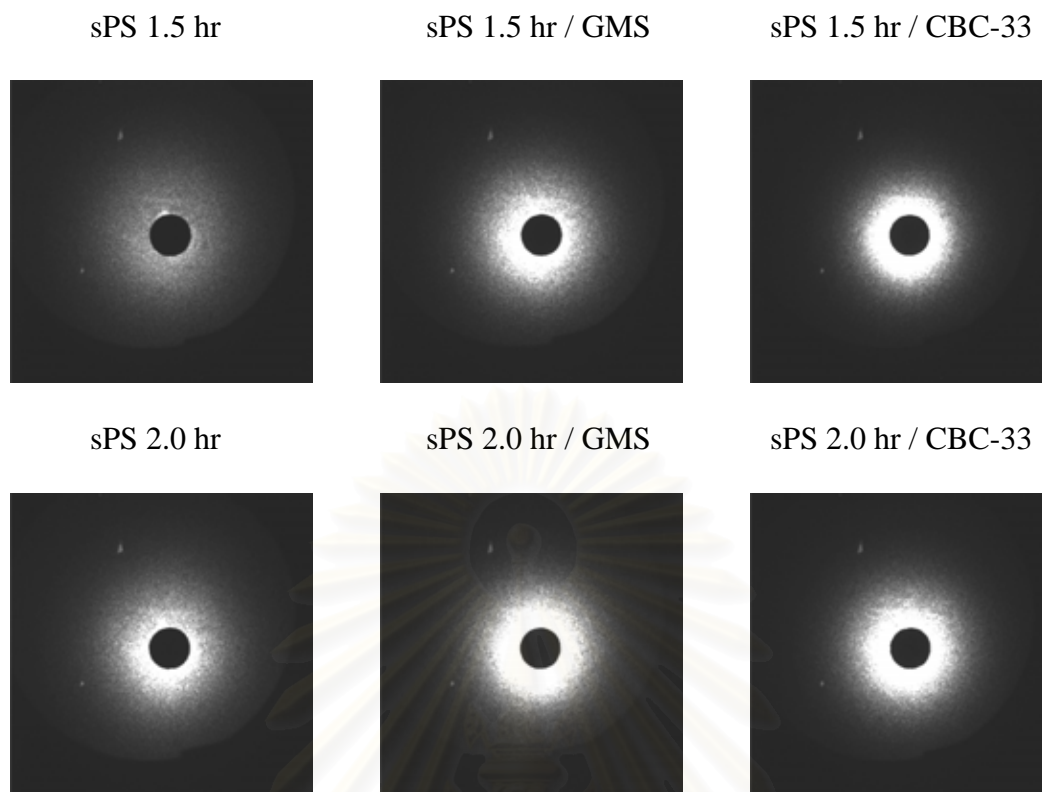


**Figure 5.19** Scattered light photographs of additives, pure polymers and their blends

#### 5.2.4.2 Digital Intensity Data

The static light scattering apparatus can provide digital intensity data for every pixel. For one light scattering photograph, it contains 49,665 data points of digital intensity and it can be plot as shown in Figure 5.20.

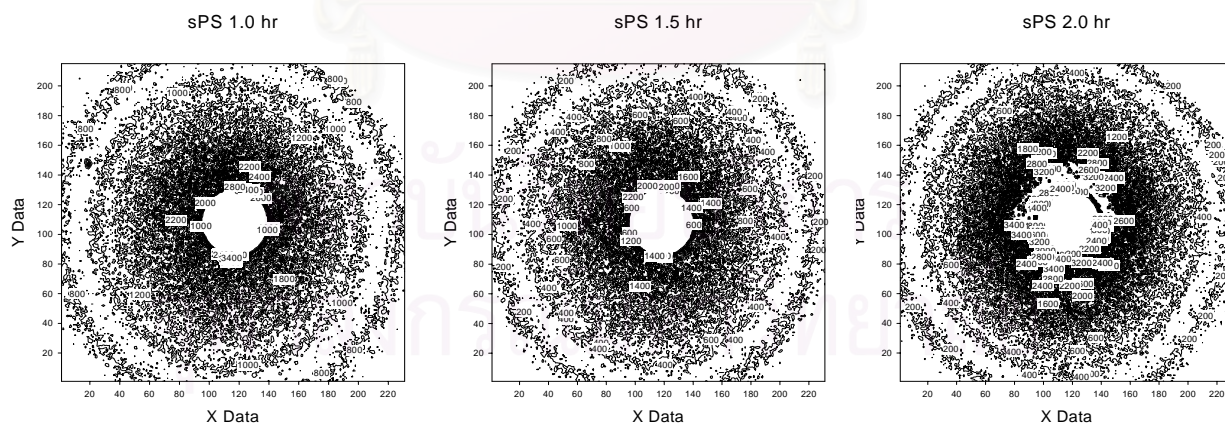


**Figure 5.20** Scattered light contour graph of pure sPS 1.0, 1.5 and 2.0 hr

Form Figure 5.20, the data points are processed as shown in the schematic diagram (Figure 5.21) in order to obtain smooth contour lines.

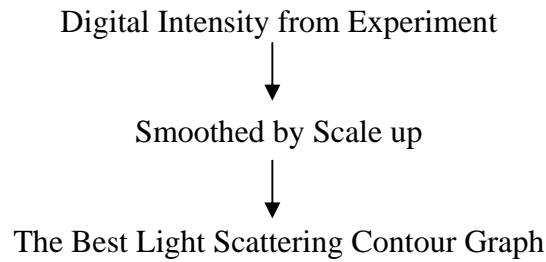


**Figure 5.21** Schematic diagram of smoothing procedure

This procedure is auto running by using sub-programming, which can be run within 3 minutes.

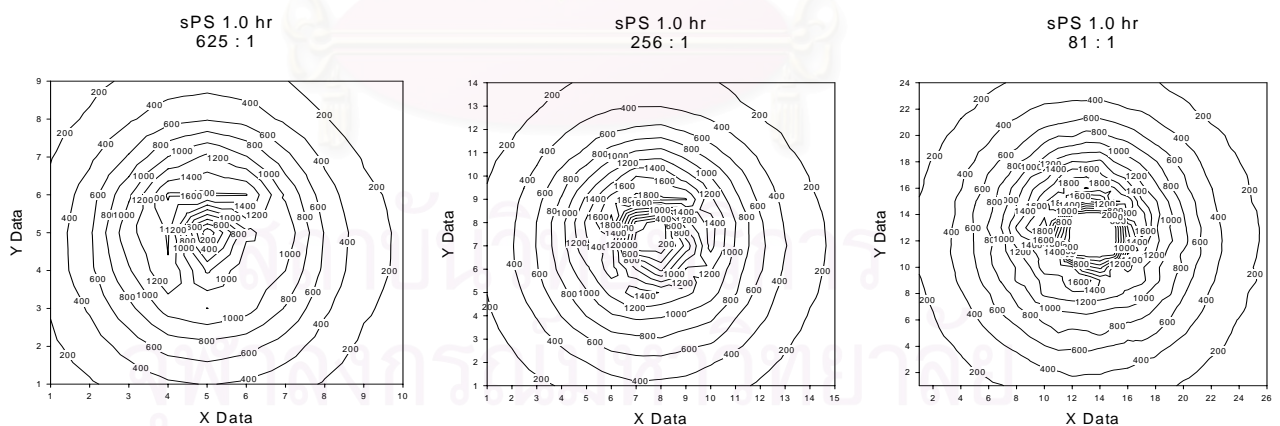
#### 5.2.4.2.1 Smoothing Digital Intensity Data

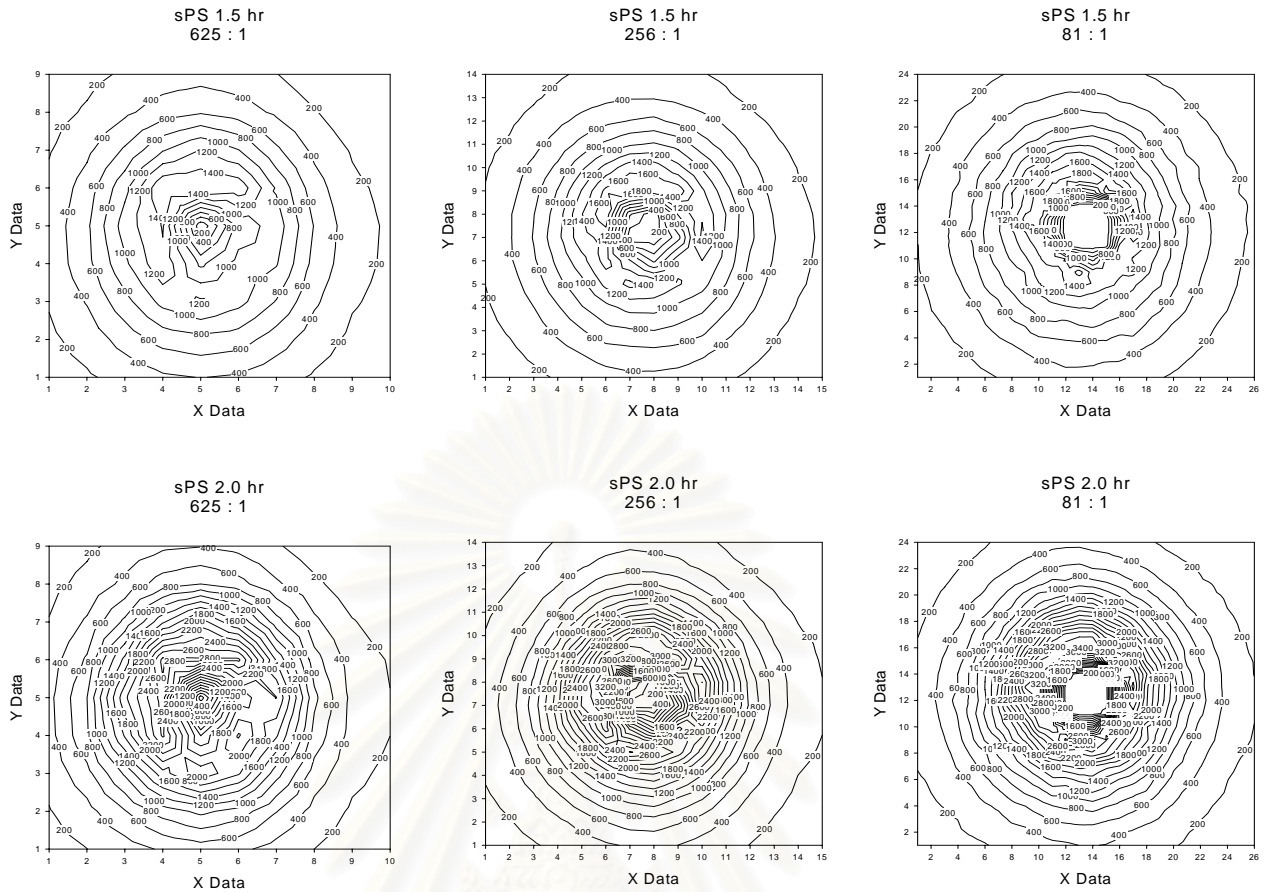
Using the average of intensity data to get better contour graphs that are clear smoothes digital intensity data and the characteristics of their curvatures are the same. In searching the standard procedure, many trials and errors were done by varying the number of intensity data, which are averaged, and collected in details. The detail of that trial can be concluded as follow.

Trial and error (the number of averaged intensity : a mean value).

- (a) 625 : 1
- (b) 256 : 1
- (c) 81 : 1

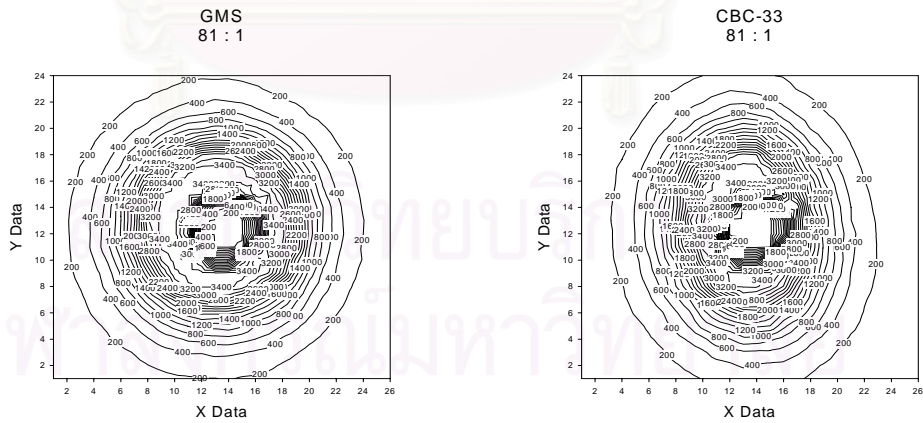
Results from trial and error are shown as contour graphs:





**Figure 5.22** Contour graphs of trial and error in smoothing intensity data

From these results, the best results is 81 : 1 because the graph fit with the scale and it is not too small graph as well as its contour line can be distinguishable.



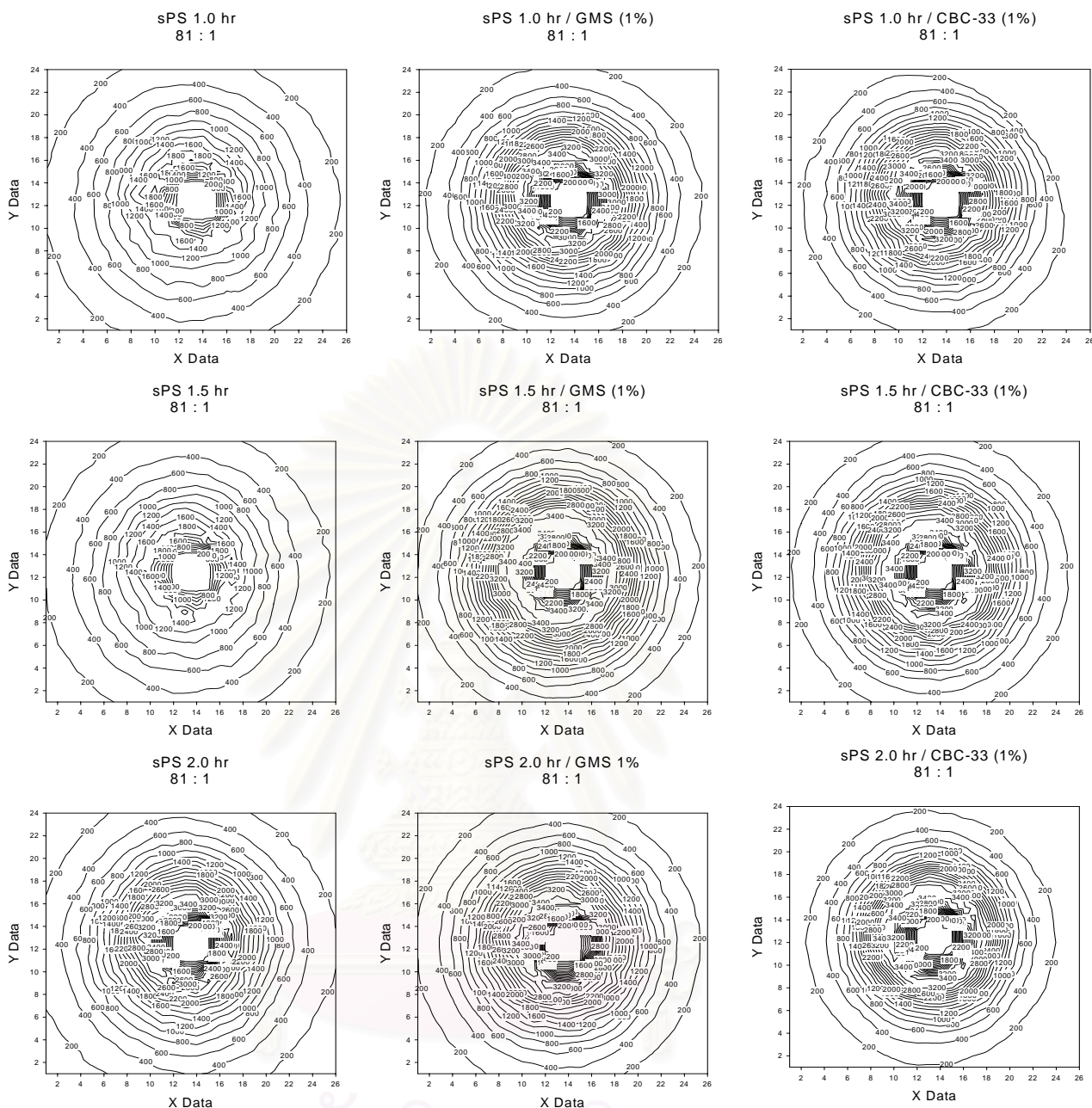


**Figure 5.23** Smoothed contour graphs of additives, pure polymers and their blends

The light scattering of polystyrene obtained with various polymerization times had the slight difference in every polymerization time. Furthermore, the addition of GMS and CBC-33 to base sPS by affected the increasing of light scattering in polymer blends due to the addition of additive to base polymer by effected to raise of the solid crystal phase.

### 5.2.5 Crystalline Structure

The additives and all polystyrene products were examined using wide-angle X-ray diffraction and the X-ray diffraction pattern were compared as shown in Figure 5.24, Figure 5.25 and Figure 5.26-5.34, respectively.

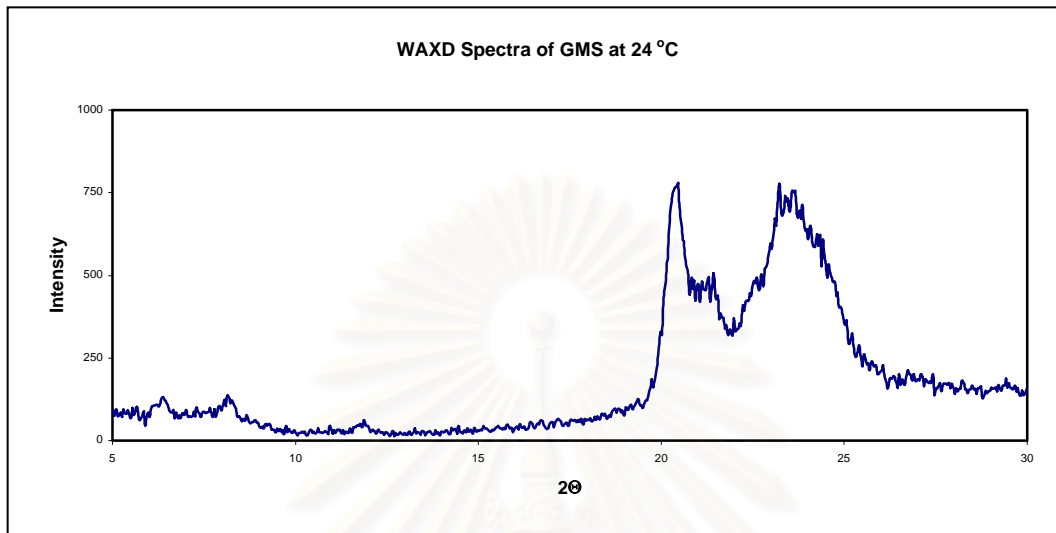


Figure 5.24 XRD patterns of GMS

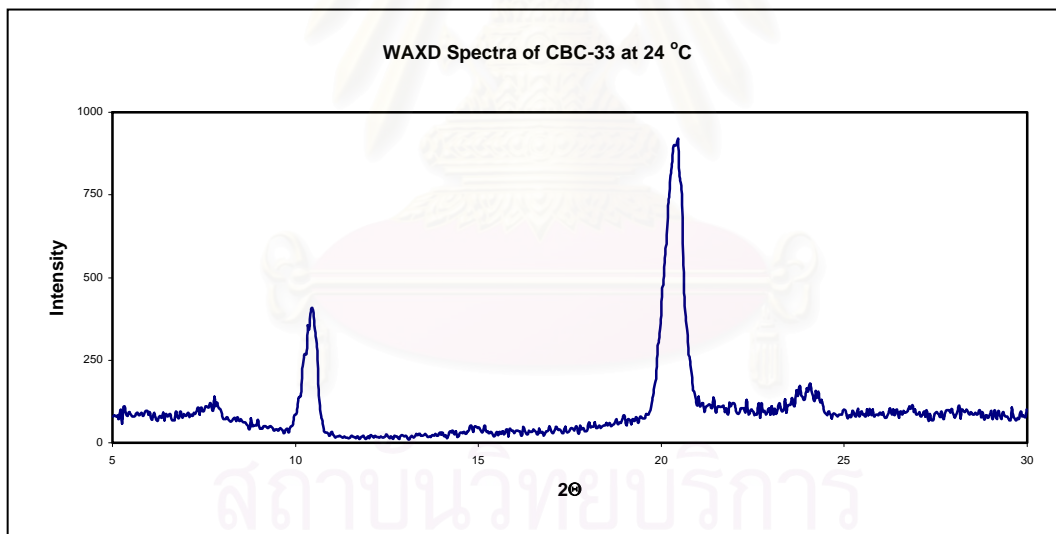


Figure 5.25 XRD patterns of CBC-33

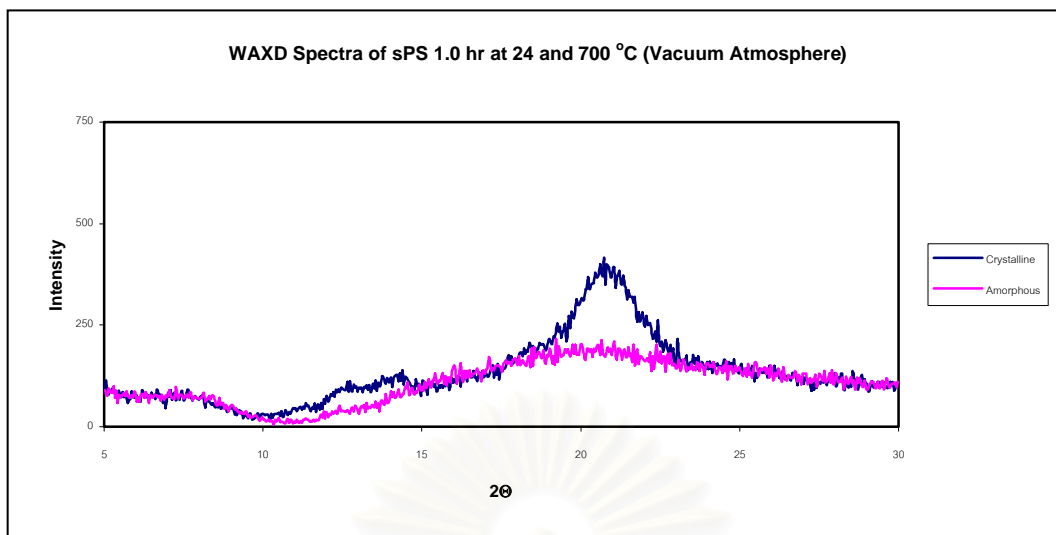


Figure 5.26 XRD patterns of polystyrene 1.0 hr

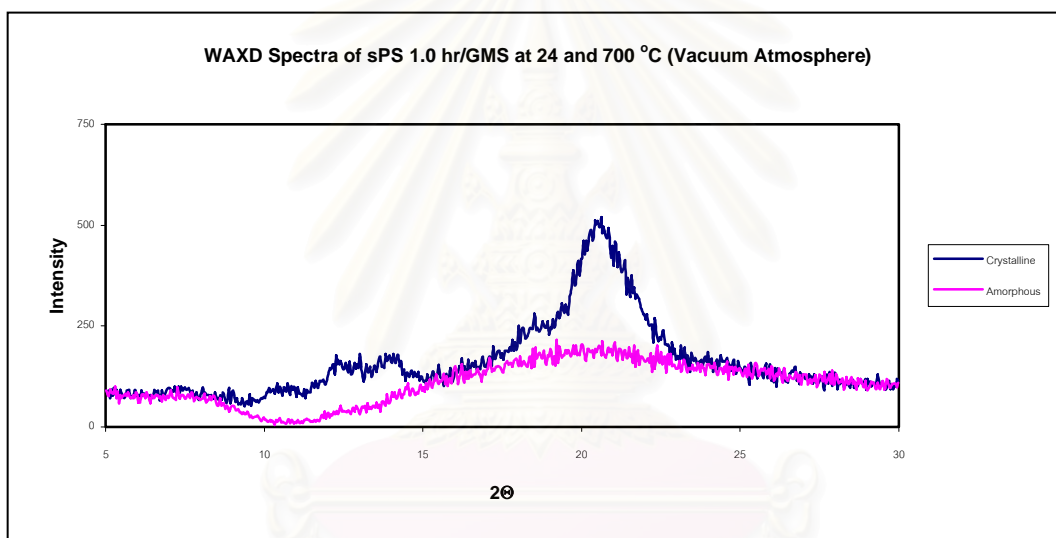


Figure 5.27 XRD patterns of polystyrene 1.0 hr blended with GMS

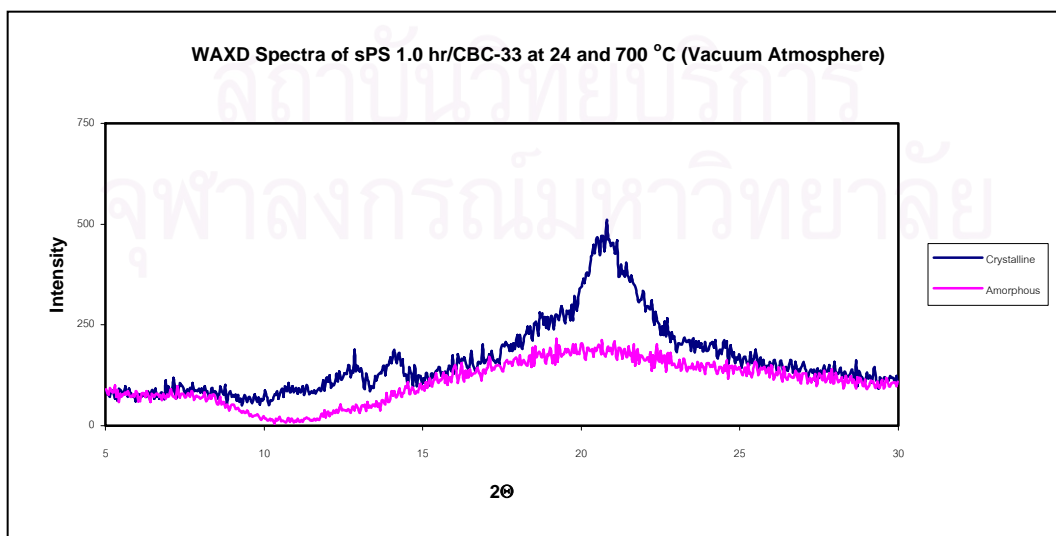


Figure 5.28 XRD patterns of polystyrene 1.0 hr blend with CBC-33



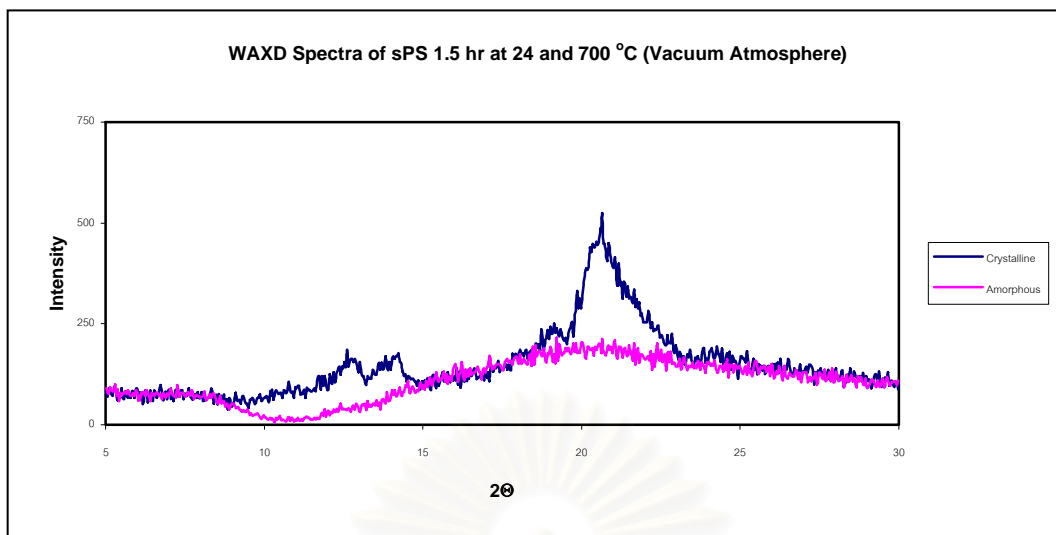


Figure 5.29 XRD patterns of polystyrene 1.5 hr

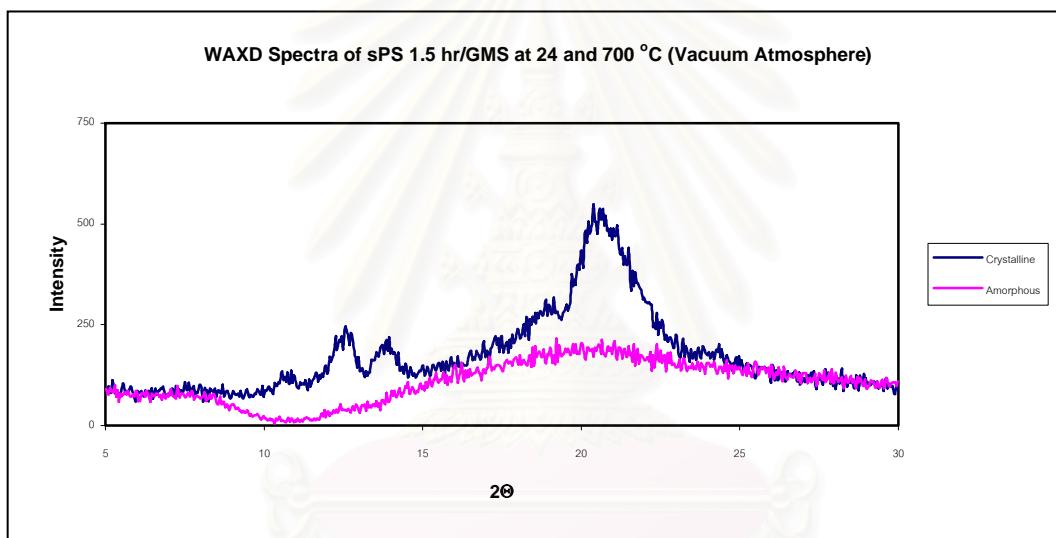


Figure 5.30 XRD patterns of polystyrene 1.5 hr blend with GMS

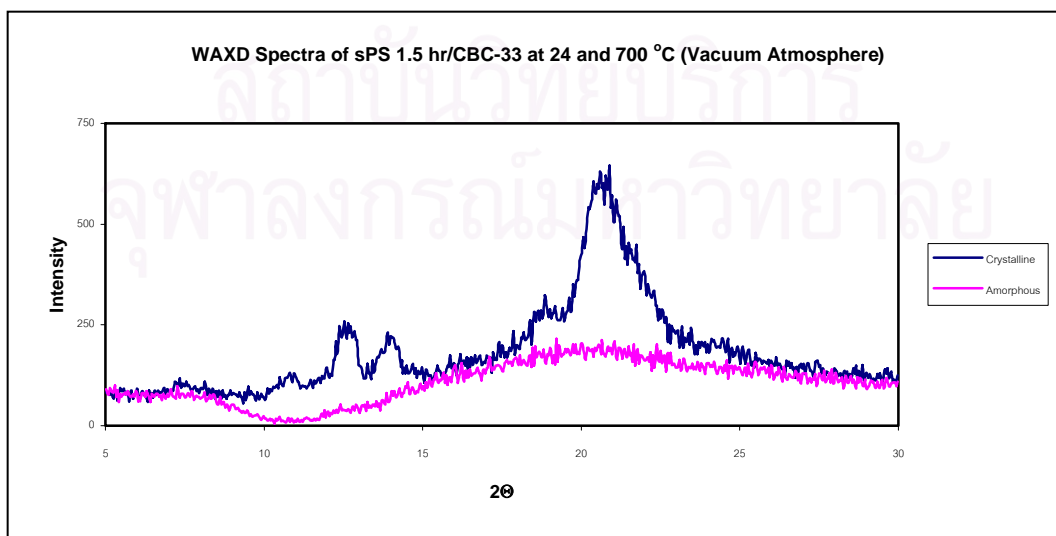


Figure 5.31 XRD patterns of polystyrene 1.5 hr blend with CBC-33

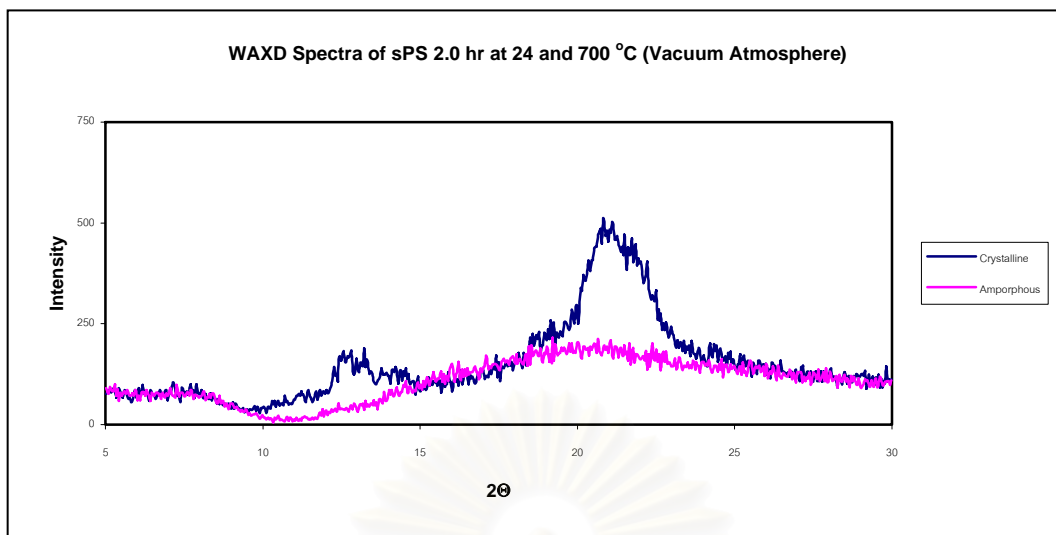


Figure 5.32 XRD patterns of polystyrene 2.0 hr

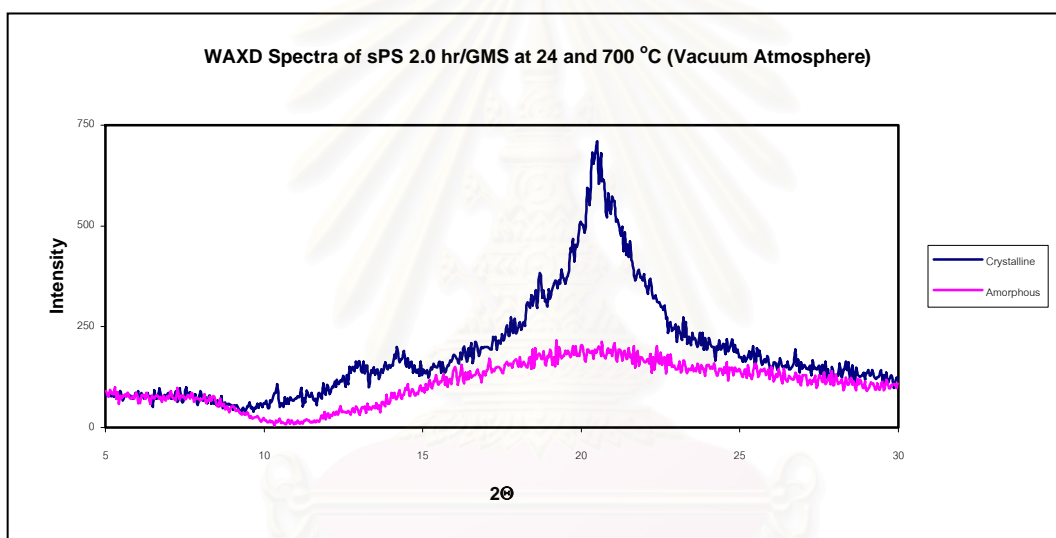


Figure 5.33 XRD patterns of polystyrene 2.0 hr blend with GMS

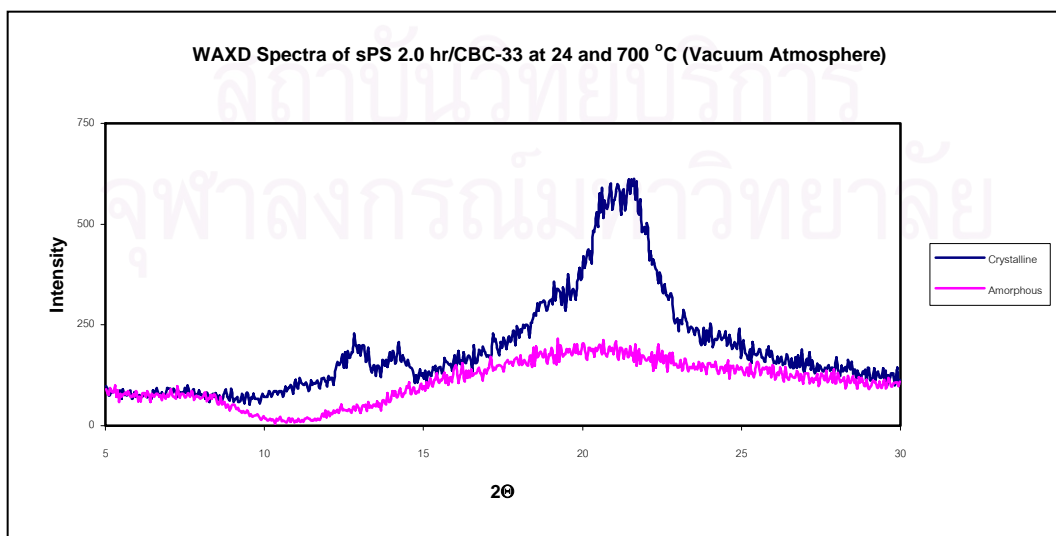
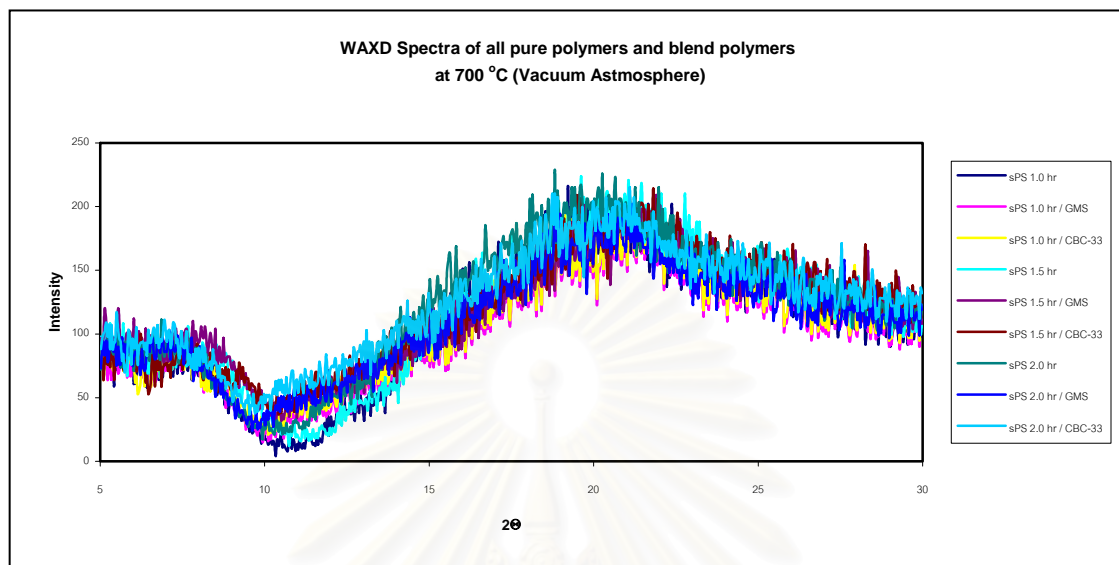


Figure 5.34 XRD patterns of polystyrene 2.0 hr blend with CBC-33

From Figure 5.26-534, we used the single standard amorphous pattern for determined the % crystallinity of polymer because all amorphous patterns of pure polymers and blend polymers were in the same form, which can be showed in Figure 5.35.



**Figure 5.35** XRD patterns of all pure polymers and blend polymers

The reason that all amorphous patterns of pure polymer and blend polymer were similarly due to the molecule of polymer was disorder as some as a bowl of spaghetti which no different or slight different in shape or structure.

Figure 5.24 was shown the X-ray diffraction patterns of GMS at room temperature under atmosphere and XRD spectra of CBC-33 was shown in figure 5.25. In Figure 5.24, XRD spectrum exhibited the diffraction peaks at about 20-25° that were the characteristic of GMS structure and XRD spectrum in Figure 5.24 exhibited the diffraction peak at about 10° and 20° that were the characteristic of CBC-33 structure.

Figure 5.26, 5.29 and 5.32 were shown the X-ray diffraction patterns of the starting syndiotactic polystyrene (sPS) with three different polymerization times at 1.0, 1.5 and 2.0 hr., respectively. From the three Figures, XRD spectrums were similarly and exhibited the diffraction peaks at about 10-15° and 20°, which were the characteristic of sPS structure. The similar diffraction peaks were observed by previous study [171-173]. The well-defined X-ray diffraction pattern of sPS was quite different from that of isotactic polystyrene (iPS). Furthermore, the identity period was twice as great as that of polyethylene (PE) and nearly equal to that of syndiotactic poly (vinyl chloride), sPVC, having a planar zigzag conformation. Therefore, that sPS had a planar zigzag conformation in the crystalline state. The crystallization rate of sPS was extremely high in comparison with that of iPS, so the solid crystal phase of iPS lesser than sPS, which was comparable to PE. sPS presented a complex polymorphism (four different crystalline from  $\alpha$ ,  $\beta$ ,  $\gamma$  and  $\delta$ ), two mesomorphic forms and various clathrate forms had been found so far. The most stable  $\alpha$  and  $\beta$  forms were characterized by chains in trans planar conformation,  $\gamma$  and  $\delta$  forms, as well as all the clathrate forms were characterized by chains in  $s(2/1)2$  helical conformation.

They were thermally unstable, hence  $\delta$  form and clathrate samples transform into  $\gamma$  form by annealing at 130 °C and transform into  $\alpha$  form by annealing at higher temperatures (180 °C). The crystallization of the  $\alpha$  and  $\beta$  forms strongly depended on the experimental conditions. It had been reported that, in the case of the crystallization from the melt, the most important factors were the maximum temperature at which the melt was heated, the permanence time of the melt at that temperature, the crystallization temperature, the cooling rate and the crystalline form of the starting material. The sample crystallized was basically in the  $\alpha$  form, as indicated by the presence of reflections at  $2\theta = 6.8^\circ$  and  $11.8^\circ$  and in the  $\beta$  form as indicated by the presence of the reflection at  $2\theta = 6.2^\circ$  and  $12.3^\circ$ . From the all spectra in the experiment, sPS contained  $\alpha$  and  $\beta$  forms. After blending sPS with GMS or CBC-33, some peaks which were characterized to sPS shift and increased of intensity as could be seen in Figure 5.26, 5.29 and 5.32 compared to Figure 5.27-5.28, 5.30-5.31 and 5.33-5.34, respectively. This indicated that there were some changed in solid crystalline phases during the preparation of blended polymer.

**Table 5.5** % Crystallinity of the obtained polymer

Type of Polymer	% Crystallinity (-)
sPS 1.0 hr	67.11
sPS 1.0 hr / GMS	75.28
sPS 1.0 hr / CBC-33	75.95
sPS 1.5 hr	72.03
sPS 1.5 hr / GMS	77.83
sPS 1.5 hr / CBC-33	79.72
sPS 2.0 hr	73.40
sPS 2.0 hr / GMS	80.90
sPS 2.0 hr / CBC-33	81.32

The increase in normalized crystallinity of sPS in the blends, was probably due to the penetration of additives into sPS domain enhanced by the molecular mobility of melt mixed blends and improved the blends melt flow properties, depended on rearrangement of the solid crystal phase was higher than origin polymer. The major effect of liquid crystal was to increase the molecular mobility of the blends when added with low concentration. GMS cloud also improved the mobility of the blend but to lesser extent and the effect did not increase at higher concentration [167,170]. On the other hand, the more LC added, the higher the mobility. Thus the mechanism, which reduced the melt viscosity in blends, might not be the same for LC and normal lubricants.

There are several methods for determining the percent crystallinity in such polymers. The first method involves the determination of the heat of fusion of the whole sample by calorimetric methods such as DSC. The heat of fusion per mole of crystalline material can be estimated independently by melting point depression experiments.

The normalized crystallinity of sPS is given by the following equation:

$$\% \text{ Crystallinity} = [(\Delta H_f / \Delta H_f^0) / \omega] \times 100$$

where  $\Delta H_f$  = the melting enthalpy of the blend  
 $\Delta H_f^0$  = the melting enthalpy of 100 % crystalline  
 $\omega$  = the weight fraction of polymer in the blend

A second method involves the determination of the density of the crystalline portion via volumetric analysis of the crystal structure and determining the theoretical density of a 100 % crystalline material. The density of the amorphous material can be determined from an extrapolation of the density from the melt to the temperature of interest. Then the percent crystallinity is given by:

$$\% \text{Crystallinity} = \left[ \frac{\rho_{exp} - \rho_{amor}}{\rho_{100\%cryst} - \rho_{amor}} \right] \times 100$$

where  $\rho_{exp}$  = the experimental density  
 $\rho_{amor}$  = the density of amorphous portion  
 $\rho_{100\%cryst}$  = the density of the crystalline portion

A third method stems from the fact that the intensity of X-ray diffraction depends on the number of electrons involved and is thus proportional to the density. Besides Bragg diffraction lines for the crystalline portion, there is an amorphous halo caused by the amorphous portion of the polymer. This last occurs at a slightly smaller angle than the corresponding crystalline peak, because the atomic spacings are larger. The amorphous halo is broader than the corresponding crystalline peak, because of the molecule disorder. This third method, sometimes called wide-angle X-ray scattering (WAXS), can be quantified by the crystallinity index (CI),

$$CI = \frac{A_c}{A_a + A_c}$$

where CI = crystallinity index or % crystallinity  
 $A_c$  = area of the crystalline fraction  
 $A_a$  = area of the amorphous fraction

Finally, from all the experimental results, WAXD results were different from DSC results because of the choiceness of the length for area under curve in DSC, which could occur at the error of % crystallinity, so the accordant of result form DSC was less accurate than XRD and the % crystallinity of XRD are more accurate than DSC because of XRD directly measure at the crystalline phase and the amorphous phase but DSC measure the energy consumed to melt the crystalline.

# CHAPTER VI

## CONCLUSIONS AND SUGGESTIONS

### 6.1 Conclusions

In this thesis,  $\text{Cp}^*\text{TiCl}_3$  catalyst was investigated for the slurry polymerization of styrene. In addition, the crystallinity of blend between syndiotactic polystyrenes and additives was also studied. The conclusions of this research can be summarized as follow:

1. % Yield of polystyrene rapidly increased at the early polymerization time and then it began to a slight increase at the finally polymerization time.
2. The catalytic activity showed a tendency to decrease with increasing polymerization time.
3. The syndiotacticity of polystyrene obtained with various polymerization times had the slight difference in degree of syndiotacticity in every polymerization time.
4. The addition of GMS and CBC-33 to base sPS by stirred melt mixer affected the increasing of  $\Delta H_{f1}$ ,  $\Delta H_{f2}$  and  $\Delta H_c$  but could reduce  $T_c$ ,  $T_{m1}$  and  $T_{m2}$  and did not effect with  $T_g$ .
5. Form DSC, the addition of GMS and CBC-33 to base sPS by affected the increasing of crystallinity in polymer blends.
6. All morphologies of pure polymers showed slight differences, it indicated that all pure polymers with the different polymerization time had closely the same chemical.
7. The SEM images of polystyrene after extraction showed similar in results. Therefore, extraction could be removed atactic part in polystyrene, also improved the morphology of polystyrene.
8. The light scattering of polystyrene obtained with various polymerization times had the slight difference in every polymerization time.
9. The addition of GMS and CBC-33 to base sPS by affected the increasing of light scattering in polymer blends.
10. All amorphous patterns form XRD of pure polymers and blend polymers were similar.

11. From XRD, the addition of GMS and CBC-33 to base sPS by affected the increasing of crystallinity in polymer blends.

12. The result from WAXD was slight different with DSC but the accordant of result from WAXD was more accurated than DSC results.

## 6.2 Suggestions

The recommendations for further research may be given as follows:

1. Another pairs between engineering polymer and additive should be chosen for studying. The better pairs of blending may be found.
2. This research can be extended to the study of the mechanism of additive that why they can increase the % crystallinity of the blends.
3. It should be interesting to study the kinetic of crystallization of crystalline polymers by using the light scattering technique.



สถาบันวิทยบริการ  
จุฬาลงกรณ์มหาวิทยาลัย

## REFERENCES

1. Aldo Guiducci, *Chemistry and Industry*, 17 June 1996, 464-465.
2. Kenneth B. Sinclair and Robert B. Wilson, *Chemistry and Industry*, 7 November 1994, 857-862.
3. W. Kaminsky, *Catalysis Today*, 62 (2000), 23-34.
4. Olagoke Olabisi, Muhammad Atiqullah and Water Kaminsky J.M.S., *Rev. Macromol. Chem. Phys.*, C37 (3), 519-554 (1997).
5. K.E. Bett, B. Crossland, H. Ford and A. K. Gardner, Proceedings of the Golden Jubilee Conference, Polyethylenes 1933-1983, The Plastics and Rubber Institute, London, (1983).
6. K. Ziegler, E. Holzkamp, H. Martin and H. Breil, *Angew. Chem.*, 67, 541 (1995).
7. K. Ziegler, *Angew. Chem.*, 76, 545 (1964).
8. G. Natta, *Mod. Plast.*, 34, 169 (1956).
9. G. Natta, *Angew. Chem.*, 76, 533 (1964).
10. J. P. Hogan and R. L. Banks, U.S. Patent, 2, 825, 721 (1958), assigned to Phillips Petroleum.
11. M. Covezzi, *Macromol. Symp.*, 89, 577 (1995).
12. Norio Kashiwa and Jun-Ichi Imuta, *Catalysis Surveys from Japan*, 1, 125-142 (1997), Baltzer Science Publishers BV.
13. Jurgen Schellenberg and Thomas H. Newman, *European Polym. J.*, 37 (2001), 1733-1739.
14. Rong Fan, Bo-Geng Li, Kun Cao, Wen-Le Zhou, Zhi-Gang Shen and Meng Ye, *J. App. Polym. Sci.*, 85, 2635-2643 (2002).
15. Seok-Ho Hwang, Myeong-Jun Kim and Jae-Chang Jung, *European Polym. J.*, 38 (2002), 1881-1885.
16. Suraphan Powanusorn, Application of Low Molar Mass Thermotropic Liquid Crystals as an Additive for Polymers, Master's Thesis, Department of Chemical Engineering, Graduate School, Chulalongkorn University, 2000.
17. Lutz, John. T. Jr. and Grossman, Richard. F., Polymer Modifiers and Additives, New York, Marcel Dekker, 2001.
18. G. Natta, P. Pino, G. Mazzanti and R. Lanzo, *Chim. Ind.*, Milan, 39, 1032 (1957).
19. D. S. Breslow and N. R. Newburg, *J. Am. Chem. Soc.*, 79, 5072 (1957).
20. A. Andersen, H. G. Corde, J. Herwig, W. Kaminsky, A. Merk, R. Mottweiler, J. Pein, H. Sinn and H. J. Vollmer, *Angew. Chem.*, 88, 689 (1976).
21. K. H. Reichert and K. R. Meyer, *Makromol. Chem.*, 169, 163 (1973).
22. H. Sinn and W. Kaminsky, *Adv. Organomet. Chem.*, 18, 99 (1980).
23. H. Sinn, W. Kaminsky, H. J. Vollmer and R. Woldt, *Angew. Chem. Int. Ed. Eng.*, 19, 392 (1980).
24. N. Ishihara, M. Kuramoto and M. Voi, *Macromolecules*, 1988, 21, 3356-3360.
25. A. Kucht and H. Kucht et al., *Organometallics*, 1993, 12, 3075-3078.
26. T. E. Ready, J. C. W. Chien and M. D. Rausch, *J. Organomet. Chem.*, 519, 1996, 21-28.
27. W. Kaminsky, S. Lenk, V. Scholz, H. W. Roesky and A. Herzog, *Macromolecules*, 30 (25), 1997, 7647-7650.
28. Q. Hu, Z. Ye and S. Lin, *Macromol. Chem. Phys.*, 198, 1823-1828 (1997).



29. P. Foster, M. D. Raush and J. C. W. Chein, *J. Organomet. Chem.*, 527, 1997, 71-74.
30. Y. Kim, B. H. Koo and Y. Do, *J. Organomet. Chem.*, 527, 1997, 155-161.
31. N. Schmeider, M. H. Proscenc and H. H. Brintzinger, *J. Organomet. Chem.*, 545-546, 1997, 291-295.
32. G. Tian, S. Xu, Y. Zhang, B. Wang and X. Zhou, *J. Organomet. Chem.*, 558, 1998, 231-233.
33. A. Buckley, A. B. Conciatori and G. W. Calundann, U.S. Patent, 4, 434, 262, 1984.
34. A. Siegmann, A. Dagan and S. Kenig, *Polymer*, 26 (1985), 1325-1330.
35. C. Schwecke and W. Kaminsky, *J. Polym. Sci. Part A: Polym. Chem.*, 39, 2805-2812, 2001.
36. Y. Kim and Y. Do, *J. Organomet. Chem.*, 655, 186-191, 2002.
37. K. Nomura and A. Fudo, *Catalysis Communications*, 4, 269-274, 2003.
38. R. Fan, K. Cao, B. Li, H. Fan and Bo-Geng Li, *European Polym. J.*, 37 (2001), 2335-2338.
39. S. K. Noh, S. Kim, Y. Yang, W. S. Lyoo and Dong-Ho Lee, *European Polym. J.*, 40 (2004), 227-235.
40. F. M. Rabagliati, M. A. Perez and R. Quijada, *Polym. Bull.*, 41, 441-446 (1998).
41. Y. C. Lin, H. W. Lee and H. H. Winter, *Polymer*, 34, 4703-4709, 1993.
42. J. C. W. Chien, Z. Salajka and S. Dong, *Macromolecules*, 25, 3199-3203 (1992).
43. Anchana Chuenchaokit, Effects of Thermotropic Liquid Crystal on Properties of Polycarbonates, Master's Thesis, Department of Chemical Engineering, Graduate School, Chulalongkorn University, 1998.
44. Noppawan Motong, Effect of Mixing and Processing on the Viscosity of Polycarbonat blends with Low Molar Mass Liquid Crystal, Master's Thesis, Department of Chemical Engineering, Graduate School, Chulalongkorn University, 2002.
45. Richard S. Stein, A. Misra, T. Yuasa, and F. Khambatta, *Pure and Appl. Chem.*, 49, 915-928 (1977).
46. J. Koberstein, T. P. Russell and R. S. Stein, 1979.
47. R. J. Tabar, A. Wasiak, S. D. Hong, T. Yuasa and R. S. Stein, 1981.
48. M. Ree, T. Kyu and R. S. Stein, 1987.
49. R. S. Stien, J. Cronauer and H. G. Zachmann, 1996.
50. R. S. Stein and K. Jacob et al., 2001.
51. Joo Young Nam, Shigenobu Kadomatsu, Hiromu Saito and Takashi Inoue, 2002.
52. J. Huang and G. L. Rempel, *Prog. Polym. Sci.*, 20, 459-526 (1995).
53. G. Natta, P. Pino, G. Mazzanti and U. Giannini, *J. Inorg. Nucl. Chem.*, 8, 612 (1958).
54. D. S. Breslow (Hercules Powder Co.), U.S. Patent, 2, 827, 446 (1958), *Chem. Abstr.*, 53, 1840i (1959).
55. H. Sinn and W. Kaminsky, *Ibid.*, 18, 99(1980).
56. R. F. Jordan, *Adv. Organomet. Chem.*, 32, 325 (1991) and *References Cited Therein*.
57. J. C. W. Chien and D. He, *J. Polym. Sci., Polym. Chem.*, Ed., 29, 1603 (1991).
58. R. Poli, *Chem. Rev.*, 91, 509 (1991).
59. R. L. Halterman, *Ibid.*, 92, 965 (1992).

60. D. J. Cardin, M. F. Lappert and C. L. Raston, Chemistry of Organo-Zirconium and -Hafnium Compounds, Wiley, New York, 1986.
61. U. Thewalt, Gmelin, Handbook of Inorganic Chemistry, Part 4 (A. Slawisch, Ed.), Springer-Verlag, Berlin, 1984.
62. P. C. Wailes, R. S. P. Coutts and H. Wegold, Organometallic Chemistry of Titanium, Zirconium and Hafnium, Academic Press, New York, 1974.
63. M. Bottrill, P. D. Gavens, J. W. Kelland and J. McMeeking, in Comprehensive Organometallic Chemistry, Vol. 3 (S. G. Wilkinson, F. G. A. Stone and E. W. Abel, Eds.) Pergamon Press, Oxford, 331 (1982).
64. D. J. Cardin, M. F. Lappert., C. L. Raston and P. I. Riley, *Ibid.*, 559.
65. T. Mise, K. Aoki, H. Yamazaki, S. Miya and M. Harada, *Proc. 34<sup>th</sup> Symp. Organomet. Chem. Jpn.*, November 1987, 79.
66. J. Okuda, *Top. Curr. Chem.*, 160, 97 (1991).
67. H. H. Brintzinger, in Transition Metals and Organometallics as Catalysts for Olefin Polymerization (W. Kaminsky and H. Sinn, Eds.), Springer-Verlag, Berlin, 1988, 249.
68. T. Mise, S. Miya and H. Yamazaki, *Chem. Lett.*, 1853 (1989).
69. J. C. Gallucci, B. Gautheron, M. Gugelchuk, P. Meunier and L. A. Paquette, *Organometallics*, 6, 15 (1987).
70. F. Nief, L. Richard and F. Mathey, *Ibid.*, 8, 1473 (1989).
71. S. Collins, Y. Hong, R. Ramachandra and N. J. Taylor, *Ibid.*, 10, 2349 (1991).
72. H. Lang and D. Seyferth, *Ibid.*, 10, 347 (1991).
73. G. A. Luinstra and J. H. Teuben, *Ibid.*, 11, 1793 (1992).
74. M. E. Huttenloch, J. Diebold, W. Rief and H. H. Brintzinger, *Ibid.*, 11, 3600 (1992).
75. Q. Huang, Y. Qian and Y. Tang, *J. Organomet. Chem.*, 368, 277 (1989).
76. J. B. Hoke and E. W. Stern, *Ibid.*, 412, 77 (1991).
77. P. Burger, K. Hortmann, J. Diebold and H. H. Brintzinger, *Ibid.*, 417, 9 (1991).
78. G. Erker and B. Temme, *J. Am. Chem. Soc.*, 114, 4004 (1992).
79. S. Collins, W. M. Kelly and D. A. Holden, *Macromolecules*, 25, 1780 (1992).
80. M. Kaminaka and K. Soga, *Makromol. Chem. Rapid Commun.*, 12, 367 (1991).
81. G. B. Sakharovskaya, N. N. Korneev, A. F. Popov, E. I. Larikov and A. F. Zhigach, *Chem. Abstr.*, 62, 2787d (1965).
82. A. Storr, K. Jones and A. W. Laubengayer, *J. Am. Chem. Soc.*, 90, 3173 (1968).
83. M. Boleslawski and S. Pasynkiewicz, *J. Organomet. Chem.*, 43, 81 (1972).
84. M. Boleslawski, S. Pasynkiewicz, K. Jaworski and A. Sadownik, *Ibid.*, 97, 15 (1975).
85. N. Ueyama, T. Araki and H. Tani, *Inorg. Chem.*, 12, 2218 (1973).
86. H. Yamamoto and H. Nozaki, *Angew. Chem. Int. Ed. Engl.*, 17, 169 (1978).
87. M. Boleslawski, S. Pasynkiewicz, A. Kunicki and J. Serwatowski, *J. Organomet. Chem.*, 116, 285 (1976).
88. A. Wolinska, *Ibid.*, 234, 1 (1982).
89. L. Siegiejezyk and L. Synoradzki, *Ibid.*, 311, 253 (1986).
90. S. A. Sangokoya (Ethyl Corp.), U.S. Patent, 5,041,583, (1991); *Chem. Abstr.*, 115, 183567a (1991).

91. N. Tomotsu and M. Kuramoto (Idemitsu Kosan Ltd.), European Patent EP, 393,358 (1990), *Chem. Abstr.*, 114, 43755q (1991).
92. S. A. Sangokoya (Ethyl Corp.), U.S. Patent, 5,099,050, (March 24, 1992), *Chem. Abstr.*, 116, 236342c (1992).
93. N. Tomotsu (Idemitsu Kosan K. K.), Japanese Patent J. P., 04,49,293 (February 1990); *Chem. Abstr.*, 117, 8699q (1992).
94. H. Sinn, J. Bliemeister, D. Clausnitzer, L. Tikwe, H. Winter and O. Zarncke, in Transition Metals and Organometallics as Catalysts for Olefin Polymerization (W. Kaminsky and H. Sinn, Eds.), Springer-Verlag, Berlin, 257 (1988).
95. G. A. Razuvaev, J. A. Sangolov, J. J. Nelkenbaum and K. S. Minsker, *Izv. Akad. Nauk SSR, Ser. Chem.*, II, 2547 (1975); *Chem. Abstr.*, 84, 59627x (1976).
96. R. Mani and C. M. Burns, *Polymer*, 34 1941 (1993).
97. D. Cam, E. Albizzati and P. Cinquina, *Makromol. Chem.*, 191, 1641 (1990).
98. T. Sugano, K. Matsubara, T. Fujita and T. Takahashi, *J. Mol. Catal.*, 82, 93 (1993).
99. S. Lasserre and J. Deronault, *Nouv. J. Chim.*, 7, 659 (1983).
100. L. Resconi, S. Bossi and L. Abis, *Macromolecules*, 23, 4489 (1990).
101. W. Kaminsky, in Transition Metal Catalyzed Polymerizations-Alkenes and Dienes, Vol.4 (R. P. Quirk, Ed.), Harwood Academic Publishers, New York, 225 (1983).
102. J. Hervig and W. Kaminsky, *Polym. Bull.*, 9, 464 (1983).
103. J. C. W. Chein and B-P. Wang, *J. Polym. Sci. Polym. Chem. Ed.*, 26, 3089 (1988).
104. F. S. Dyachkovskii, *Vysokomol. Soedin.*, 7, 114 (1965); *Chem. Abstr.*, 63, 4394 (1965).
105. O. N. Babkina, E. A. Grigorian, F. S. Dyachkovskii, A. E. Shilov and N. M. Shuvalov, *Ah. Fiz. Khim.*, 43, 1759 (1969); *Chem. Abstr.*, 71, 123380x (1969).
106. J. J. Eisch, A. M. Piotrowski, S. K. Brownstein, E. J. Gabe and F. Lee., *J. Am. Chem. Soc.*, 107, 7219 (1985).
107. R. F. Jordan, *J. Chem. Educ.*, 65, 285 (1988).
108. X. Yang, C. L. Stern and T. J. Marks, *J. Am. Chem. Soc.*, 113, 3623 (1991).
109. C. Shishta, R. M. Hathorn and T. J. Marks, *Ibid.*, 114, 1112 (1992).
110. E. Giannetti, G. M. Nicoletti and R. Mazzocchi, *J. Polym. Sci. Polym. Chem. Ed.*, 23, 2117 (1985).
111. M. Bochmann and A. J. Jaggar, *J. Organomet. Chem.*, 424, C5 (1992).
112. R. F. Jordan, C. S. Bajgur, R. Willett and B. Scott, *J. Am. Chem. Soc.*, 108, 7410 (1986).
113. J. J. Eisch, K. R. Caldwell, S. Werner and C. Kruger, *Organometallics*, 10, 3417 (1991).
114. G. G. Hlatky, H. W. Truner and R. R. Eckman, *J. Am. Chem. Soc.*, 111, 2728 (1989).
115. D. J. Crowther and R. F. Jordan, *Makromol. Chem. Macromol. Symp.*, 66, 121 (1993).
116. J. Cihlar, J. Mejzlik, O. Hamrik, P. Hudec, J. Majer, *Ibid.*, 181, 2549 (1980).
117. S. A. Reddy, G. Shashidhar and S. Sivaram, *Macromolecules*, 26, 1180 (1993).

118. S. A. Reddy and S. Sivaram, in Polymer Science-Recent Advances (I. S. Bhardwaj, ed.), Allied Publishers, New Delhi, 1994.
119. A. V. Agasaryan, G. P. Belov, S. P. Davtyan and M. L. Eritsyanyan, *Eur. Polym. J.*, 17, 443 (1981).
120. W. Kaminsky, A. Bark, R. Spiehl, N. Moler-Linderhof, S. Neidoba, in Transition Metals and Organometallics as Catalysts for Olefin Polymerization (W. Kaminsky and H. Sinn, Eds.), Springer-Verlag, New York, 291 (1988).
121. W. Kaminsky and R. Steiger, *Polyhedron*, 7, 2375 (1988).
122. M. H. Prosenc, C. Janiak and H. H. Brintzinger, *Organometallics*, 11, 4037 (1992).
123. J. C. W. Chien and B. Wang, *J. Polym. Sci. Part A: Polym. Chem.*, 28, 15 (1990).
124. J. C. W. Chien and A. Razavi, *J. Polym. Sci. Part A: Polym. Chem.*, 26, 2369 (1988).
125. J. C. W. Chien and B-P. Wang, *J. Polym. Sci. Part A: Polym. Chem.*, 26, 3089 (1988).
126. W. Kaminsky, K. Kuiper, and S. Niedoba, *Makromol. Chem. Makromol. Symp.*, 3, 377 (1986).
127. J. C. W. Chien and R. Sugimoto, *J. Polym. Sci. Chem.*, 29, 459 (1991).
128. B. Rieger, X. Mu, D. T. Mallin, M. D. Rausch and J. C. W. Chien, *Macromolecules*, 23 3559 (1990).
129. N. Herfert and G. Fink, *Makromol. Chem.*, 193, 1359 (1992).
130. J. A. Canich, European Patent, 0,420,436 (1991) assigned to Exxon Chemical Co.
131. H. W. Turner, European Patent, 0,226,463 (1987) assigned to Exxon Chemical Patents, Inc.
132. H. W. Turner, International Patent, WO 87/03,604 (1987) assigned to Exxon Chemical Patents, Inc.
133. E. Giannetti, G. M. Nicoletti and R. Mazzocchi, *J. Polym. Sci. Polym. Chem. Ed.*, 23, 2117 (1985).
134. A. Zambelli, P. Longo and A. Grassi, *Macromolecules*, 22, 2186 (1989).
135. M. Bochmann, *Angew. Chem.*, 104, 1206 (1992).
136. X. Yiang, C. L. Stern and T. J. Marks, *J. Am. Chem. Soc.*, 116, 10015 (1994).
137. G. G. Hlatky, H. W. Turner and R. R. Eckmann, *Organometallics*, 11, 1413 (1992).
138. J. A. Ewen and A. Razavi, U.S. Patent, 4, 892,851 (1990), assigned to Fina Technology, Inc.
139. J. C. W. Chein, W. M. Tsai and M. D. Rausch, *J. Am. Chem. Soc.*, 111, 2728 (1991).
140. G. G. Hlatky, H. W. Turner and R. R. Eckmann, *Ibid.*, 116, 10015 (1989).
141. L. Jai, X. Yang, A. Ishihara and T. J. Marks, *Organometallics*, 14, 3135 (1995).
142. C. Pellecchia, A. Proto, P. Longo and A. Zambelli, *Makromol. Chem. Rapid Commun.*, 12, 663 (1991).
143. C. Pellecchia, A. Proto, P. Longo and A. Zambelli, *Ibids.*, 13, 227 (1992).
144. Hoechst Aktiengesellschaft, European Patent, 0,384,263 (1993).

145. H. W. Turner, European Patent, 0,277,004 (1988) assigned to Exxon Chemical Patents, Inc.
146. G. G. Hlatky, H. W. Turner and R. R. Eckmann, *J. Am. Chem. Soc.*, 111, 2728 (1992).
147. N. Herfert and G. Fink, *Makromol. Chem. Macromol. Symp.*, 66, 157 (1993).
148. A. R. Siedle, W. M. Lamana, R. A. Newmark, J. Stevens, A. E. Richardson and M. Ryan, *Makromol. Chem. Macromol. Symp.*, 66, 215 (1993).
149. J. A. Ewen and M. J. Elder, *Makromol. Chem. Macromol. Symp.*, 66, 179 (1993).
150. K. Soga and D. H. Lee, *Makromol. Chem.*, 193, 1687 (1992).
151. M. Takahashi, Metalocene' 95, (Proceedings of the International Congress on Metallocene Polymers), Scotland Business Research Inc., Brussels, 61 (1995).
152. L. Luciani, M. Federico, G. Liiana and B. Evelina, European Patent, 0,595,390 (1994) assigned to Enichem S. P. A.
153. F. Milani, L. Lucian0, P. Bruno and L. Antonio, European Patent, 0,588,404A2 (1994) assigned to Enichem S. P. A.
154. D. Fischer, S. Junglin and R. Mulhaupt, *Makromol. Chem. Macromol. Symp.*, 66, 191 (1993).
155. Hans R. Kricheldorf, Handbook of Polymer Synthesis, Part A, Marcel Dekker, Inc., New York, 1992.
156. Netfirms, Introduction to Liquid Crystals, Available from <http://adminnet.eng.ox.ac.uk/lc.research/introf.html>.
157. Netfirms, Polymer Liquid Crystals, Available from <http://plc.cwru.edu/tutorial/enhanced/files/lindex.html>.
158. Gray, G. W., Molecular Structure and the Properties of Liquid Crystals, London, Academic Press, 1962.
159. Demus, D. Goodby, J. Gray, G. W. Spiess, H. W. and Vill, V., Handbook of Liquid Crystals, Vol. 2A: Low Molecular Weight Liquid Crystals I, New York, Wiley-VCH, 1998.
160. Cifferri, A. Krigbaum, W. R. and Meyer, Robert B., Polymer Liquid Crystal, London, Academic Press, 1982.
161. Prasit Pattananuwat, Siriprapa Pattanakit and Set Siriwat, Metallocene Catalyst for Syndiotactic Polymerization of Styrene, Bachelor's Senior Project, Department of Material Science and Engineering, Faculty of Engineering and Industrial Technology, Silpakorn University, 2001.
162. R. PO and N. Cardi, *Prog. Polym. Sci.*, 21 (1996), 47-88.
163. L. H. Sperling, Introduction to Physical Polymer Science, 3<sup>rd</sup> Ed., John Wiley & Sons, Inc., 2001.
164. R. S. stein and M. B. Rhodes, *Journal of Applied Physics*, 31 , 11 (1960).
165. R. S. Stein and T. Hotta, *Journal of Applied Physics*, 35 , 7, 2237-2242 (1964).
166. Netfirms, Phthalate Plasicizers, Available from [http://www.eng.buffalo.edu/Courses/ce435/2001ZGu/Phthalate\\_Plasticizers/PhthalatePlasticizersReport.htm](http://www.eng.buffalo.edu/Courses/ce435/2001ZGu/Phthalate_Plasticizers/PhthalatePlasticizersReport.htm).
167. S. Wacharawichanant, *Private Communication*, 2002.
168. Shengqing Xu, Bin Chen, Tao Tang and Baotong Huang, *Polymer*, 40 (1999) 3399-3406.

169. Netfirms, Polystyrene, Available from <http://www.psrc.usm.edu/macrog/styrene.htm>.
170. S. Wacharawichanant, S. Thongyai, S. Tanodekaew, J. S. Higgins and N. Clarke, *Polymer*, 45 (2004), 2201-2209.
171. N. Ishihara, T. Seimiya, M. Kuramoto and M. Uoi, *Macromolecules*, 1986, 19, 2465-2466.
172. Yuying Li, Jiasong He, Wei Qiang and Xiao Hu, *Polymer*, 43 (2002), 2489-2494.
173. Claudio De Rosa, Odda Ruiz de Ballesteros, Massimo Di Gennaro and Finizia Auriemma, *Polymer*, 44 (2003), 1861-1870.
174. Eakkalak Singnoo, Effects of Low Molar Mass Liquid Crystal Addition on Crystal Structure of Isotactic Polypropylene, Master's Thesis, Department of Chemical Engineering, Graduate School, Chulalongkorn University, 2003.



สถาบันวิทยบริการ  
จุฬาลงกรณ์มหาวิทยาลัย



**APPENDIX**

สถาบันวิทยบริการ  
จุฬาลงกรณ์มหาวิทยาลัย

## Appendix A: The Data of DSC Characterization

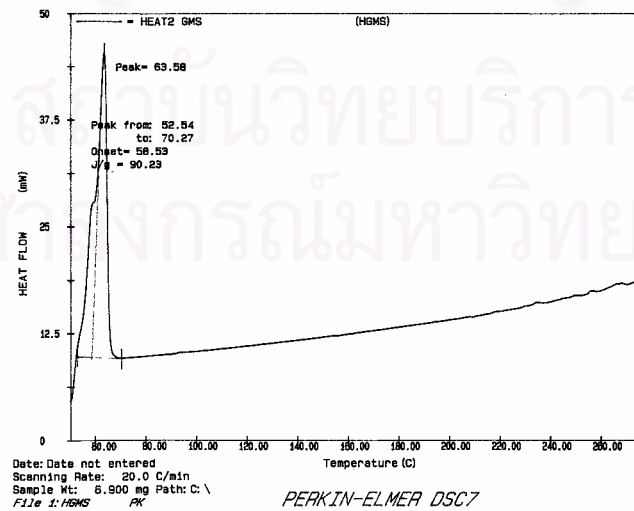
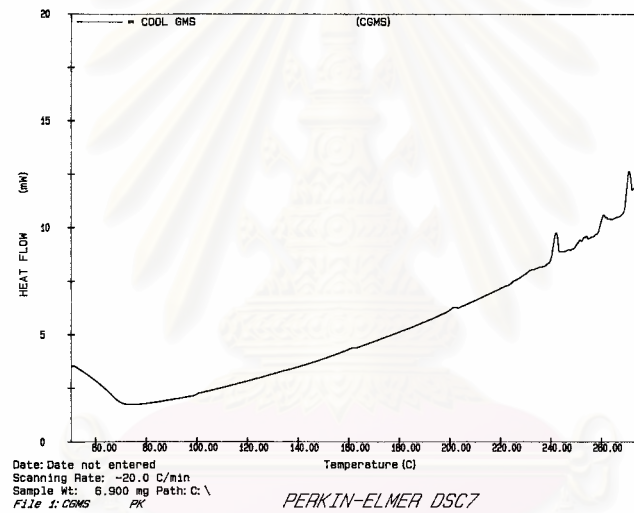
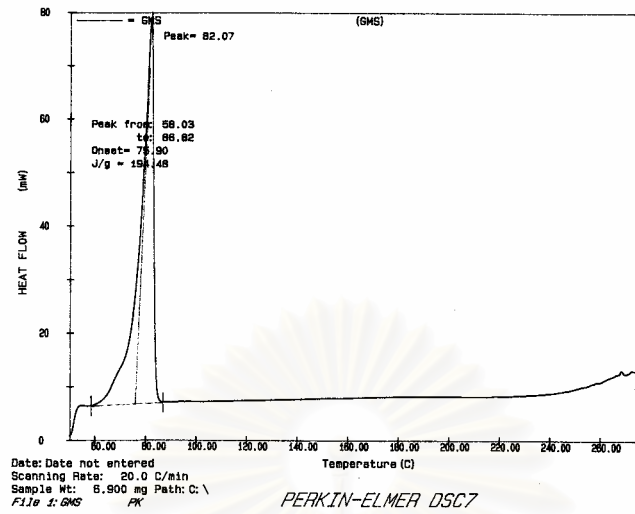


Figure A.1 DSC curve of GMS



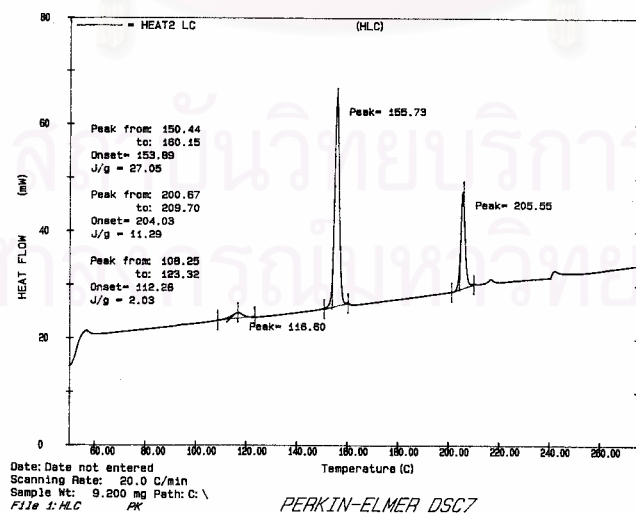
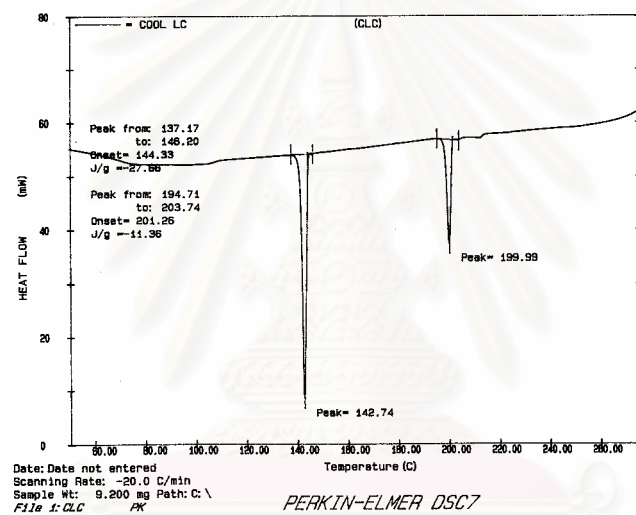
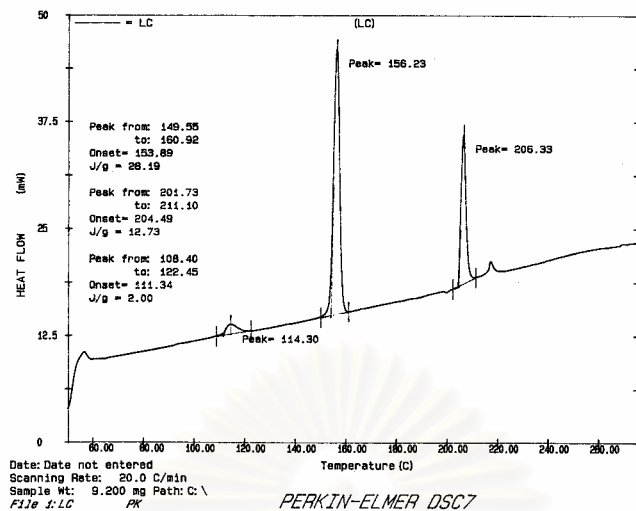


Figure A.2 DSC curve of CBC-33

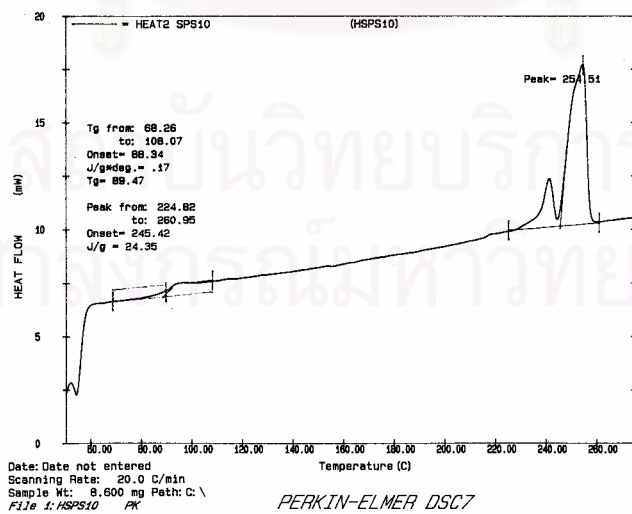
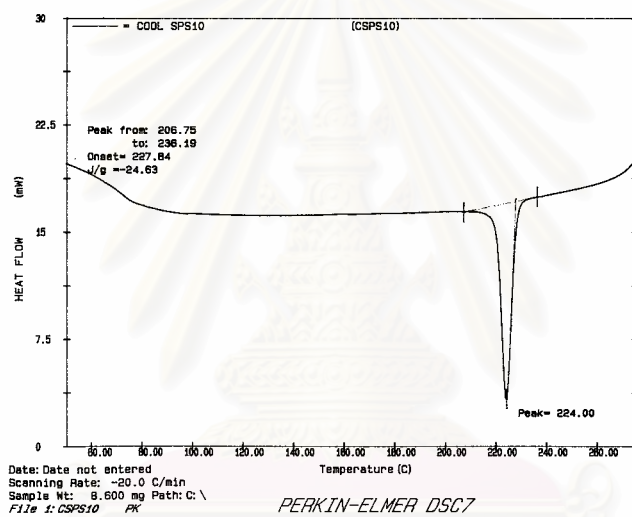
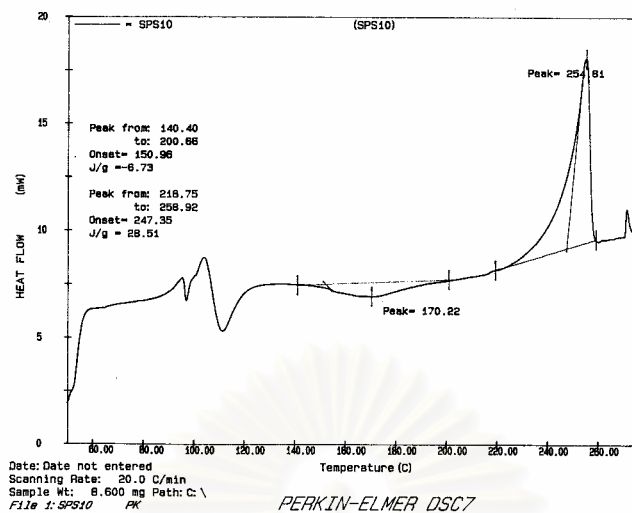


Figure A.3 DSC curve of polystyrene 1.0 hr

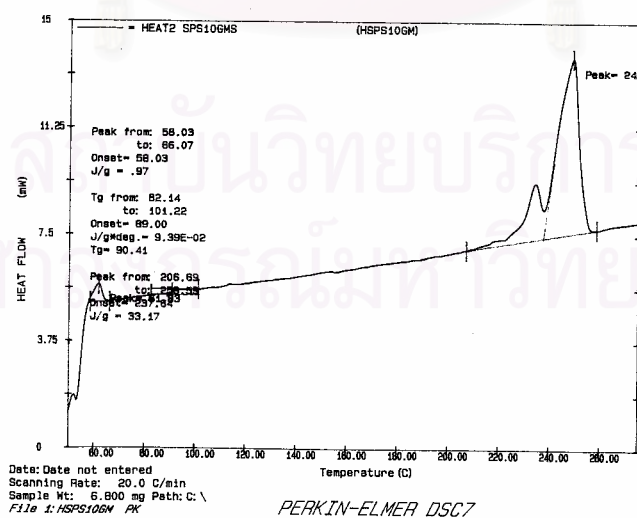
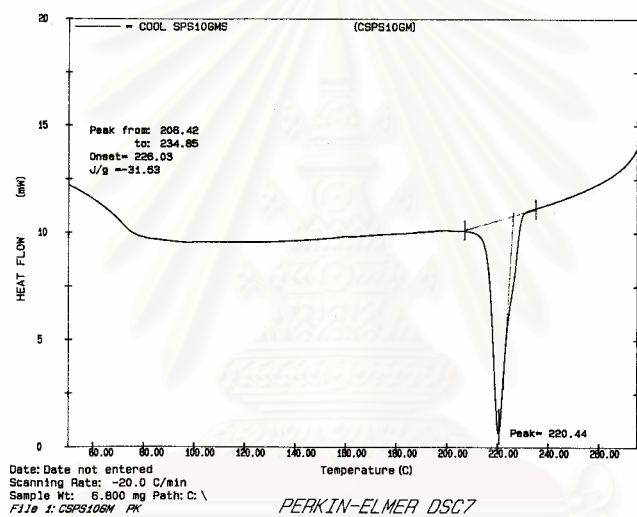
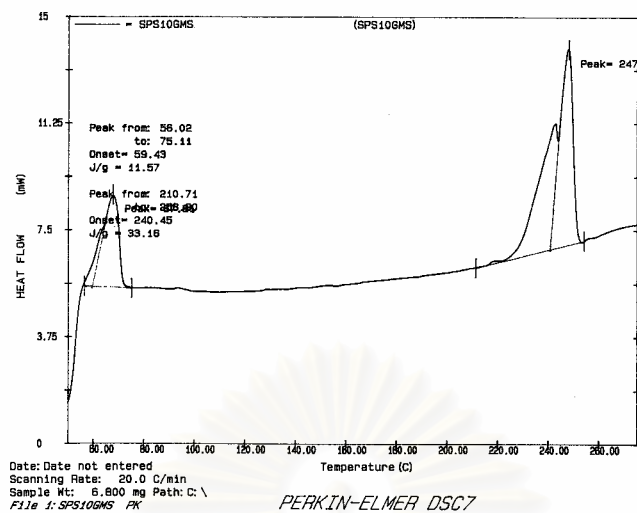


Figure A.4 DSC curve of polystyrene 1.0 hr blended with GMS

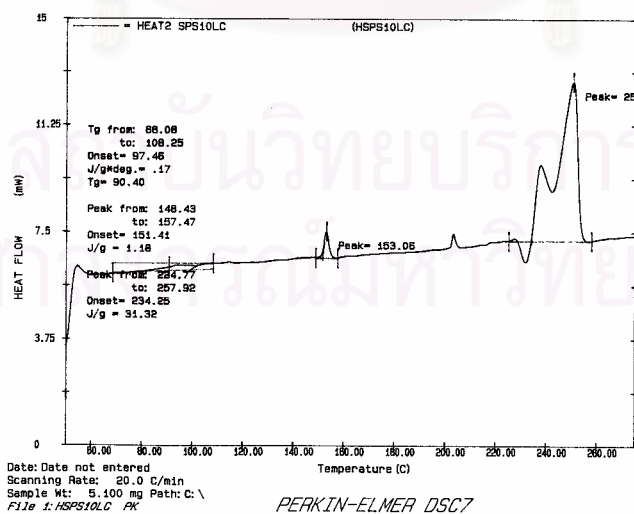
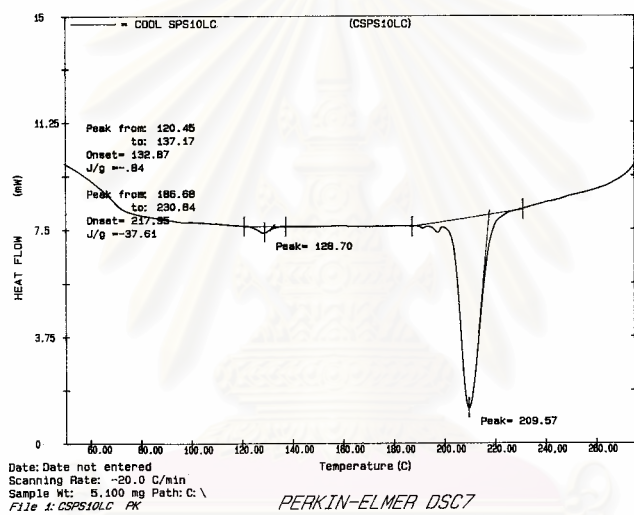
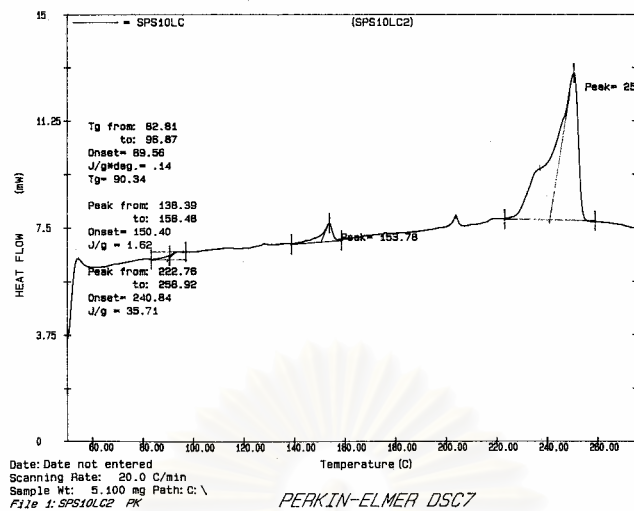


Figure A.5 DSC curve of polystyrene 1.0 hr blended with CBC-33

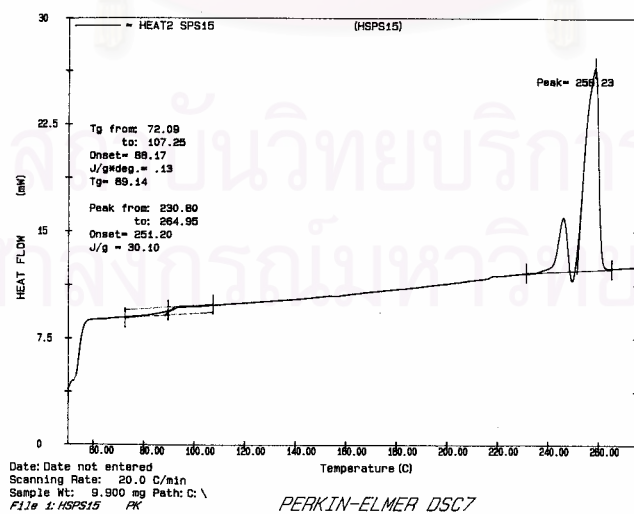
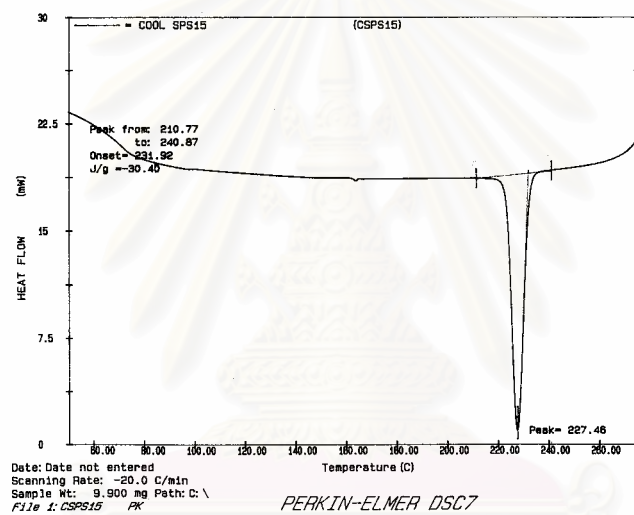
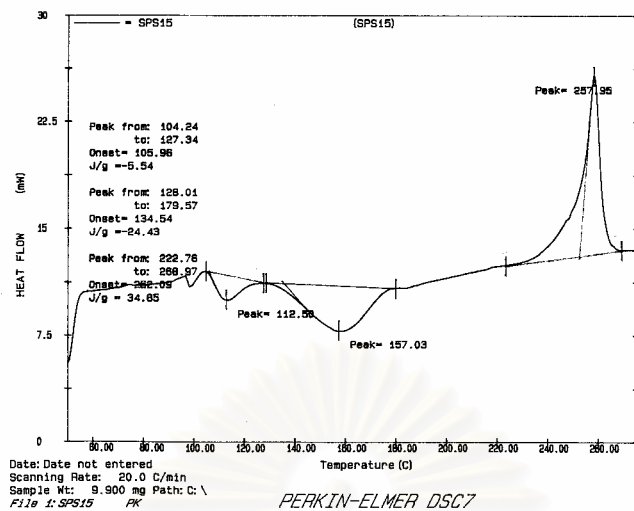


Figure A.6 DSC curve of polystyrene 1.5 hr

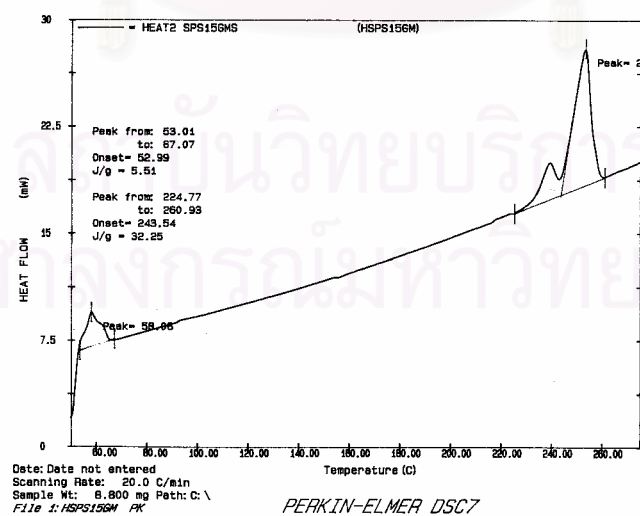
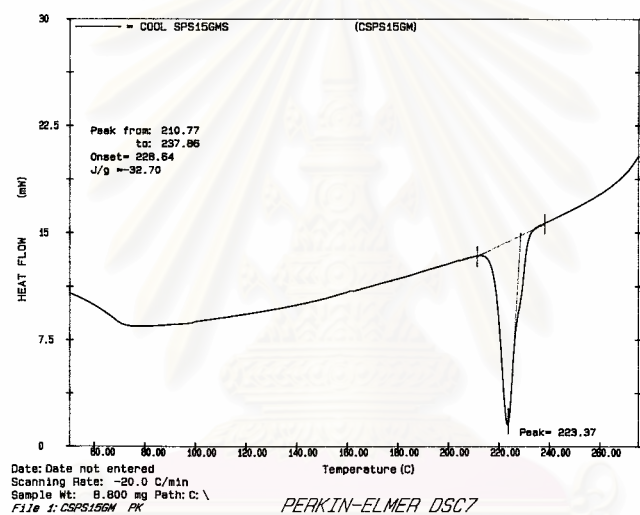
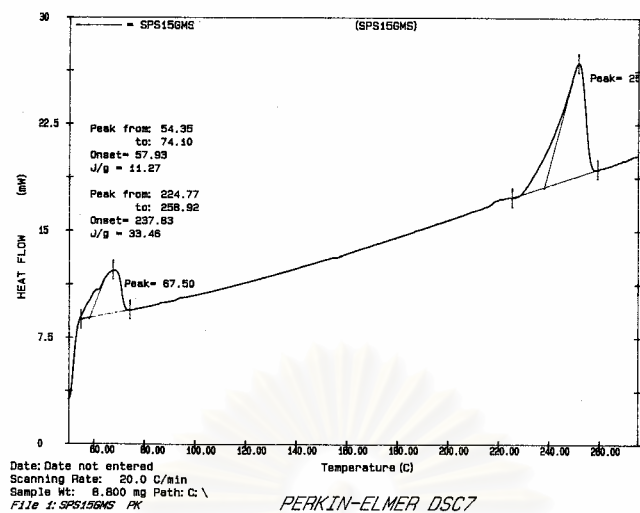


Figure A.7 DSC curve of polystyrene 1.5 hr blended with GMS

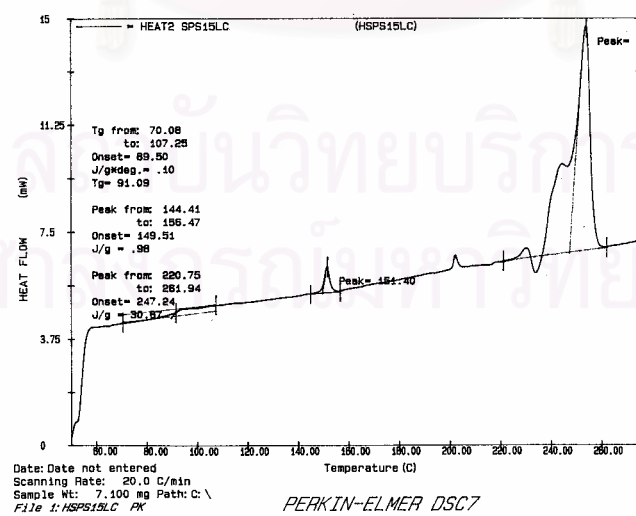
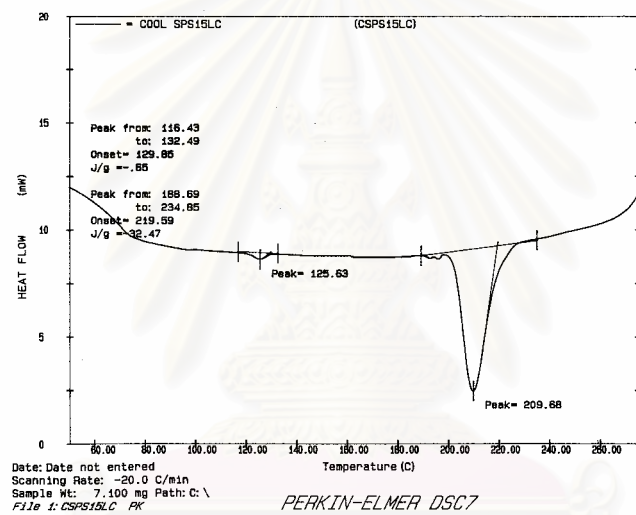
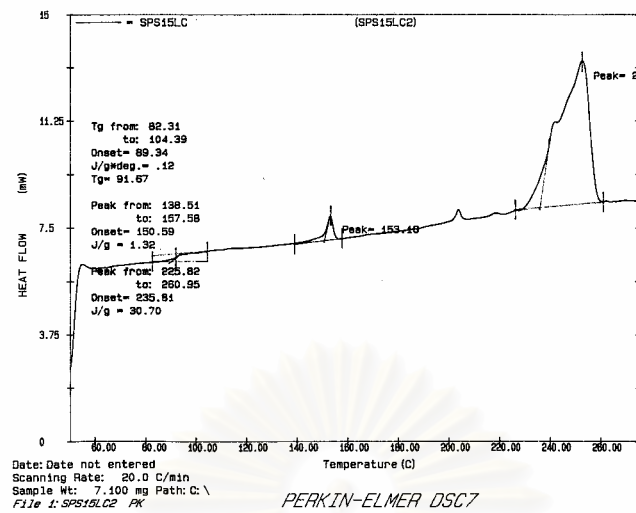


Figure A.8 DSC curve of polystyrene 1.5 hr blended with CBC-33

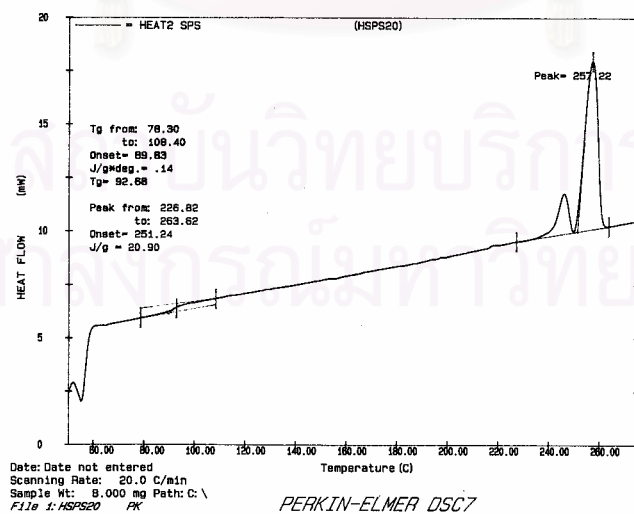
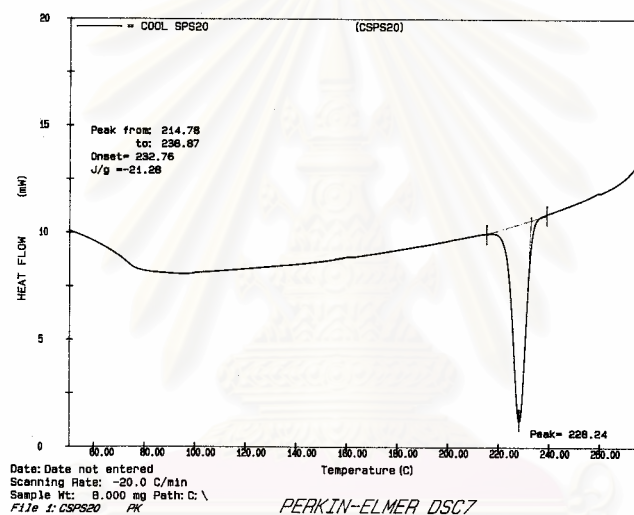
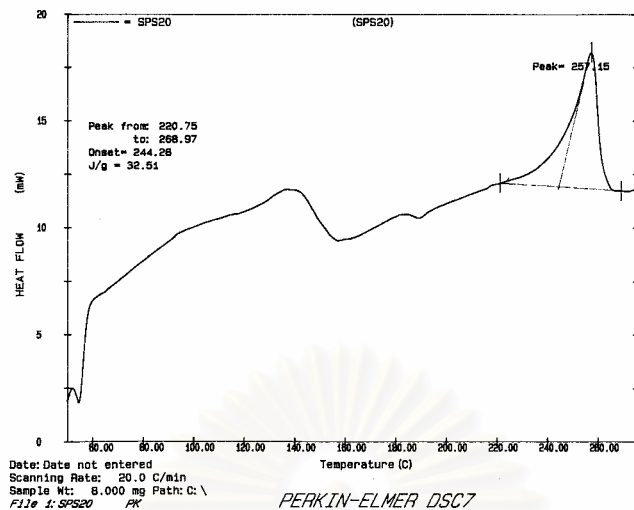


Figure A.9 DSC curve of polystyrene 2.0 hr



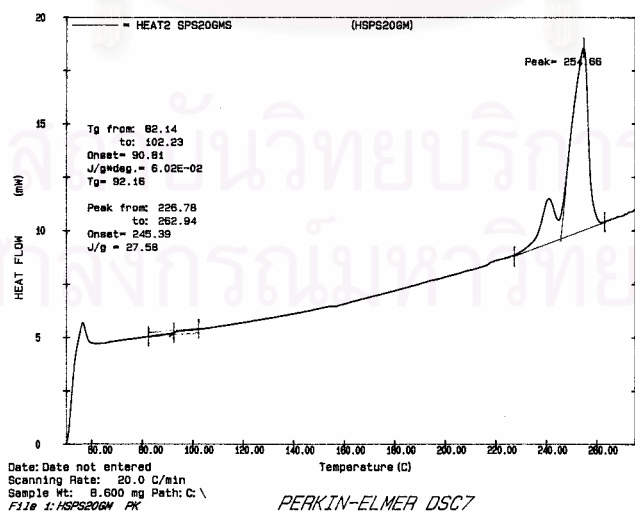
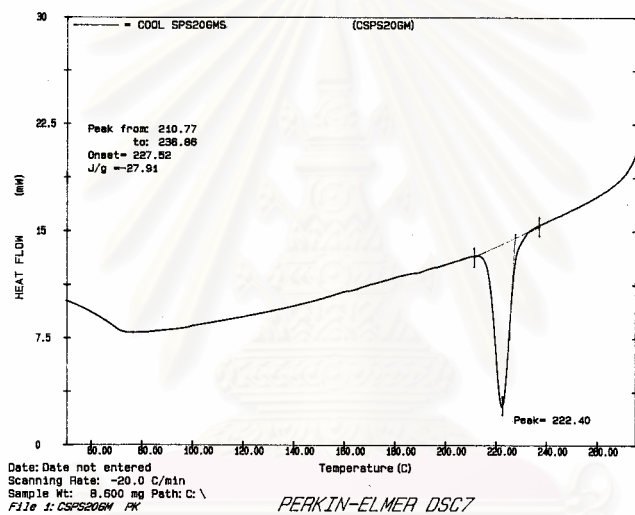
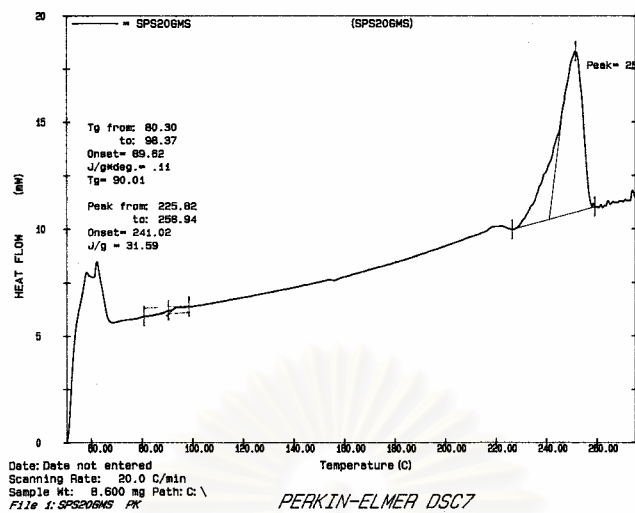


Figure A.10 DSC curve of polystyrene 2.0 hr blended with GMS

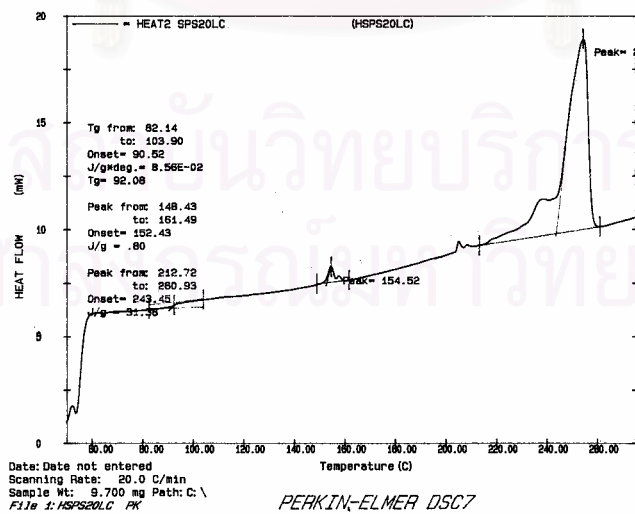
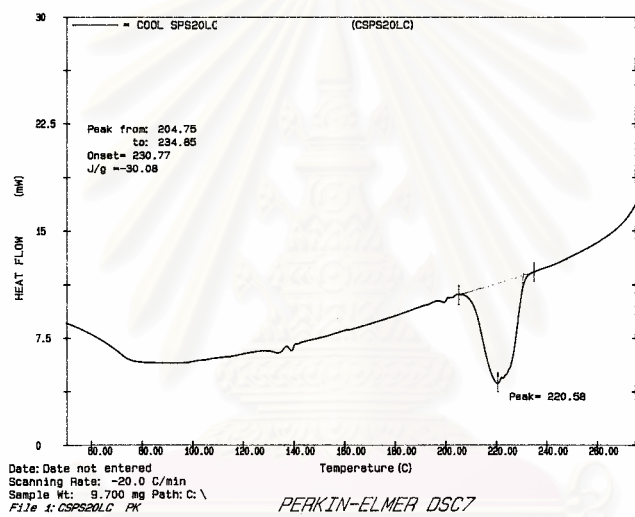
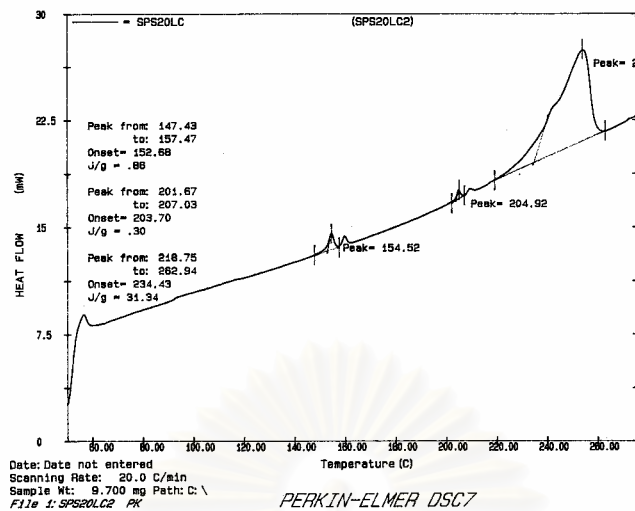


Figure A.11 DSC curve of polystyrene 2.0 hr blended with CBC-33

## VITA

Mr. Achanai Buasri was born in Nakhonsawan, Thailand on February 13, 1980. He received the Bachelor Degree of Engineering in Petrochemicals and Polymeric Materials from the Department of Material Science and Engineering, Faculty of Engineering and Industrial Technology, Silpakorn University in 2001. He entered the Master of Engineering in Chemical Engineering Program at Chulalongkorn University in 2002.



สถาบันวิทยบริการ  
จุฬาลงกรณ์มหาวิทยาลัย